

THESIS

TAXONOMIC DISTINCTIONS IN THE 3D MICROMORPHOLOGY OF TOOTH MARKS
WITH APPLICATION TO FEEDING TRACES FROM MIDDLE BED II, OLDUVAI GORGE,
TANZANIA

Submitted by

Matthew V. Muttart

Department of Anthropology

In partial fulfillment of the requirements

For the Degree of Master of Arts

Colorado State University

Fort Collins, Colorado

Summer 2017

Master's Committee:

Advisor: Michael C. Pante

Jason LaBelle
Randall Boone

Copyright by Matthew V. Muttart 2017

All Rights Reserved

ABSTRACT

TAXONOMIC DISTINCTIONS IN THE 3D MICROMORPHOLOGY OF TOOTH MARKS WITH APPLICATION TO FEEDING TRACES FROM MIDDLE BED II, OLDUVAI GORGE, TANZANIA

Reconstructing the ecology of Early Stone Age archaeological sites is critical to understanding the conditions and behaviors that led to these accumulations, particularly as hominins encroached upon the larger carnivore guild by regularly consuming flesh and marrow from mammal carcasses; a dietary shift which is often considered a catalyst towards increased brain and body size. However, due to the paucity of both hominin and carnivore body fossils in the archaeological record, little is known about the specific carnivore taxa that hominins were competing and interacting with. The abundance of carnivore tooth marked bone at these early archaeological sites highlights the potential of these traces to help refine our knowledge of past hominin and carnivore interactions by linking specific carnivore taxa to the feeding traces found on fossil bones.

This thesis seeks to determine if variations in a carnivore's tooth mark morphology can be used to differentiate between carnivore actors using feeding traces found in the archaeological record. Previous research seeking to link carnivores to their feeding traces have examined gross bone damage capabilities, gnawing damage patterns, and measurements of tooth pits from digital photographs. These findings have only been able to link body size of consumers to the levels of damage or size of tooth marks inflicted on bone surfaces during feeding. These findings are

limited by the qualitative or two-dimensional analyses on which they are based, but highlight the potential for more advanced techniques of data collection and analysis.

Controlled feeding experiments were conducted for seven species of modern mammalian carnivores and a single species of crocodile. Scans of individual tooth marks were produced using a Nanovea white-light confocal profilometer, while 3D models of the marks were analyzed with Digital Surf's Mountains Software. Tooth marks found on fossils from Middle Bed II, Olduvai Gorge, were scanned and compared against an actualistic sample of tooth marks.

Quantitative analysis and statistical comparison of 3D measurements can be used to characterize taxonomic distinctions of tooth mark morphology between certain species as well as to link some fossil feeding traces to specific carnivore taxa. This method provides a means to identify specific carnivore actors from their feeding traces, potentially enhancing our ecological reconstructions of Early Stone Age archaeological sites and understanding of hominin-carnivore interactions as they relate to early hominin diet and behavior.

ACKNOWLEDGEMENTS

Foremost I would like to thank my advisor Michael Pante for his guidance and help in this project and mentoring my development as a writer, researcher, and academic. I would like to thank my committee members, Jason LaBelle and Randall Boone for their help and encouragement throughout the many stages of my degree and project. I would like to thank Mica Glantz and Ann Magennis for their honest and always appreciated advice and encouragement over the last two years. I would also like to thank Robert Lee from the Zoology and Microbiology Department for his generous help with the logistical issues related to processing my sample and giving me permanent space to work in his lab during my project.

I would like to thank those who provided funding for the many components of my project and degree including Colorado State University Anthropology Department for not only funding my degree but also my conference travel, Kathy Schick and Nick Toth of the Stone Age Institute for facilitating my field work and professional development in Olduvai Gorge, Susan Omori and everyone at the Colorado Archaeology Society for funding my project and inviting me to present my research during their fall meetings.

This project was greatly improved by the generosity of researchers in my field allowing me to incorporate their published work into my thesis. I would like to thank Brianna Pobiner for her African lion sample, Robert Blumenshine for his spotted hyena sample, and Jackson Njau for his Nile crocodile sample. I would also like to thank Ignacio de la Torre for allowing me to incorporate archaeological traces from his excavations in Olduvai Gorge, Tanzania into my project.

I would like to thank everyone at the Denver Zoo for helping with the many stages of this project, even when my protocols and goals must have seemed alien to them. Without the

organization, care, and persistence of Sharon Joseph I don't think the collaboration with the Denver Zoo would have happened, and thanks to Matthew Lenyo and Steve Venne, the curators of carnivores at Denver Zoo, for rooting through the grass for whatever bone fragments the hyenas had left behind. I would also like to thank Abby Matzke, Michelle Proulx, and Robert Proulx from the Rist Canyon W.O.L.F Sanctuary for allowing me to include their wolves into this project but also for letting me interact and learn about the rescue and rehabilitation efforts needed for wolves in North America.

Lastly to my friends and family; for their support and motivation I would not be here today. To my parents, Arpi Panossian Muttart and Daved Muttart, whose guidance, love, and inexorable support are the foundation of every one of my successes. To my undergraduate advisor, Yin Lam, who has always offered encouragement and support throughout my academic career: I am indebted and fortunate. My friends and colleagues who have always been a source of motivation and support have been critical to my success and sanity in this pursuit, Kristen and Neil Porasz, for being my test audience for presentations and edits to get my work to where it is now, and especially to Trevor Keevil for all his help throughout this project and for making staying in the lab until dawn on too many occasions almost socially acceptable. And finally, to my partner Elizabeth, my greatest source of motivation and happiness, without her I would still be "writing"!

DEDICATION

For Camilo

TABLE OF CONTENTS

ABSTRACT.....	ii
ACKNOWLEDGEMENTS.....	iv
DEDICATION.....	vi
LIST OF TABLES.....	ix
LIST OF FIGURES.....	xi
CHAPTER 1 INTRODUCTION.....	1
1.1 Problem Statement.....	1
1.2 Zooarchaeological and Taphonomic Theory.....	3
1.3 Scope of Thesis and Sample Characteristics.....	6
1.4 Summary.....	7
CHAPTER 2 BACKGROUND & LITERATURE REVIEW.....	8
2.1 Hominin – Carnivore Interactions: Carcass Acquisition Sequences and Hominin Evolution.....	8
2.2 Biomechanical Analysis of Carnivore Feeding Morphology.....	12
2.2.1 Functional Appendicular Morphology.....	13
2.2.2 Paranasal Sinus Cavity.....	13
2.2.3 Tooth Size, Root Morphology & Breakage.....	15
2.2.4 Mandibular Force Profiles.....	16
2.3 Biomechanical Modeling of Extinct Carnivores.....	18
2.4 Previous Approaches for Carnivore Feeding Trace Identification and Distinction.....	21
2.4.1 Gnawing Patterns & Gross Bone Damage.....	22
2.4.2 Tooth Mark Frequency & Morphology.....	23
2.5 Review of High-Resolution 3D Methods in Archaeology and Taphonomy.....	24
2.5.1 Digital Microscopy.....	26
2.5.2 Digital Microphotogrammetry.....	29
2.5.3 Non-Contact Profilometer.....	30
2.6 Conclusion.....	31
CHAPTER 3 MATERIALS AND METHODS.....	39
3.1 Sample.....	39
3.2 Modern Sample: Naturalistic Observations of Wild Animals.....	42
3.2.1 Spotted Hyena, n=28 (from Blumenschine 1988).....	42
3.2.2 African Lion, n=28 (from Pobiner 2007).....	42
3.3 Modern Sample: Controlled Feeding Observations of Captive Animals.....	43
3.3.1 Nile Crocodile, n=48 (from Njau & Blumenschine 2006).....	43
3.3.2 Grey Wolf, n=29 (from Rist Canyon W.O.L.F Sanctuary).....	43
3.3.3 African Wild Dog, n=31; Spotted Hyena, n=30; Striped Hyena, n=30; African Lion, n=30; North American Brown Bear, n=28 (from Denver Zoo).....	43

3.4	Archaeological Sample	44
3.5	Preparation of Sample for Analysis	45
3.5.1	Bone collection	45
3.5.2	Cleaning	45
3.6	Profilometer – Scanning Procedure.....	46
3.6.1	Profilometer & Software.....	46
3.6.2	Scanning & Analysis Protocol	47
3.6.3	3D data processing.....	47
3.6.4	3D data measurement.....	48
3.6.5	Profile extraction.....	49
3.6.6	Profile measurement	50
3.7	Statistical Methods – Treatment of Results.....	51
CHAPTER 4	RESULTS	53
4.1	Testing the Applicability of Replicas.....	53
4.2	Comparison of Inter-Carnivore Samples.....	54
4.3	Analysis of Individual Measurement Metrics	57
4.4	Multivariate Linear Discriminate Analysis	71
4.4.1	Potential to Discriminate Between Actors	71
4.4.2	Comparisons Between Animal Pairs	79
4.4.3	Inferred fossil trace marks	80
CHAPTER 5	DISCUSSION.....	82
5.1	Interpretation of Results	83
5.1.1	Potential and Accuracy of Molding Materials	83
5.1.2	Sources of Variation between wild and captive animals	84
5.1.3	Potential to discriminated between actors.....	85
5.1.4	Inferred Fossil Trace Marks.....	92
5.2	Weaknesses, Limitations, & Future Work	93
CHAPTER 6	CONCLUSION	97
REFERENCES	99
APPENDIX A	– ALL MEASURED DATA FROM CAPTIVE AND WILD CARNIVORES	115
APPENDIX B	– ALL MEASURED DATA FOR MARKS INFERRED ON FOSSILS	125
APPENDIX C	– ALL MEASURED FROM TESTING THE ACCURACY OF REPLICAS ..	127

LIST OF TABLES

Table 1 – Summary of species included within this study.....	6
Table 2 - Detailed overview of high-resolution 3d scanning applications in archaeology.....	35
Table 3 - Summary of species and corresponding sample included within this study.	40
Table 4 - Characteristics of fossils included within this study..	41
Table 5 - Summary statistics of tooth marks between original and replica.	54
Table 6 - Summary statistics for tooth marks produced by wild and captive african lions.....	55
Table 7 - Summary statistics for tooth marks produced by wild and captive spotted hyenas	56
Table 8 - Summary statistics for tooth marks produced by spotted hyenas and striped hyenas...	57
Table 9 – Kruskal-wallis and mann-whitney U tests for surface area (3D) measurements between all carnivore species	59
Table 10 - Kruskal-wallis and mann-whitney U tests for volume (3D) measurements between all carnivore species tooth marks.....	60
Table 11 - Kruskal-wallis and mann-whitney U tests for maximum depth (3D) measurements between all carnivore tooth marks.....	61
Table 12 - kruskal-wallis and mann-whitney U tests for mean depth (3D) measurements between all carnivore species tooth marks.....	62
Table 13 – Kruskal-wallis and mann-whitney U tests for maximum length (3D) measurements between all carnivore species tooth marks.	63
Table 14 - Kruskal-wallis and mann-whitney U tests for maximum width (3D) measurements between all carnivore species tooth marks.....	64
Table 15 – Kruskal-wallis and mann-whitney U tests for maximum depth (profile) measurements between all carnivore species tooth marks.....	65
Table 16 - Kruskal-wallis and mann-whitney U tests for area (profile) measurements between all carnivore tooth marks.	66
Table 17 - Kruskal-wallis and mann-whitney U tests for width (profile) measurements between all carnivore tooth marks.	67
Table 18 - Kruskal-wallis and mann-whitney U tests for roughness (profile) measurements between all carnivore tooth marks.....	68
Table 19 - Kruskal-wallis and mann-whitney u tests for opening angle (profile) measurements between all carnivore tooth marks.....	69
Table 20 - Kruskal-wallis and mann-whitney u tests for floor radius (profile) measurements between all carnivore tooth marks.....	70
Table 21 - Summary and descriptions of all linear discriminant analyses.	71
Table 22 - Confusion matrix for linear discriminant analysis between all species.	72

Table 23 - Confusion matrix for linear discriminant analysis between all species at the family level.....	73
Table 24 - Confusion matrix for linear discriminant analysis between all african species..	74
Table 25 - Confusion matrix for linear discriminant analysis between all african species at the family level.	75
Table 26 - Confusion matrix for linear discriminant analysis between all species grouped biomechanically.	76
Table 27 - Confusion matrix for linear discriminant analysis between all african species grouped biomechanically.	77
Table 28 - Confusion matrix for linear discriminant analysis between reptilia and mammalia species classes.....	78
Table 29 - Species comparisons between every carnivore included in this study.	79
Table 30 – Classifications for fossil trace marks.	81

LIST OF FIGURES

Figure 1 - Two studiabiles from a single spotted hyena tooth mark.....	48
Figure 2 - Measurements taken during 3d analysis.	49
Figure 3 - Sample image of a crocodile tooth marked bone, extracted scanning surface, and cross-sectional profile taken across the deepest profile of the mark.	50
Figure 4 - Area of a hole from the profile extracted from the deepest profile.....	51
Figure 5 – Contour analysis showing opening angle and floor radius of the tooth mark with the remaining bone outside of the mark removed.....	51
Figure 6 - Principal component analysis between original and replica scans.....	53
Figure 7 – Box and whisker plots for surface area (3D) measurements between all carnivore species tooth marks.	59
Figure 8 - Box and whisker plots for volume (3D) measurements between all carnivore species tooth marks.....	60
Figure 9 - Box and whisker plots for maximum depth (3D) measurements between all carnivore species tooth marks.	61
Figure 10 - Box and whisker plots for mean depth (3D) measurements between all carnivore species tooth marks.	62
Figure 11 - Box and whisker plots for maximum length (3D) measurements between all carnivore species tooth marks.	63
Figure 12 - Box and whisker plots for maximum width (3D) measurements between all carnivore species tooth marks.	64
Figure 13 - box and whisker plots for maximum depth (profile) measurements between all carnivore species tooth marks.....	65
Figure 14 - box and whisker plots for area (profile) measurements between all carnivore species tooth marks.....	66
Figure 15 - Box and whisker plots for width (profile) measurements between all carnivore species tooth marks.	67
Figure 16 - Box and whisker plots for roughness (profile) measurements between all carnivore species tooth marks.	68
Figure 17 - Box and whisker plots for opening angle (profile) measurements between all carnivore species tooth marks.....	69
Figure 18 - Box and whisker plots for floor radius (profile) measurements between all carnivore species tooth marks.	70
Figure 19 - Graph showing results of linear discriminant analysis between all species as 95% confidence intervals.	72

Figure 20 - Graph showing results of linear discriminant analysis between all species at the family level as 95% confidence intervals.	73
Figure 21 - Graph showing results of linear discriminant analysis between all african species as 95% confidence intervals.	74
Figure 22 - Graph showing results of linear discriminant analysis between all african species at the family level as 95% confidence intervals.	75
Figure 23 - Graph showing results of linear discriminant analysis between all species grouped biomechanically as 95% confidence intervals.	76
Figure 24 - Graph showing results of linear discriminant analysis between all african species grouped biomechanically as 95% confidence intervals.	77
Figure 25 - Graph showing results of linear discriminant analysis between reptilia and mammalia species class as 95% confidence intervals.	78
Figure 26 - Graph showing results of limited discriminant analysis as convex hulls with fossil trace marks within the african family level discriminant analysis.	80
Figure 27 - Sample tooth marks of african lion and spotted hyena	88
Figure 28 – Sample tooth marks of spotted hyena and nile crocodile.	90
Figure 29 – Sample tooth marks of african wild dog and african lion.	91
Figure 30 – Sample tooth marks of north american brown bear and grey wolf	92

CHAPTER 1 INTRODUCTION

1.1 Problem Statement

Linking specific carnivore species to feeding traces found on fossil bones is critical to reconstructing the ecological and behavioral contexts of Early Stone Age archaeological sites. The Plio-Pleistocene boundary is marked by a drastic shift in hominin behavior and diet as hominins encroached on the larger carnivore guild by regularly consuming nutrient dense flesh and marrow from large mammal carcasses. This dietary shift is often considered as a catalyst towards increasing brain and body size in the genus *Homo* (Aiello & Wheeler 1995; Wood & Collard 1999; Ragir 2000; Stanford & Bunn 2001; Aiello & Wells 2002; Larsen 2003; Leonard et al. 2007; Anton & Snodgrass 2012). Faunal remains in the Pleistocene archaeological record sometimes bear dual-patterned bone with both tooth marks from carnivore feeding action and cut marks from hominin butchery action. However, understanding carcass acquisition sequences – if hominins accessed meat through hunting or scavenging from carnivore kills remains a long-standing debate (Binford 1981; Brain 1981; Bunn 1982; Domínguez-Rodrigo and Barba, 2006; Blumenschine et al. 2007; Domínguez-Rodrigo et al. 2010, 2011, 2012; McPherron et al. 2011; Pante et al. 2015; Parkinson et al. 2015; Thompson et al. 2015). Due to the paucity of carnivore remains in the archaeological record, we cannot determine the specific carnivore actor with which hominins were interacting and competing, limiting our inferences regarding hominin carcass acquisition strategies and sequences. Therefore, the precise and accurate characterization of carnivore feeding trace marks left on bone is critical to our understanding of hominin-carnivore interactions, the ecological context of archaeological sites, and behaviors related to the dietary shift that may have been crucial to hominin evolution.

Carnivore feeding traces found on bone provide an accurate resource to link causal agents and their behaviors to faunal assemblages. Actualistic carnivore feeding and butchery experiments indicate that tooth and cut mark morphology as well as frequency is directly related to the relative timing of hominin and carnivore access and flesh availability on carcasses (Blumenschine 1988; Blumenschine & Marean 1993; Capaldo 1998; Nascou & Morin 2014). Therefore, if specific carnivore actors can be identified by tooth marks left on bone, analysis utilizing known feeding behavior and ecological contexts can be used to infer flesh availability and timing of access for early hominins. The exact nature of hominin-carnivore interactions has important implications for early hominin subsistence strategies and evolution, shaping behavioral traits such as foraging patterns, habitat preference, and social behaviors (Hunt 1994; Ragir 2000; Larsen 2003; Dunbar & Shultz 2007).

Previous approaches seeking to link specific carnivore taxa to their feeding traces have been conducted by analyzing qualitative aspects of tooth mark morphology (Dominguez-Rodrigo 2001; Njau and Blumenschine 2006; Coard 2007), gnawing patterns (Haynes 1983; Pobiner & Blumenschine 2003; Burke 2013), and an assessment of a carnivore's ability to delete bone portions (Blumenschine & Marean 1993; Pobiner 2007; Yravedra et al. 2014). Previous quantitative attempts to link tooth mark morphology to specific carnivore taxa have only displayed a weak correlation between tooth mark size and carnivore body size (Delaney-Rivera 2009; Dominguez-Rodrigo and Piqueras 2003). These previous approaches have been unsuccessful due to the methodological constraints of qualitative or two-dimensional analysis, which measure length and width of tooth pits from digital photographs; however, the findings of these previous analyses highlight the potential of feeding traces to refine our knowledge of past hominin and carnivore interactions with improved methods.

The current project uses high-resolution 3D scanning to produce a more accurate and precise characterization of carnivore tooth mark morphology. Additionally, the methodological improvements including the quantitative approach utilized here, will allow archaeologists to more accurately discern specific carnivore agents from trace marks left in the archaeological record. The goals of this thesis, therefore, are twofold:

1. To determine if micromorphological variations in carnivore tooth mark morphology can be used to quantitatively discriminate between carnivore actors, and identify specific carnivore taxa by the feeding traces left on bone.
2. To apply the findings of this actualistic study to tooth-marked fossil bones from a Middle Bed II (1.7 mya) archaeological site in Olduvai Gorge, Tanzania in order to identify carnivores responsible for feeding traces on these archaeological remains.

Achieving these goals will allow archaeologists to better understand hominin-carnivore interactions, ecological contexts, and behaviors that led to these fossil bone accumulations.

1.2 Zooarchaeological and Taphonomic Theory

The theoretical concepts utilized in this thesis are uniformitarianism, actualism, analogy, and middle range research applied towards understanding unknown aspects of the past. Uniformitarianism grounds the methodology and validates the theoretical approaches of using modern analogs in actualistic studies. Uniformitarianism hypothesizes that natural processes are continuous, universal, and governed by natural laws allowing for past products to be attributed to analogous processes currently in operation (Gould 1965; Lyman 1994). The principles of

uniformitarianism allow for the application of actualistic studies and inferences regarding past behaviors through analogous processes currently in operation.

Middle range theory provides connections between the behaviors of modern causal agents and feeding traces seen in the present, with those in the fossil record allowing reliable application to the analysis of feeding traces found in the archaeological record (Binford 1981). For instance, tooth-marked bones are found in both archaeological and contemporary settings, and processes related to creating tooth marked bone (carnivore feeding), can be observed in the present as the responsible action for the final product; therefore, inferences can be made regarding similar processes being practiced in the past to create trace marks found in the archaeological record (Lyman 1994).

Actualistic approaches seek to connect present observable behaviors and their final products to archaeological remains in order to infer the taphonomic processes that led to their archaeological deposit (Rudwick 1976). Actualistic applications in paleoarchaeology are known as neotaphonomy, where naturalistic and experimental procedures are used to directly observe the relationship between cause and archaeological effect (Lyman 1994). Ultimately, actualistic studies can uncover equifinalities (different events, causes, or behaviors that produce the same result or effects) by establishing a distinct causal link between archaeological products through observation of modern processes and their products (Marean 1995).

Identification of appropriate resources or actors to be used in an actualistic approach is through relational analogy (Gifford-Gonzalez 1991). Gifford-Gonzalez (1991) established a nested model for identifying modern taphonomic processes and their causal relations to traces found in the archaeological record. The levels within this nested model are as follows:

1. Identify the trace on an archaeological product that has undergone a taphonomic process.
2. Identify the effector, material, or process that modified the archaeological product.
3. Identify the causal agent or physical processes responsible for the trace.
4. Determine the behavioral context.
5. Determine the ecological context.

The goal of this thesis is to link the trace (carnivore tooth mark) to the actor responsible (specific carnivore species). These goals are accomplished through a neotaphonomic approach utilizing controlled feeding experiments of wild and captive carnivores in order to define and observe the causal relationship between process and product, carnivore actor and feeding trace. Middle range theory advocates for an accurate means of identification through a scientific approach in order to further the science of archaeology, bringing scientific methods into archaeological research in lieu of inference, creating a rich body of actualistic research in its wake:

“What we are seeking through middle-range research are accurate means of identification... reliable cognitive devices... Rosetta stones that permit accurate conversion from observation on statics to statement about dynamics... to build a paradigmatic frame of reference for giving meaning to selected characteristics of the archaeological record through a theoretically grounded body of research.” Binford 1981:25

Neotaphonomic approaches utilizing middle range research have interpreted a wide-range of effectors and agents responsible for patterns found in the archaeological record such as post-depositional fluvial action (Pante & Blumenschine 2010), butchery traces (Blumenschine 1988; Selvaggio 1994), butchery trace mark morphology (Bello & Soligo 2008; Boschin & Crezzini 2012; Bello et al. 2016; Braun et al. 2016; Pante et al. 2017), lithic typology and wear (Lin et al.

2010; Caruana et al. 2014; Lemorini et al. 2014), and carnivore feeding traces (Njau & Blumenschine 2006; Delaney-Rivera et al. 2009; Pobiner 2007; Pobiner 2015; Pante et al. 2017); all of which have greatly improved our understanding of past hominin behaviors and evolutionary precursors. This thesis seeks to build upon this great body of actualistically-based research by furthering our understanding of carnivore tooth mark morphology by advancing the methods of linking carnivore to archaeological trace.

1.3 Scope of Thesis and Sample Characteristics

This thesis is comprised of two components. The first component is based upon actualistic feeding experiments to study the feeding traces and tooth mark morphology of eight mammalian carnivores and one crocodylian in both naturalistic and captive environments (Table 1). The second component of this thesis is the analysis and comparison of archaeological trace marks to the actualistically generated sample. The archaeological sample consists of 30 tooth marks found on faunal remains from a Middle Bed II site in Olduvai Gorge, Tanzania, dating to approximately 1.7 million years.

Table 1 – Summary of species included within this study.

Common Name	Scientific Name	Setting	Number of Individuals	Number of Tooth Marks
African Wild Dog	<i>Lycaon pictus</i>	Captive	4	31
Grey Wolf	<i>Canis Lupus</i>	Captive	1	29
Spotted Hyena	<i>Crocuta crocuta</i>	Wild	N/A	28
Spotted Hyena	<i>Crocuta crocuta</i>	Captive	3	30
Striped Hyena	<i>Hyaena hyaena</i>	Captive	2	30
African Lion	<i>Panthera leo</i>	Wild	N/A	28
African Lion	<i>Panthera leo</i>	Captive	4	30
Brown Bear	<i>Ursus arctos</i>	Captive	2	28
Nile Crocodile	<i>Crocodylus niloticus</i>	Captive	4	48
Total				282

1.4 Summary

This thesis seeks to build upon zooarchaeological and taphonomic bodies of research that seek to link specific actors to their fossil traces; specifically, to link carnivores to micromorphological variables in tooth mark morphology. The methodology applied in this thesis has been successfully proven to be accurate and precise between observers as well as capable of discerning carnivore tooth marks from stone tool cut marks with 97.5% accuracy (Pante et al. 2017). This method is further developed and the dataset is significantly increased within this thesis.

Chapter 2 provides an overview of biomechanical research of the carnivore feeding apparatus connected to maximum bite force and gross bone damage as it relates to identifying carnivores responsible for archaeological assemblages. Following this, previous approaches to identifying carnivores by their feeding traces is examined, leading to a review of high-resolution 3D scanning applications in the field of archaeology and taphonomy.

Chapter 3 provides a description of the methodological protocols used within this thesis: methods followed for both naturalistic and controlled feeding observations; post carnivore feeding collection, storage, and bone cleaning methods; the high-resolution 3D scanning protocol used; and lastly, the statistical method of analyses utilized in this study is defined.

Chapter 4 and 5 present the results from the actualistic experiments and an analysis of the archaeological trace marks against the actualistic sample. Chapter 6 summarizes the major findings of this thesis, and outlines future research I hope to undertake.

CHAPTER 2 BACKGROUND & LITERATURE REVIEW

The analysis of carnivore tooth marks can be used to infer carcass consumption sequences between distinct carnivores and hominins. The extent of damage and consumption inflicted by feeding carnivores corresponds to the amount of edible flesh and bone available to subsequent consumers of the carcass (Pobiner 2015). Members of the order Carnivora possess a wide-range of feeding behaviors and niches, each providing a variable amount of resources for scavenging hominins (Van Valkenburgh 1996; Van Valkenburgh & Molnar 2002; Pobiner 2007; Van Valkenburgh 2007; Pobiner 2015). Therefore, the specific carnivore species hominins were interacting with is directly related to resources availability and the overall diet breadth of hominins. Hominin dietary strategies must be analyzed alongside an ecological, behavioral, and taphonomic perspective of the greater carnivore guild in order to understand the effect of specific carnivores on spatially and temporally governed hominin behaviors related to their subsistence strategies.

This chapter will provide an overview of the biomechanical research of the carnivore feeding apparatus connected to maximum bite force and gross bone damage. Subsequently, previous approaches to identifying carnivores by their feeding traces are examined. Lastly, a review of the application of high-resolution 3D scanning and photogrammetry in the field of archaeology and taphonomy is provided.

2.1 Hominin – Carnivore Interactions: Carcass Acquisition Sequences and Hominin Evolution

The ecological dynamic between hominins and carnivores has impacted the evolutionary trajectory of the genus *Homo*. Understanding the ecological contexts and human-carnivore interactions as animal source foods were introduced into hominin diet are critical for

understanding the effects this diet change would have had on hominin brain and body morphology (Shipman & Walker 1989; Aiello & Wheeler 1995; Wood & Collard 1999; Stanford & Bunn 2001; Aiello & Wells 2002; Leonard et al. 2007; Anton & Snodgrass 2012), the driving forces behind hominin tool development and complexity (Harris & Capaldo 1993; Roche et al. 1999; Leigh 2012; Ruck 2014), the social organization and cultural complexity (Foley 2001; Dunbar & Shultz; Anton & Snodgrass 2012; Leigh 2012; Pradhan et al. 2012), and the overall ecological changes affecting hominin subsistence strategies (Clark & Kurashina 1979; Rogers et al. 1994; Potts 1998; Plummer et al. 1999; Ungar et al. 2006). Furthermore, the new dietary and behavioral practices of hominins such as opportunistic and power scavenging (Blumenschine & Cavallo 1992; Oliver 1994; Capaldo 1997; Bunn 2001; Pante et al. 2012), led to increased competition for resources, causing hominin induced changes to the carnivore guild (Agudo et al. 2010; Yirga et al. 2012), and increased risk of predation or injury from carnivores (Treves & Treves 1999; Njau & Blumenschine 2012; Moleon et al. 2014; Camaros et al. 2016).

The exact precursor towards inclusion of meat in early hominin diet remains unknown. Environmental and ecological contexts provide the most parsimonious explanation of the driving forces behind hominin diet change as the Pleistocene boundary is marked by increased seasonality (Ungar et al. 2006). The loss of stable resources such as fruits and tubers may have driven early hominins towards scavenging carcasses, a feeding strategy made easier by a loss of carnivore density and species richness, reducing competition at this time (Bunn & Ezzo 1993; Lewis 1996; Werdelin & Lewis 2005; Koch & Barnosky 2006). Resources such as tree-stored leopard kills and abandoned kills from larger felids would have provided substantial flesh in the same way these carnivores and their modern analogs still do today (Cavallo & Blumenschine 1989; Van Valkenburgh et al. 2002; Pobiner 2007; Van Valkenburgh 2007). However, the exact

strategies of early hominin carcass acquisition, as either obligate scavengers or hunters, remains as a long-standing and controversial debate (Binford 1981; Brain 1981; Bunn 1982; Domínguez-Rodrigo and Barba, 2006; Blumenschine et al. 2007; Domínguez-Rodrigo et al. 2010, 2011, 2012; McPherron et al. 2011; Pante et al. 2015; Parkinson et al. 2015; Thompson et al. 2015).

Analytical models aimed at deciphering the sequence of carcass access by hominins and carnivores include skeletal part profiles (Dart 1949; Binford 1981, 1984; Potts 1983; Blumenschine 1986; Bunn 1986; Bunn & Kroll 1986; Stiner 1991; Marean et al. 1992; Marean 1998; Marean & Kim 1998; Bartram & Marean 1999), mortality profiles (Vrba 1975, 1980; Klein 1982; Lyman 1987; Stiner 1990; Pickering 2002; Steele 2003) and cut mark frequency and location (Domínguez-Rodrigo et al. 1997; 2006; Lupo & O'Connell 2002; Pickering & Egeland 2006; Merritt 2015). These models provide a means to infer primary or secondary access to carcasses with a certain degree of accuracy, but taphonomic processes such as degree of carnivore modification, differential transport, and degree of preservation can alter assemblage representation and inferences (Binford 1981; Gifford 1981; Behrensmeyer 1991; Gifford-Gonzalez 1999; Denys 2002;).

Modern carnivores are not homogenous in their feeding behaviors and bone modification capabilities; identifying a carnivore's specific taphonomic trace is needed in order to better understand hominin-carnivore interactions related to hominin diet and subsistence. Approaches towards this goal include hypothesizing scales of flesh availability to secondary hominin actors (Blumenschine 1986, 1988; Turner 1992, 1998; Marean & Ehrhardt 1995; Arribas and Palmqvist 1999; Dominguez-Rodrigo 2001; Palmqvist et al. 2011; Nasau & Morin 2015; Pobiner 2015). Taphonomic analysis of specific carnivores have also been conducted to understand their feeding behaviors and the traces they would have left in the archaeological record; most studies have

focused on the most effective bone crunchers, the spotted hyenas (Haynes 1983; Binford et al. 1988; Blumenschine 1988; Cruz-Uribe 1991; Marean & Spencer 1991; Lam 1992; Marean et al. 1992; Blumenschine & Marean 1993; Capaldo & Blumenschine 1994; Selvaggio 1998; Capaldo 1998; Dominguez-Rodrigo 1999; Pickering 2002; Faith 2007; Pobiner 2007; Lansing et al. 2009; Dominguez-Rodrigo 2013; Arrizia 2017). However, other species that alter bone and leave archaeological traces such as felids (Haynes 1983; Cavallo & Blumenschine 1989; Dominguez-Rodrigo 1999; Pobiner & Blumenschine 2003; Pobiner 2007; Dominguez-Rodrigo & Pickering 2010; Gidna et al. 2013), canids (Haynes 1980, 1983; Fiorillo 1991; Monahan 1999; Yravedra et al. 2012), ursids (Haynes 1982, 1983), crocodylians (Njau & Blumenschine 2006; Baquedano et al. 2012), baboons (Dominguez-Rodrigo et al. 1998; Dominguez-Rodrigo et al. 1999), and chimpanzees (Pickering & Wallis 1997; Plummer & Stanford 2000; Tappen & Wrangham 2000) have also been studied individually.

Comparative analysis between carnivores and their taphonomic traces are largely based on tooth mark morphology and patterns of gross bone damage (Binford 1981; Selvaggio & Wilder 2001; Dominguez-Rodrigo & Piqueras 2003; Pobiner & Blumenschine 2003; Pickering et al. 2004; Delaney-Rivera et al. 2009; Pobiner 2015). These comparative analyses have observed a wide range of overlap between carnivore actors, thus providing only general guiding principles based on weak correlation between a carnivore's body size and tooth pit size. More recently, high resolution 3D scanning and micro-photogrammetric techniques have displayed the ability to differentiate between cut marks produced by different tool types (Bello & Soligo 2008; Boschine & Crezzini 2012; Mate-Gonzalez et al. 2015). This points towards the potential of this technology to distinguish between the tooth marks inflicted by different carnivore species.

2.2 Biomechanical Analysis of Carnivore Feeding Morphology

Biomechanical approaches, modeling cranial and appendicular morphology of extant carnivores can provide insights into extinct carnivore feeding behaviors. This is especially critical for smaller extinct carnivores, which exhibit biomechanical adaptations for extremely high bite force (Wroe et al. 2005) that do not coincide with the findings of tooth mark size correlation to carnivore body size and in turn could produce faulty references regarding flesh availability for scavenging hominins (Dominguez-Rodrigo & Piqueras 2003; Delaney-Rivera et al. 2009). Therefore, in order to better understand the ecology and energetics of hominin scavenging or hunting opportunities, two developments are needed.

1. Improve the quantitative methods employed in the analysis of individual carnivore tooth mark morphology.

2. Connect quantitative methods of tooth mark identification to a biomechanical understanding of a carnivore's cranial and appendicular feeding apparatus to model extinct carnivore trace marks.

This approach will provide a complementary framework to neotaphonomic findings, identifying feeding behaviors and traces of extinct carnivores unknowable through previous approaches. Ultimately guiding inferences regarding extinct carnivore feeding traces found on faunal remains in the archaeological record.

The order Carnivora occupies a wide-range of feeding niches that can be seen in the diversity of their cranial, dental, and appendicular form. These morphological variations are linked to the properties of foods ingested and masticated by these carnivores. A biomechanical approach investigating the relationship between niche specialization and morphological characteristics of extant carnivores could identify feeding niches and biodiversity of extinct

carnivores critical to the ecological reconstruction of Early Stone Age archaeological sites. This section will outline four distinct biomechanical characteristics of carnivore morphology and how they relate to feeding biology and impacts to analysis of the archaeological record.

2.2.1 Functional Appendicular Morphology

The forelimbs of predators are an essential mechanism for prey capture, killing and carcass transport (Van Valkenburgh 1985). Comparisons of forelimb length and robusticity within extant carnivore guilds highlights their relation to niche dynamics, and can be extrapolated to infer hunting behaviors and guild dynamics between extinct carnivores as well as anthropoids (Van Valkenburgh & Molnar 2002). Felids that hunt larger prey species have more robust forelimbs in comparison to smaller prey specialists such as servals which have longer and less robust forelimbs to facilitate speed (Meachen-Samuels & Van Valkenburgh 2009).

Functional shortening of limb bones in larger prey specialists facilitates the mechanical advantage needed to subdue and restrain prey before administering a killing bite (Meachen-Samuels & Van Valkenburgh 2009). In extant canids, forelimb robusticity increases to support body weight (Wayne 1986). Shortened distal limb bones and extreme robusticity seen in the extinct giant hyena *Pachycrocuta brevirostris* are believed to have developed to transport large carcasses back to dens (Palmqvist et al. 2011). Biomechanical analysis of the appendicular form provides a foundation to infer diet breadth, prey size preference, and carcass acquisition strategies.

2.2.2 Paranasal Sinus Cavity

The interior paranasal sinus cavity affects the configuration of the frontal bone, altering skull morphology as well as overall strength by dissipating stress more evenly, allowing for a higher bite force. All bone-cracking hyaenids have large and elongated frontal sinuses that

coincide with the domed arc needed to dissipate bite force stress (Curtis & Van Valkenburgh 2014; Tanner et al. 2008). These morphological characteristics are seen in correlation with prey size in other carnivores, indicating that these traits are directly linked to frontal bone vaulting to dissipate stress and facilitate higher bite force (Curtis & Van Valkenburgh 2014; Tseng and Wang 2010). There is a tradeoff in bite force and sinus shape, larger felids with stronger bite force for killing bites have relatively wide sinus cavities restricted to the frontal portion of the crania as they do not require the morphology to dissipate the higher post-canine bite force stress associated with bone cracking behavior (Slater & Van Valkenburgh 2009). Increasing bone volume in the skull by limiting sinus size allows for non-bone cracking carnivores to dissipate torsional loads needed to subdue, restrain, and shear their prey, whereas the larger sinus cavity in bone cracking carnivores allows for linear load dissipation needed for breaking bone and accessing within bone nutrients (Curtis & Van Valkenburgh 2014).

The strong correlation between sinus cavity shape and size is indicative of overall bite force as seen in Curtis and Van Valkenburgh's (2014) comparison between felids, canids, and hyaenids. These findings indicate maximums of feeding behavior related to prey size preferences and gross bone damage capabilities; however, carnivores display a wide-range of opportunistic feeding behaviors, leading to very diverse faunal assemblages (Lam 1992). Obligate scavengers do produce a more defined assemblage of fractured large ungulate bone, concentrating on marrow rich elements such as the tibia and femur, often leaving the bones of smaller prey or marrow depleted bones complete (Binford 1981; Palmqvist et al. 2011). A 3D volumetric analysis of extinct carnivores may further indicate their bone cracking abilities and effects that would have on the archaeological record. The relationship between sinus morphology and bite force indicates that species with larger sinus cavities would create larger tooth marks.

2.2.3 Tooth Size, Root Morphology & Breakage

One of the most distinct morphological and biomechanical traits associated with mammalian carnivores is their variable dentition, which has evolved to fit a wide range of ecological and feeding niches. Both tooth crown and tooth root morphology can be used to infer feeding behavior. Crown morphology is directly linked to different feeding biology such as killing bites, shearing of meat from bone, and bone crushing ability (Van Valkenburgh 1996). Analyzing the maximum stress exerted on a tooth crown before breakage threshold indicates bone crunching carnivores such as hyenas can withstand significantly higher stress compared to canids and felids; this is largely due to the buttressed mandible that facilitates stress distribution throughout the cranium (Tseng and Binder 2008). Overall changes to tooth shape and size can also differentiate between carnivorous and herbivorous ursids, where individuals with a carnivorous diet possess smaller molars and carnassial blades (Sacco & Van Valkenburgh 2004). Furthermore, prey size preference can be determined in felids by overall robusticity of canines; however, there is no link to bite force through this method. as the larger canines are weaker than smaller canines under certain torsional and linear stresses (Meachen-Samuels & Van Valkenburgh 2009). Tooth root morphology can also be used to infer bite force potential, where larger roots and robust mandibular symphysis indicate an individual's adaptation to processing harder foods (Kupczik & Stynder 2011).

Analysis of tooth and root size can trace the phylogeny of a species through their evolutionary history (Sacco & Van Valkenburgh 2004). Furthermore, prey size as well as ecological contexts of extinct carnivores can be inferred through analysis of craniodental morphology, where predators would have adapted tooth morphology to the characteristics of prey within their feeding niche (Meachen-Samuels & Van Valkenburgh 2008). Feeding behavior

and ecological reconstructions can also be inferred by the high frequencies of broken or fractured tooth crowns found in the archaeological record. For instance, a high amount of broken tooth crowns found at Rancho La Brea, California, belonging to *Canis Lupus*, indicate possible resource scarcity and this species' attempts to crack bone for marrow (Binder et al. 2002). When tooth root size is adjusted to relative skull size, *C. lupus* has similarly sized pre-carnassial tooth roots compared to hyenas, indicating their ability to process large ungulate bones (Van Valkenburgh 2009). Large tooth roots seen in *C. lupus* would also facilitate stress dissipation of the initial high loads associated with bone processing (Christiansen & Wroe 2007).

Tooth crown and tooth root morphology can be correlated to overall bite force and its relation to gross bone destruction and tooth mark morphology. The individual teeth of a carnivore are unlikely to provide much insight into tooth mark morphology. For example, the characteristic teeth of crocodylians leave behind distinct bisected pits; however, this diagnostic trait is only present on 10% of faunal remains (Njau & Blumenschine 2006). Predicted bite force from tooth crown and tooth root analysis is much more helpful to understand the maximum bite force of canines, a critical adaptation for head hunters (Van Valkenburgh 2009). Predicted bite force from tooth crown analysis can infer bone cracking abilities of extinct carnivores and how this ability would manifest in skeletal part profiles; however, the biomechanical characteristics of the mandible and cranial vault is much more diagnostic for bone cracking and gross bone damage abilities in carnivores.

2.2.4 Mandibular Force Profiles

Craniodental evolution via functional morphology directly influences a carnivore's feeding niches and success of a species. Biomechanical linkages to diet can differentiate hypercarnivore taxa to more generalist carnivores through predicted bite force analysis and

relative cranial morphology (Tseng & Flynn 2015). Biomechanical approaches to mandibular force profiles analyze interdental gaps (Therrien 2005), symphyseal shape related to load dissipation (Wroe 2007), muscle arm momentum (Cassini & Vizcaino 2012), beam analysis of flex and maximum bending stress of the mandible (Sacco & Van Valkenburgh 2004), and finite element analysis of stress distribution along cranial arcs and forehead vaults (Tanner et al. 2007). Species capable of high gross bone damage exhibit increased dorsoventral buttressing under the premolars and the post-carnassial molars. Furthermore, for the mandible to withstand the bending force exerted while cracking bone, the arc of stress needs to be dissipated through a vaulted forehead towards the sagittal crest; therefore, dense mandibular bone between the mandibular corpus and the articular condyle and elongated frontal and temporal bones are necessary and indicative of a carnivore's ability to withstand the stress of cracking bone (Tanner et al. 2007; Sacco & Van Valkenburgh 2004).

Mandibular force profiles and overall craniodental size can be used to infer diet breadth. Morphological comparison of extant carnivores to anthropoids display anthropoids were highly carnivorous with no indication of omnivory, suggesting a restricted dietary breadth or lack of resource diversity (Van Valkenburgh 2007). Furthermore, these characteristics are a large determinant of rank within a guild, and can therefore be related to feeding behaviors such as pack hunting or scavenging (Van Valkenburgh & Molnar 2002). These morphological distinctions also indicate inter-taxonomic variations as seen in studies between herbivorous and omnivorous ursids and can be used to infer diet breadth and bite force related to gross bone damage of extinct ursids (Sacco & Van Valkenburgh 2004). However, it is of note that herbivorous ursids such as *Ailuropoda melanoleuca* possess the strongest bite force of all ursids

indicating overall bite force is not reliable for omnivorous species and only indicate the ability to process dense foods (Kupczik & Stynder 2011).

When applied to extinct carnivore species such as the marsupial lion *Thylacoleo coarnifex*, it is clear this species' distinct cranial and dental morphologies related to bite force do not have a modern analog (Wroe 2008). Loading stress of the crania and mandible, analyzed from the bilateral bite force at the canines, bilateral bite force at the carnassial notch, and unilateral bite force at the carnassial notch indicate *T.coarnifex* possessed a bite force stronger than any felid or similarly sized carnivore as well as possessing the dorsoventrally buttressing and symphyseal shape needed to withstand the stresses related to cracking the bones of large ungulates (Wroe et al. 2005). Earlier inferences of the feeding behavior of *T.coarnifex* based on body size led to the belief it had a similar bite force and feeding niche as smaller felids such as the serval (Wroe et al. 2005). Body size is often used to correlate or infer tooth mark size (Dominguez-Rodrigo & Piqueras 2003; Delaney-Rivera 2009); however, the extreme bite force understood only through biomechanical analysis of *Thylacoleo coarnifex* indicates that this species would have been capable of extreme gross bone damage and left tooth marks larger than modern felids at a quarter of the body size (Wroe 2008).

2.3 Biomechanical Modeling of Extinct Carnivores

Over the past 60 million years there have been many successive clades of carnivores, many of which follow patterned and repeated ecological replacement within distinct feeding niches (Van Valkenburgh 2007). Hypercarnivores fulfill one of the most distinct feeding niches, hunting of prey significantly larger than themselves, but also exhibit the most evolutionary and ecological failures due to their large size and hunting behaviors (Werdelin & Lewis 2005; Van Valkenburgh et al. 2004). Hypercarnivores are characterized by their deep jaws relative to

overall size, large canines and incisors designed for strong killing bites and shearing meat, as well as minimal grinding surface area on molars (Van Valkenburgh & Koepfli 1993). The emergence of the hypercarnivore feeding niche is believed to have developed due to an energetic tradeoff, where hunting smaller prey became too costly relative to resources gained (Van Valkenburgh 2009). The evolutionary adaptation that drove larger body size to facilitate hunting larger animals, Cope's Rule, may have assisted the individual but it also facilitated the eventual failure of the clade in times of resource scarcity and ecological shifts (Van Valkenburgh et al. 2004). Pleistocene hypercarnivores would have provided abundant carrion for scavenging carnivores including hominins, similar to the ecological role modern felids serve today (Pobiner 2007; Van Valkenburgh et al. 2004).

The evolutionary incentive from a more specialized to generalized carnivore can be seen in the biomechanical adaptation of the giant hyena *Pachycrocuta brevirostris*. The overall height of *P.brevirostris* was not much larger than modern hyenas; however, its robusticity and greater size was facilitated by the shortening of the radius and tibia relative to the humerus and femur (Palmqvist et al. 2011). These adaptations facilitated the ability to carry larger carcasses over longer distances, a necessary trait for predominately scavenging carnivores. Additionally, larger post-canine teeth and robusticity of the mandible placed this hypercarnivore squarely within the scavenger niche. This is evidenced by the lack of forelimb motor function and lower bite force, relative to modern hyenas, seen in the incisors and canines, displaying a lack of adaptation for subduing a prey or administering a killing bite needed for hunting the large prey they subsisted on (Palmqvist et al. 2011).

The biomechanical understanding of *P.brevirostris*'s feeding niche (scavenging) and extinction coincides with saber-toothed cats such as *Megantereon whitei* (hunting) which would

have provided abundant carcasses to scavenge from, providing a clear indication of carcass acquisition sequence and behaviors that would have led to skeletal part profiles and fracture patterns seen in archaeological assemblages. This behavioral marker is in stark contrast to modern hyaenids who are seen to hunt upwards of 76% of the time in the Ngorongoro Crater (Honer et al. 2002).

The shift to a more generalized behavior seen in modern hyenas was likely brought on by the loss of hypercarnivores that provided readily accessible and abundant carcasses to scavenge (Van Valkenburgh 1999; Koch & Barnosky 2006). This can also be seen in the transition between *Homo habilis* and *Homo erectus*, towards a larger body size which is thought to have facilitated in longer ranging, increasing overall resource availability, as well as the ability to successfully ambush hunt smaller animals as scavengeable carcasses became less common place across the landscape (Hunt 1994; Ragir 2000 Lieberman et al. 2009). From this ecological and biomechanical understanding of the evolving carnivore guild we can infer *P.brevirostris* would have produced skeletal part profiles with heavy element deletion as well as tooth marks larger than modern hyenas. Research focused on saber-toothed cats is needed to understand their bone crunching ability related to gross bone damage and skeletal part profiles; based on their carnassial teeth and weakness towards bilateral force in their canines, researchers believe saber-toothed cats did not possess the cranial morphology or bite force necessary for bone cracking (Anyonge 1996; Biknevicius & Van Valkenburgh 1996; Van Valkenburgh et al. 1990). However, analysis of prey size preference and transport ability indicate sabre-toothed cats were effective at body part disarticulation and transport (Marean & Earhardt 1995; Arribas & Palmqvist 1999). These findings suggest hypercarnivores would have provided a moderate but viable and economic food source for scavenging hominins.

2.4 Previous Approaches for Carnivore Feeding Trace Identification and Distinction

Analyzing the biomechanical adaptations of carnivores provides evidence for maximum and minimum gross bone damage capabilities and how that would manifest in skeletal part profiles. These values can be determined through bone density analysis, the energetic value of skeletal parts, and the ecological contexts that have shaped the biomechanical characteristics of extant carnivores. The behavioral shift towards hunting in modern hyaenids and more generalist behavior such as facultative scavenging in felids and canids can be traced to the changing ecological contexts where populations of large prey needed for hypercarnivore subsistence decreased (Werdelin & Lewis 2005; Gibbard et al. 2010). However, this is problematic due to the highly variable feeding behaviors exhibited by carnivores, such as hunting versus scavenging frequency (Kruuk 1972), bone cracking performance (Sacco & Van Valkenburgh 2004), and prey choice (Lam 1991), which are not consistent across distinct and related carnivore populations. Furthermore, hypercarnivores outside of the hyena family that display the biomechanical ability to fracture bone for the extraction of marrow would have likely exploited this energetic resource if given the opportunity. However, the ability and behavior of bone cracking in hypercarnivores may have only been utilized at the later stages of their existence in times of resource scarcity or ecological shifts when carcasses could not be abandoned to scavengers (Van Valkenburgh et al. 1990). A modern analogue to this can be seen in captive carnivores who exploit resources to a greater degree and delete or fracture bones during fasting periods relative to periods of abundant food resources (Faith et al. 2007). Unfortunately, the majority of analyses of a carnivore's ability to damage bone have been either qualitative (Bunn 1983; Binford et al. 1988; Dominguez-Rodrigo 1999; Haynes 1982; Palmqvist & Arribas 2001),

anecdotal (Lam 1992, Dominguez-Rodrigo 1997, 1999), or inferential based on analysis of archaeological assemblages (Cruz-Uribe 1991; Pickering 2001).

2.4.1 Gnawing Patterns & Gross Bone Damage

The relationship between distinct carnivore taxa and maximum gross bone damage capabilities has been shown through a quantitative approach controlling prey body size (Bunn 1982; Pobiner & Blumenschine 2003; Pobiner 2007). However, these experiments were conducted with fully fleshed carcasses and model early-access predatory behavior rather than late-access scavenging behavior. The influence of prey body size on the level of skeletal damage is not well documented when carnivores are scavenging hominin refuse or vice versa beyond a single study of carcass acquisition sequences (Blumenschine 1988). Marean and Spencer (1991) suggest that prey body size is significant when elements have first been fractured by primary acting carnivores or hominins, as the small epiphyses of small prey are swallowed whole whereas large prey epiphyses are not. Therefore, the ratio of long bone epiphysis to shaft fragments in an archaeological assemblage may indicate levels of carnivore ravaging; however, this is likely to vary with prey body size, degree of competition, and resource scarcity (Marean & Spencer 1991; Blumenschine & Marean 1993). Understanding the biomechanical traits of a carnivore's maximum gross bone damage ability relative to prey size, alongside actualistic studies of modern carnivore gross bone damage can predict skeletal part profile patterns of analogous extinct carnivores. A higher predicted bite force ascertained from biomechanical interpretations can inform analysis of the possible ranges of bone damage extinct carnivores would have been capable of.

Incorporating an energetic and mechanical understanding of bone can assist in characterizing feeding behavior and amount of flesh available to secondary consumers. Bone

density analysis, related to an animal's size class is critical to understanding whether a carnivore would possess the ability to destroy certain bone elements (Lyman 1984; Marean 1991; Lam et al. 1999). A biomechanical approach alongside an understanding of bone density can inform analyses of minimum and maximum bone damage capabilities of distinct carnivores in order to rule out carnivore agents based on skeletal part profiles (Pobiner 2007). For instance, Pobiner (2007) found modern felids are shown to leave substantial flesh on size 3 & 4 carcasses but not on size 1 & 2 carcasses. These findings can guide analysis of skeletal part profiles to better infer actors feeding on larger size 3 & 4 prey but due to gross bone damage overlap and comparable bone deletion capabilities, determining carnivore actors which fed on smaller size 1 & 2 prey is not possible (Pobiner 2007). Ultimately, due to the wide overlap of carnivores with similar bite force related to gross bone damage, analyzing gnawing and damage patterns is not sufficiently accurate for taxonomic distinction.

2.4.2 Tooth Mark Frequency & Morphology

Analysis of individual tooth marks provides the most reliable resource for identifying traces to specific carnivore agent. The majority of tooth mark identification studies are qualitative or infer the identities of the carnivores responsible for archaeological assemblages by only analyzing archaeological remains rather than by demonstrating connections of actor to trace through actualistic studies (Collinson & Hooker 2000; Erickson & Olson 1996).

Tooth mark distribution and frequency have been used to infer carcass consumption sequences (Blumenschine & Marean 1993; Blumenschine 1995) and to infer specific carnivore taxa responsible for feeding traces (Egeland et al. 2004). These studies are applicable to certain carnivores such as hyaenids who leave relatively high proportions of tooth marked shafts to epiphyses compared with smaller carnivores such as leopards or jackals that leave very few

traces on bone shafts (Pobiner 2007). However, tooth mark distribution and frequency are largely unreliable methods to infer which specific carnivore taxa were responsible for skeletal part profiles or feeding traces as there is considerable overlap of tooth mark frequencies between taxa (Pobiner 2007).

Previous approaches measuring length and width of tooth pits from 2D digital images displayed trends between carnivores but no statistical distinguishability. A weak correlation between carnivore body size and tooth mark size was observed (Dominguez-Rodrigo & Piqueras 2003; Delaney et al. 2009). Tooth mark size and morphology provides a means to differentiate between the larger and smaller carnivores responsible for these traces, however, as mentioned above, the large overlap between tooth mark morphology analyzed through current 2-dimensional methods is insufficient for taxonomic classification.

A biomechanical approach can assist with inferences related between overall bite force and tooth mark morphology where carnivores with stronger bite force would leave behind larger tooth marks. Unfortunately, a solely biomechanical approach fails to address the confounding factor of tooth mark morphology overlap correlated to body size. Knowledge of the biomechanical capabilities of extinct carnivores can assist in inferring possible actor to skeletal part profiles or tooth marks found in the archaeological record especially in outlier cases as seen with *T. coarnifex*. However, a more quantitative method is required to accurately identify tooth mark morphology to distinct carnivore taxa.

2.5 Review of High-Resolution 3D Methods in Archaeology and Taphonomy

High-resolution 3D scanning and photogrammetric methods have found a wide range of applications in biological and archaeological sciences. These 3D scanning technologies have the ability to revolutionize methods of analysis and to improve the accuracy of inferences made from

archaeological remains. Previous methods of analysis were limited in quantitative metrics and relied primarily on qualitative descriptors. For instance, identification of taphonomic traces found on bone from hominin butchery or carnivore feeding action have largely been conducted through qualitative descriptors of overall trace mark morphology (Behrensmeier et al. 1986; Binford 1981; Blumenschine 1995; Blumenschine et al. 1996; Bunn 1981; Lyman 1996; Potts and Shipman 1981), which has led to long-standing debates regarding methodological accuracy and causal links of trace marks (Blumenschine et al. 1996; Dominguez-Rodrigo et al. 2010; Thompson et al. 2015). Similarly, biomechanical analyses relying on osteometric comparisons have been limited by qualitative assessment as well as varying protocols, leading to problematic conclusions that could not be replicated (Sholts et al. 2010). High-resolution 3D methods provide quantitative and standardized protocols between researchers, strengthening the accuracy of our interpretations of the past.

Due to the methodological limitations of qualitative data, researchers have turned to high-resolution 3D scanning and photogrammetric methods that can quantify morphometrics not observable or recordable through traditional methods. Optic microscopy provided the first quantitative method of analysis for micro-morphological traces (Dominguez-Rodrigo & Pickering 2003; Ungar 2004). The development of scanning electron microscopy (SEM) and digital imaging techniques provided two-dimensional images that were able to be analyzed three-dimensionally. However, drawbacks of SEM such as high cost, the time needed to setup and take each photo, the possible damage to materials, the limitations of the hardware itself (only able to process small objects), and its overall lack of accuracy, limited widespread use of SEM technology (Schroettner et al. 2006). Furthermore, both of these methods were not explicitly quantitative and relied upon qualitative descriptors of trace mark morphologies. Advances in

high-resolution 3D technologies have produced a wide-range of accessible hardware, eliminating the majority of the difficulties associated with SEM. These technological advances provide researchers with a rapid means of analyzing data; an entire cranium can be scanned in 10-15 minutes following the protocol established by Sholts et al. (2010) and high resolution scans of materials such as cut marks left on bone surfaces can be scanned with up to 40 nm accuracy in under an hour (Pante et al. 2017).

High-resolution 3D scanning and photogrammetric methods have a wide-range of applications in archaeology such as: biomechanical analysis of cranial morphology for the purpose of taxonomic distinction and adaptive radiation lineages, lithic analysis for the purpose of morphological and typological distinction as well as use wear patterns, dental morphology and wear analysis for the purpose of evolutionary distinctions and dietary analysis, and taphonomic analysis of cut and tooth marks left on bone in order to discern specific actors present (a detailed synopsis of these applications can be seen at the end of the chapter in Table 2).

This review section is concerned with high-resolution 3D scanning and photogrammetric methods as applied to the taphonomic analysis of stone and metal tool cut marks and carnivore tooth marks left on bone in order to discern specific effector and actor.

2.5.1 Digital Microscopy

The first proposals for high-resolution quantitative analysis of trace marks found in the archaeological record utilized SEM analysis (Potts & Shipman 1981). However, due to the limitations of the technology it did not see widespread use and qualitative approaches such as blind-testing for the degree of correspondence between analysts was relied upon (Blumenshine et al. 1996).

Bello and Soligo (2008) introduced a new method to quantify and analyze cut marks left on bone. Cut marks were experimentally produced using a metal knife and a flint flake on freshly butchered ribs of domestic pigs. Three angles of incision were used at approximately 25°, 45°, and 90° to the bone surface in order to provide a range of cut mark morphologies. Scans of the entire marks, ranging from 9.5 to 13.5 mm were taken, seven perpendicular profiles of the marks were used for analysis which were taken at 0.5 mm intervals along the mark and analyzed individually. Bello and Soligo (2008) introduced measurement parameters for their analysis which had been unattainable with previous methods: slope angles, opening angle, bisector angle, shoulder height, floor radius, and depth of cut. Only two of the six parameters displayed a statistical difference between tool types (slope and floor radius). Nevertheless, this paper set the foundation for future quantitative micromorphological analyses.

The novel method proposed by Bello and Soligo (2008) was then adapted to almost a dozen experimental and archaeological datasets (Table 2). Bello et al. (2009) analyzed cut marks found at a 0.5 million-year-old Acheulean butchery site (Boxgrove, England) against experimental butchery marks made by a replica handaxe. Scanning resolution was lowered to 4 µm vertically and laterally from 0.2µm, the resolution used in Bello and Soligo (2008), in order to cut down scan times without a tangible loss in scan quality. Additionally, the seven profiles taken at 0.5mm intervals were dropped in lieu of only analyzing the central profile. Cut marks observed from the experimental butchery created more acute opening angles, and smaller floor radii and were generally shallower. Bello et al. (2009) speculated these differences could be due to the experimental handaxes being sharper, and not as dulled from repeated use, or from a lack of control of force in the experimentally created marks. Bello et al. (2009) concluded that the

robusticity of *Homo heidelbergensis* may have factored into the greater force indicated by the larger marks, displaying the need to control force in actualistic models.

Further work analyzed Gough's Cave, a later Upper Palaeolithic site, with cut marked human remains that had led previous researches to believe that these marks indicated cannibalistic behavior (Bello 2011). Bello (2011) compared the Boxgrove data from Bello et al. (2009) as well as cut marks found on faunal remains in the site to show that much more force would have been needed to produce the cut marks seen at Gough's Cave. The comparison of these micromorphological characteristics led Bello (2011) to conclude that the larger floor radius and opening angles were due to the human bodies being stiffer in rigor mortis and the tools used becoming dull by the high amount of force needed for ritual defleshing. Bello (2001) therefore concluded that these traces were not indicative of cannibalism as previously thought but rather a product of ritual burial practices.

Boschin and Crezzini (2012) built upon previous work by increasing the number of stone and metal tool types analyzed. Twenty marks were created for each tool type (Copper blade, bronze blade, steel blade, flint flake, and a retouched flint flake) used during actualistic butcheries of cattle metapodials. Additionally, to test the comparative value of these experiments, 34 cut marks found on pigs from the Iron Age settlement of Trebbio, Italy were tested alongside their actualistic sample. Measurement metrics outlined in Bello and Soligo (2008) were used, excluding bisector angles due to the angle of the tool not being held constant during butchery. Additionally, breadth at the floor and opening of the mark was measured. A principal component analysis of all metrics displayed 83% accuracy in determining tool type of experimental marks and 59% accuracy of fossil cut marks.

More recently, Bello et al. (2016) analyzed three Serbian sites with human cut marked bone against the Gough's Cave human cut marked bone. Measurement metrics analyzed were breadth at floor and opening of the mark adapted from Boschini and Crezzini (2012), opening angle of the mark, and depth of the mark adapted from Bello et al. (2008). Marks were analyzed from human bones as well as non-human bones found at the sites. Bello et al. (2016) characterized two distinct types of marks found on human bones, marks made from disarticulation, and marks made from filleting which were likely due to the processing being conducted after bodies had decayed for a certain amount of time.

2.5.2 Digital Microphotogrammetry

High-resolution digital microphotogrammetry methods have shown very interesting and positive results in the analysis of cut and tooth mark morphology. Digital microphotogrammetry captures a high volume of photographs of trace marks from multiple angles in order to produce high-resolution 3D model of the trace marks. This methodology provides a low cost and rapid method of capturing and characterizing the morphology of trace marks.

Mate-Gonzalez et al. (2015) developed a method and protocol for the analysis of cut marks. Measurement metrics that are capable of being analyzed via digital microphotogrammetry include width of the incision surface, width of the incision mean, width of the incision at the bottom, opening angle, depth, and angle of the tool impact. This method was applied to the analysis of flint, copper, and quartzite cutting tools and could differentiate between these tools with roughly 70% accuracy according to their multivariate analysis (Mate-Gonzalez et al. 2016).

This method has since been applied to the analysis of carnivore tooth mark morphology, in the only high-resolution 3D assessment of carnivore feeding traces other than this thesis (Arriaza et al. 2017). Arriaza et al. (2017) analyzed tooth marks created from naturalistic feeding

experiments of spotted hyena and African lion. Arriaza et al. (2017) report the ability to differentiate between these carnivore actors, following their methodology, with 76% accuracy.

2.5.3 Non-Contact Profilometer

The precision of the methods listed above have yet to be demonstrated or replicated. In the initial pilot study, Bello and Soligo (2008) reported only mean errors between observers (17.2%). However, a large portion of the protocol established in that paper has now been dropped in lieu of qualitative descriptors, leaving readers without a standardized and precise method to replicate these studies.

Pante et al. (2017) provide a completely quantitative method to distinguish cut and tooth marks as well as a detailed and standardized protocol that was tested against inter-observer error prior to its application of fossil remains. Twelve cut marks and ten tooth marks were scanned and analyzed separately by three observers to test the precision of Pante et al.'s (2017) method. Profiles for analysis were extracted from the center and deepest point of the marks. Results displayed errors as low as 4.7% for maximum length and up to 35.9% for radius of the mark. Additionally, comparisons of central profiles were statistically different between observers, and therefore removed from analysis. Comparisons of profiles from the deepest point of the mark were statistically indistinguishable and recommended as the only profile to be measured due to the ability to accurately replicate this profile location. For this reason, it is important to note that the entirety of high-resolution 3D analysis of taphonomic traces prior to Pante et al. (2017) has only analyzed the less accurate and replicable central or interval profiles of trace marks. Furthermore, profile measurements vary in their values drastically throughout the tooth mark and interval profiles may not be relevant or representative of trends in tooth mark morphology.

Limiting profile analysis to the deepest profile provides a constant and comparable and replicable profile for accuracy and precise comparison between trace marks.

High-resolution 3D scanning techniques provide researchers with the ability to analyze micromorphological characteristics of individual profiles of marks. However, no research prior to Pante et al. (2017) analyzed the entire 3D area of these trace marks. Analyzing the entirety of these marks through metrics such as surface area, volume, maximum depth, mean depth, maximum length, and maximum width can further develop comparative measurement metrics and produce more informative analysis. If software limits the use of the 3D analysis of entire mark morphologies, ArcGIS as described by Caruana et al. (2014) can be used for similar analytical strength. It is through this high-resolution 3D scanning method that the analysis of carnivore tooth marks was conducted in this thesis; providing, for the first time, a quantitative characterization of 3D features in carnivore tooth marks.

2.6 Conclusion

A biomechanical approach to carnivore feeding traces displays the wide-range of behaviors and niches present among taxa during the Pleistocene that are not seen in extant carnivores (Lewis 1996; Van Valkenburgh & Molnar 2002). The most critical biomechanical finding is the presence of bone cracking ability in many carnivores outside of the hyena family. Carnivores such as ursids (Haynes 1980; Sacco & Van Valkenburgh 2004), felids (Therrien 2005), canids (Wroe et al. 2005), crocodylians (Njau & Blumenschine 2006), and certain marsupials (Attard et al. 2011) were capable of maximum gross bone damage similar to hyaenids. Gross bone damage, tooth mark frequency, and tooth mark morphology can be used to infer ecological contexts as well as the degree of competition and resource abundance

(Blumenschine & Marean 1993). However, as a marker for identifying the individual taxa responsible for archaeological assemblages these methods are insufficient.

The analysis of tooth marks has been used to infer carnivore presence and action, as well as to ascertain carcass consumption sequences between distinct carnivore agents and hominins. Through middle range research tooth mark and gross bone damage analysis has been used to infer how known and observable carnivore behaviors create distinct faunal assemblages and traces. To date, the use of tooth marks to identify specific carnivore taxa has only shown a weak correlation between body size and tooth mark size (Dominguez-Rodrigo & Piqueras 2003; Delaney-Rivera 2009). Specific carnivore actors such as crocodiles possess unique tooth morphology and can be identified by their distinct bisected pits; however, these distinct traces are not consistently present on faunal remains providing a low degree of identification (Njau & Blumenschine 2006). Furthermore, the qualitative nature and limited quantitative methodologies of tooth mark identification has led to long standing debates regarding trace mark identification (Selvaggio & Wilder 2001; Dominguez & Piqueras 2003; Pobiner & Blumenschine 2003).

Binford's (1981) argument for middle range research can be credited for the drive and eagerness to develop quantitative and replicable methods with high-resolution 3D scanning photogrammetry to answer archaeological questions. However, a significant number of the case studies reviewed lack a clearly standardized and tested protocol. The first step in establishing a new methodology should be to test the accuracy and precision of the method against control samples and previous methods. Recently, Molina and Heras (2015) have stressed the implications of the high inter-observer errors produced in their study, making the dearth of inter-observer protocol studies in the field of dental morphology problematic. Sholts et al. (2010) provided a foundational protocol, initially tested for inter-observer error with a small known

sample, which then went to guide subsequent research. Lithic typology and wear studies have developed numerous distinct protocols and methods which may in turn lead to discrepancies and disagreements when datasets or 3D models are compared in future works, something quantitative research typically aims to avoid. Karasik and Smilansky (2008) utilized CLSM in order to create 3D models for reconstruction and typological comparison, their initial research endeavor was to establish a means to efficiently scan their materials as well as clearly provide a replicable methodology for future researchers to build upon. Similarly, Pante et al. (2017) have provided a protocol and baseline for future taphonomic research.

Sample sizes between research projects were highly variable, with many insufficient for sound statistical analysis (Table 2). Additionally, inappropriate use of fossil samples for comparison without established actualistic samples is widespread. For example, Stemp et al. (2010) compared four experimentally created flint flakes, two of which were used intensively on conch shells and two on dry antler in order to quantify use wear. A sample of 2 for each variable is not sufficient, nor can “intensive use” be quantified for comparison or replication in future research. Sample sizes can also easily be falsely inflated by utilizing multiple profiles of a single mark or inter-landmarks (Bello et al. 2011; Bello et al. 2013; Bocaege et al. 2010; Friess 2010; Guy et al. 2013; Molina & Heras 2015; Stemp et al. 2010); this practice would produce unreliable interpretations or inferences of archaeological remains.

3D scanning techniques provide quantitative metrics to further strengthen the analysis of archaeological remains. Standardizing protocols provides a means for researchers to collaborate and compare replicable datasets, greatly increasing the accuracy of inferences and our understanding of the past. The full potential of these methods will take years to realize and conducting analysis without standardized protocols or control samples has the possibility of

diminishing the reputation and hence the application of high-resolution 3D scanning and photogrammetry. Despite the benefits discussed within this review, 3D scanning methods should not be used solely in research and analysis; a more holistic approach utilizing traditional methods in tandem with 3D scanning will provide stronger inferential power.

Through the biomechanical analysis of extant carnivores, specific feeding behaviors such as prey size preference, hunting adaptation, and bite force of extinct carnivores can be inferred. The inferential power of biomechanics falls short of being able to link specific carnivore taxa to carnivore feeding traces found in the archaeological record; however, it provides a baseline for inferring characteristic traces such as gross bone damage, overall tooth mark size, and ecological contexts of extinct carnivores. An integrated approach combining actualistic studies of modern carnivore feeding behavior, a biomechanical understanding of the carnivore feeding apparatus, and a quantitative method to assess tooth mark morphology will provide the most holistic and accurate means to identify specific carnivore taxa to the trace marks left in the archaeological record. This will provide novel interpretations of the past that were previously unattainable.

Table 2 - Detailed overview of high-resolution 3D scanning applications in archaeology.

Topic	Device & Software	Lens & Resolution	Sample Type & Size	Description	Results	Reference
Biomechanics and Craniometrics	Micro scribe 3D digitizer (Immersion Corporation). No software specified.	N/A	17 male & 17 female crania from each species: <i>G. gorilla</i> , <i>P. paniscus</i> , <i>P. troglodytes</i> , <i>H. Sapiens</i> (native Israeli), 13 casts of <i>H. erectus</i> from Asia, Europe, and Africa. (N=170)	6 landmarks of the mandibular fossa were measured for inter and intra-level comparisons of each species.	Statistical separation between each species. Statistical separation between geographically distinct <i>H. erectus</i> species. Correlation between African <i>H. erectus</i> and modern <i>H. Sapiens</i> .	Barash 2015
Biomechanics and Craniometrics	Breuckmann Smartscan Stereo (www.Breuckmann.com). No software specified.	Optical Resolution of 0.26mm	3 crania each species: <i>H. erectus</i> , <i>H. neanderthalensis</i> , <i>H. heidelbergensis</i> , <i>H. sapiens</i> , 1 <i>H. rhodesiensis</i> . (N=13)	24 craniometric landmarks generated 580 semi landmark measurements in order to assess calvarial shape variation and changes in ancestral lineage.	Statistical distinctions between each species. No morphological link between <i>H. rhodesiensis</i> and <i>H.sapiens</i> , should be lumped with <i>H. erectus</i> .	Friess 2010
Biomechanics and Craniometrics	NextEngine Desktop 3D Scanner model 2020i. NextEngine ScanStudio HD software.	Optical Resolution of 0.127mm.	19th-20th century US males and females of black and white ancestries from the Terry Collection (Smithsonian Museum). 30 Black females, 33 Black males, 26 White females, 30 White males. (N=119)	13 linear distances measured between 7 cranial landmarks (Following Sholts et al. 2010) on browridges and mandibles in order to quantify discrete traits related to sexual dimorphism.	A linear discriminate function was able to discern ancestry with 87% accuracy and sex with 79% accuracy analyzing browridges. Mandible error values much higher.	Garvin & Ruff 2012
Biomechanics and Craniometrics	FastSCAN Cobra (Polheus Inc). No software specified.	N/A	30 unidentified crania. (N=30)	26 line distance measurements from the lambda as well as seven breadth parameters were taken. Two examiners scanned each crania twice in order to test 3D laser scanning measurement accuracy to conventional methods.	There was no statistical difference between 3D scanning measurements or measurements taken through conventional methods.	Park et al. 2006
Biomechanics and Craniometrics	NextEngine Desktop 3D Scanner. NextEngine ScanStudio HD software.	N/A	5 modern human crania. (N=5)	Establishing a protocol for cranial measurements using 3D laser scanning techniques and testing the accuracy between observers.	Errors between observer models produced no more than 0.3% error for surface area and 0.2% for volume.	Sholts et al. 2010
Biomechanics and Craniometrics	NextEngine Desktop 3D Scanner. NextEngine ScanStudio HD software.	N/A	30 crania from 3 modern human population: Norwegian, Chinese, and Native Californian. (N=90)	13 linear distances measured between 7 cranial landmarks was used to identify ancestral group affinity between crania.	This method was able to correctly differentiate population with 87-90% accuracy.	Sholts et al. 2011
Lithic Typology and Wear	Alicona Infinite Focus microscope. MeX software.	2.5x objective lens, 10µm vertical and lateral resolution	An experimental knapping hammer made from whitetail deer antler. (N=1)	Quantitatively characterize use-damage of knapping tools used to manufacture stone tools.	Displaying microscopic features diagnostic to knapping behaviour. However, no further comparative work was done.	Bello et al. 2013

Table 2 – Continued

Lithic Typology and Wear	smartSCAN3D-HE, Breuckmann GmbH. OPTOCAD software.	Lateral resolution of 40 μ m and 2 μ m for vertical	150 cores and 250 blades randomly selected from the Yabroud II site, Syria from five stratigraphic layers. (N=400)	Presenting a method to quantify new metrics displaying morphological variations between distinct stone tool technologies and cultures.	Using quantitative metrics such as longitude and transversal convexity, morphological differences can be seen between certain stratigraphic layers.	Bretzke & Conard 2012
Lithic Typology and Wear	NextEngine Desktop 3D Scanner. ArcGIS 10.2 software.	N/A	19 archaeological, 20 experimental, and 11 naturally pitted cobbles. (N=40)	Developing a protocol to quantify anthropogenically-generated damage patterns on percussive tools from naturally damaged river cobbles.	Spatial autocorrelation analysis found naturally damaged cobbles have percussion marks with more depth and internal surface roughness than cobbles used as tools.	Caruana et al. 2014
Lithic Typology and Wear	Microscribe-3DX. Inscribe32 Software.	N/A	Scar patterns on 55 cores. (N=55)	Developing a mathematical formula for describing scar patterning seen in high-resolution 3-D scans in order to identify core preparation and reduction methods.	Mean scar pattern angle displays a consistent progression (increased angle) from blade cores to polyhedrons. Levallois cores display a normal distribution, whereas Acheulian handaxes possess random scar patterns.	Clarkson et al. 2006
Lithic Typology and Wear	Polygon Technology (Specific model not specified). QTS sculptor software.	N/A	90 Acheulian handaxes from three Lower Paleolithic sites in Israel. Umm Qatafa (26), Ma'ayan Barukh (39), Nahal Zihor (25). (N=90)	Developing new metrics to document and determine typology of lithic artifacts. (Center of mass position, volume, surface area).	New metrics support temporal separation of tool cultures, Accuracy with 3D scanning was significantly higher than standard methods such as length values which saw extremes of 48% measurement error and 1.4% interobserver error with 3D scanning.	Grossman et al. 2008
Lithic Typology and Wear	Konica Minolta Sensing Vivid 190 3D Digitizer. Geomagic Studio 9.0 Software.	N/A	30 experimentally created cores (N=30)	Improving methods of measuring cortex in order to better assess artifact transportation and assemblage formation.	Quantifying cortex volume with 3D scanning provides more accurate cortex ratio values than ordinarily estimated values (1.98-7.96%).	Lin et al. 2010
Lithic Typology and Wear	UBM laser profilometer	N/A	Four experimentally created flint flakes, intensively used for 20mins on either conch shells or dry deer antler. (N=4)	Testing whether the surface roughness measured on experimentally worn stone tools used on different materials can be discriminated.	Length-scale fractal analysis and overall roughness can be used to identify distinct use-wear patterns associated with different materials (shell and antler).	Stemp et al. 2010
Dental Morphology	Alicona Infinite Focus microscope. MeX software.	20x lens. 0.4 μ m lateral and 0.01 μ m vertical resolution	Three teeth from a juvenile from a Medieval cemetery sample from Abingdon, Oxfordshire. 1 lower central incisor, 1 upper central incisor, and 1 upper lateral incisor. (N=3)	Testing a 3-D technique to reconstruct dental growth profiles by analyzing the number and spacing of perikymata markings on enamel surfaces.	Individual perikymata grooves can be unambiguously identified and isolated with method, allowing for direct distances from successive pairs to be measured. This method can quantify perikymata spacing allowing for confident age estimates of individuals.	Bocage et al. 2010
Dental Morphology	μ m-CT VISCOM X8050. Avizo 7.0 Software	N/A	Molars from 2 Gibbons, 4 Gorillas, 3 Chimpanzees, 4 modern humans, 6 Cercopithecoids, and 1 South American monkey (<i>Lagothrix</i>). (N=20)	Establishing a quantitative method for comparing enamel and enamel-dentine junction surfaces.	Quantifying dental topography displays an overlap in variables but statistical trends such as Occlusal enamel thickness for the purpose of taxonomic identification from dental topography. Expansion of sample size may provide stronger statistical significance.	Guy et al. 2013

Table 2 – Continued

Dental Morphology	Device not specified. Match 3D V1.6 Software.	N/A	Twelve patients were given full dentures. (N=12)	To compare the use of different variables to measure clinical wear of denture tooth materials.	Multiwear studies should only concentrate on specific parameters, high interobserver error was recorded, protocols need to be established to keep error levels manageable or wear measurements obtained from other centers cannot be compared.	Molina & Heras 2015
Dental Morphology	Identica Structured Light 3D Scanner. Software not specified.	N/A	Dental casts from 160 Greek subjects (80 males, 80 females) from the records of the Department of Orthodontics of the University of Athens.	To evaluate shape variation, allometry, and sexually dimorphic differences between male and female maxillary and mandibular first permanent molar occlusal surfaces.	No shape dimorphism was observed, molars of males were marginally larger than females (3.2%). Upper and lower molar sizes were significantly correlated ($r^2=0.689$) owing to efficient masticatory function.	Polychronis et al. 2013
Tooth and Cut Mark Morphology	Alicona Infinite Focus microscope. Infinite Focus IFM 2.0 software.	10x lens. 0.2 μ m vertical resolution and 0.8 μ m lateral resolution	3 cut marks made with a modern metal knife, 3 cut marks made with a flint flake. 7 profiles from each cut mark were analyzed. (N=6)	To test the applicability of 3D scanning to quantifying cut mark morphology to improve identification and information regarding butchery behaviour with new measurement metrics.	This method provides additional measurement metrics unattainable with previous methods. New measurement metrics (Table 3) were able to distinguish tool type.	Bello & Soligo 2008
Tooth and Cut Mark Morphology	Alicona Infinite Focus microscope. MeX software.	5x lens. Vertical and lateral resolution of 4 μ m.	44 cut marks found on faunal fossil remains. 76 cut marks from experimental butchery. (N=120)	To infer lower Paleolithic hominin butchery techniques, identification of tool type by cut marks left on bone.	Statistical difference in cut mark morphology between experimental and fossil assemblage, likely due to the greater robusticity and force applied by <i>Homo heidelbergensis</i> .	Bello et al. 2009
Tooth and Cut Mark Morphology	Alicona Infinite Focus microscope. MeX software.	5x lens. Vertical and lateral resolution of 1.75 μ m.	Case Study 1: 27 cut marked human bone, 16 cut marked faunal bone Gough's Cave (Upper Paleolithic, England). Case Study 2: 25 cut marks from Boxgrove (Lower Paleolithic, England) and 23 from Gough's Cave. (N=91)	To interpret the difference between cut marks related to faunal butchery and cannibalism. To identify tool diversity by analyzing micromorphological cut mark characteristics.	Much more force was used for the human butchery as seen in wider and deeper cut marks compared to faunal butcher, possibly due to rigor mortis and human butchery being part of ritual burial and not cannibalism.	Bello 2011
Tooth and Cut Mark Morphology	Alicona Infinite Focus microscope. MeX software.	5x lens. Vertical and lateral resolution of 14.9 μ m.	Three experimentally created cut marks and two types of moulds for each mark. (N=9)	To test the accuracy of moulding materials to create replicas of trace marks left on bone such as cut marks.	Scans of original marks and scans of the replicas were statistically indistinguishable. Moulding materials can confidently be used when original trace marks cannot be scanned.	Bello et al. 2011
Tooth and Cut Mark Morphology	Alicona Infinite Focus microscope. MeX software.	5x lens. 1 μ m vertical resolution and 3.28 μ m lateral resolution	16 engraved marks on reindeer antler Magdalenian site of Neschers, France. 12 engraved marks on horse metatarsal Magdalenian site of Courbet Cave, France. (N=28)	Provide a new technique for recognizing and interpreting incised features on archaeological specimens.	3D analysis provides a quantitative way to interpret and describe engravings. Similarities between engraving techniques were identified.	Bello et al. 2013
Tooth and Cut Mark Morphology	Alicona Infinite Focus microscope. MeX software.	5x lens. 1.775 μ m vertical resolution and 0.9 μ m lateral resolution	Cut marked bone from four sites. 237 human, 147 faunal Gough's Cave, England. 43 human, 91 faunal Lepenski, Serbia. 2 human, 64 faunal Padian, Serbia. 63 human Vlasac, Serbia. (N=647)	To differentiate between cannibalized human remains and secondary burial modification such as scalping and filleting disarticulation actions.	A distinction between cannibalism and secondary modification of human bones after death and partial decomposition can be made based on frequency, distribution, and micromorphological characteristics of cut marks.	Bello et al. 2016

Table 2 – Continued

Tooth and Cut Mark Morphology	Hirox KH-7700, OL-140II lens. KH-7700 3D viewer 1.2.0 software.	10x lens. 14 μ m vertical resolution, 7 μ m lateral resolution.	20 experimentally created cut marks from 5 tool types (copper blade, bronze blade, steel blade, flint flake, retouched flint flake). 34 cut marks on faunal remains from Trebbio, Italy an Iron Age site. (N=134)	To test the applicability of 3D scanning to quantifying cut mark morphology from distinct tool types with new measurement metrics expanded from Bello & Soligo 2008.	A principal component analysis of previously established and new metrics displayed a 83% accuracy in determining tool type of experimental marks and 59% accuracy with fossil marks.	Boschin & Crezzini 2012
Tooth and Cut Mark Morphology	Nanovea ST400. Expert 3D software.	3x lens. 5 μ m vertical resolution, 10 μ m lateral resolution.	51 cut experimentally created cut marks. 29 known tooth marks from a spotted hyena feeding experiment.	Testing inter-observer error and to establish a standardize protocol for 3D scanning micromorphological traces left on bone.	Inter-observer error ranged from 4.7% to 35.9% depending on measurement metric. Central profiles of marks were found to be too variable and unreliable between oververs, only analyzing the deepest produced replicable and precise results between observers.	Pante et al. 2017
Tooth and Cut Mark Morphology	Scanner developed by the Institute of Medical Physics Erlangen, Germany. Impact View Software.	N/A	N/A	Develop a method to identify tool/weapon with cut mark left on bone.	3D scanning provides a opportunity to correlate tool to cut mark, however for the application to forensic anthropology, the back and forth movement to dislodge a weapon after stabbing diminishes the ability to identify the weapon responsible.	Thali et al. 2003
Tooth and Cut Mark Morphology	Leica TCS SP2 True Confocal Scanner. Software not specified.	N/A	N/A	Testing the application of 3D scanning on forensic material such as gun shot residue and gun shot wounds.	High resolution scanning can identify micromorphological features related to distinct gun shot residues left on skin.	Turillazzi 2008
Pottery Morphology	Polygon Technology (Specific model not specified). QTS sculptor software.	N/A	Approximately 1000 pot shards from several sites. (N=1000)	A method for rapids scanning of shards (500 per day) is introduced. Axis of symmetry and mean profiles are determined for the purpose of reconstruction from sherds.	The efficiency of the model provides a means for rapid print-quality scans. Additionally, multiple typological profiles were identified which will allow for more confident computerized reconstructions.	Karasik & Smilansky 2008
Pottery Etching	Uscan Nanofocus. Usoft software.	Lateral and Vertical resolution of 15 μ m	Two pottery shards with visible carved inscriptions. (N=2)	Developing a method to improve visual quality and decipherment of illegible carved inscriptions.	The high resolution scans uncovered several unreadable inscriptions (by naked eye or photogrammetry methods). Implementation of 3D scanning will aid in deciphering inscriptions and in turn improve knowledge of ancient populations.	Montani et al. 2012

CHAPTER 3 MATERIALS AND METHODS

The neotaphonomic study undertaken in this thesis is designed to create a controlled sample representative of specific carnivore tooth mark morphologies to compare to carnivore trace marks found on fossil bones in the archaeological record. This thesis sample consists of actualistic feeding trails at the Denver Zoo and Rist Canyon Wolf Sanctuary, as well as materials from published naturalistic feeding experiments (Blumenschine 1988; Njau & Blumenschine 2006; Pobiner 2007). Table 3 details the characteristics of the animals and samples included in this thesis. The actualistic sample is also applied to interpret fossil trace marks found on faunal remains from a Middle Bed II site in Olduvai Gorge Tanzania dating to approximately 1.7 million years ago. Table 3 details the characteristics of the fossils included in this thesis. A Nanovea ST400 white-light non-contact confocal profilometer was utilized to characterize individual tooth marks at the level of detail and accuracy needed to achieve the goals of this thesis.

3.1 Sample

Previous studies that analyzed carnivore feeding traces observed that tooth mark morphology varies with prey size as well as the anatomical location on bone of the feeding traces (Lam 1999; Pobiner 2007, Delaney-Rivera et al. 2009; Andres et al. 2012; Nascou & Morin 2014). These findings led this study to focus the feeding trials on size 3 cow limb bones and to only analyze marks found on the midshafts of the bones, ignoring tooth marks on or near the softer bone of the epiphyses (Animal size groups are based on Bunn 1982. Size 1 <23kg; Size 2, 23-114kg; Size 3, 114-341kg.). Feeding trials were limited to less than 24-hour periods in order to limit feeding traces such as gross gnawing. Furthermore, feeding trials were conducted on fasting days for the animals, driving more interest in the bones to better replicate wild feeding

behavior. All tooth scores and tooth pits as defined by Selvaggio (1994) found on the midshaft portion of bones were included into analysis; gnaw marks, furrowing, and overlapping tooth marks were ignored.

Table 3 - Summary of species and corresponding sample included within this study.

Common Name	Setting	Number of Individuals	Age (years)	Sex	Average Weight (kg)	Number of Bones	Sample Size
African Wild Dog	Captive	3	4	2 Female, 1 Male	35	6	31
Grey Wolf	Captive	1	11	1 Female	45	4	29
Spotted Hyena	Wild	N/A	N/A	N/A	N/A	9	28
Spotted Hyena	Captive	3	3	2 Female, 1 Male	46	6	30
Striped Hyena	Captive	2	18	1 Female, 1 Male	59	6	30
African Lion	Wild	N/A	N/A	N/A	N/A	9	28
African Lion	Captive	4	2	4 Male	145	4	30
Brown Bear	Captive	2	15	1 Female, 1 Male	250	6	28
Nile Crocodile	Captive	4	N/A	N/A	N/A	6	48
Total						56	282

Table 4 - Characteristics of fossils included within this study. See Bunn (1982) for body size classes.

Identification Number	Prey Taxon	Skeletal Element	Body Size	Tooth Mark Location	Tooth Mark Type
HWKEE 1652	Bovid	Radius	3	Near Epiphysis	Score
HWKEE 2908A	Bovid	Calcaneum	3	Calcaneum	Score
HWKEE 2908B	Bovid	Calcaneum	3	Calcaneum	Score
HWKEE 4107	Bovid	Metapodial	3	Midshaft	Score
HWKEE 4242	Bovid	Metacarpal	3	Epiphysis	Score
HWKEE 4268	Indeterminate	Femur	3	Midshaft	Score
HWKEE 60025	Indeterminate	Long Bone	3	Midshaft	Pit
HWKEE 2743	Indeterminate	Long Bone	3	Midshaft	Score
HWKEE 356	Indeterminate	Tibia	3	Midshaft	Pit
HWKEE 3833A	Indeterminate	Tibia	3	Midshaft	Score
HWKEE 3833B	Indeterminate	Tibia	3	Midshaft	Pit
HWKEE 4168	Bovid	Humerus	3	Epiphysis	Score
HWKEE 4176A	Bovid	Radius	3	Midshaft	Score
HWKEE 4176B1	Bovid	Radius	3	Midshaft	Score
HWKEE 4176B2	Bovid	Radius	3	Midshaft	Score
HWKEE 4176B3	Bovid	Radius	3	Midshaft	Pit
HWKEE 1975	Indeterminate	Long Bone	3	Near Epiphysis	Pit
HWKEE 677A	Indeterminate	Humerus	3	Head	Pit
HWKEE 677B	Indeterminate	Humerus	3	Head	Score
HWKEE 1045A	Indeterminate	Humerus	3	Near Epiphysis	Pit
HWKEE 1045B	Indeterminate	Humerus	3	Near Epiphysis	Score
HWKEE 1045C	Indeterminate	Humerus	3	Near Epiphysis	Score
HWKEE 3969	Indeterminate	Cervical Vertebra	2	Zygopophysis	Score
HWKEE 1886A	Indeterminate	Scapula	2	Blade	Score
HWKEE 1886B	Indeterminate	Scapula	2	Blade	Pit
HWKEE 60021A	Indeterminate	Metapodial	3	Midshaft	Score
HWKEE 60021B	Indeterminate	Metapodial	3	Midshaft	Pit
HWKEE 600275	Indeterminate	Rib	2	Head	Score
HWKEE 60050	Indeterminate	Long Bone	3	Midshaft	Score

3.2 Modern Sample: Naturalistic Observations of Wild Animals

3.2.1 Spotted Hyena, n=28 (from Blumenschine 1988)

Spotted hyena (*Crocuta crocuta*) tooth marks were collected from Robert Blumenschine's sample of carnivore only experiments conducted in the Ngorongoro Conservation Area, Tanzania. Tooth marks found on the midshafts of size 3 bovids were included in this thesis. Bones from this sample were sent to Colorado State University for analysis. A total of 10 bone fragments from Blumenschine's study were included within this thesis. Spotted hyena feeding, defleshing and demarrowing were only partially observed by Blumenschine so other consumers and their traces cannot be completely ruled out.

3.2.2 African Lion, n=28 (from Pobiner 2007)

African Lion (*Panthera Leo*) tooth marks were collected from Brianna Pobiner's sample of naturally consumed bone in Ol Pejeta Conservation Area, Kenya. African lion tooth marks from the midshafts of size 3 equids were included in this thesis. Tooth marks were molded using 3M ESPE Express Vinyl Polysiloxane Impression Material Putty Base and Catalyst, molds were sent to Colorado State University for analysis. A total of 9 bones and 29 tooth marks from Pobiner's study were included within this thesis. African lion feeding was observed by Pobiner; however, it was not observed from start to completion and therefore other consumers and their traces cannot be ruled out with absolute certainty. Pobiner stipulates that the Ol Pejeta Conservation Area has a very low population of hyenas and jackals and it was unlikely that they came into contact with the carcasses. When hyena ravaging was apparent, samples were discarded and not included into Pobiner's study.

3.3 Modern Sample: Controlled Feeding Observations of Captive Animals

3.3.1 Nile Crocodile, n=48 (from Njau & Blumenschine 2006)

Nile Crocodile (*Crocodylus niloticus*) tooth marks were collected from Njau and Blumenschine's (2006) sample of controlled feeding observations of captive crocodiles in Bagamoyo, Tanzania. A total 48 tooth marks on six size 3 bovid bones from Nile crocodiles feeding trials in Njau and Blumenschine's study were included in this thesis. Entire feeding episodes were observed by Jackson Njau, and bones were collected after 24 hours from the crocodile enclosures.

3.3.2 Grey Wolf, n=29 (from Rist Canyon W.O.L.F Sanctuary)

Captive feeding observations of grey wolves (*Canis lupus*) were conducted at a private rehabilitation sanctuary for wolves in Colorado, USA. The sanctuary houses over 30 wolves of varying pedigree and admixture with domestic dog species. For this reason, only Isabeau, a solitary and believed to be "pure" wolf was included for feeding trials. Wolves were fed moderately fleshed bones on a bi-weekly basis on fasting days. Feeding behavior was observed during the active phase of the feeding episode and bones were collected from the enclosure after 20-24 hours. While the wolves were fed a wide range of bones from different animals and size classes, only tooth marks from the midshafts of size 3 bovids were included in this thesis for consistency with the remainder of the sample. A total of four bones from four distinct feeding trials were included in this thesis.

3.3.3 African Wild Dog, n=31; Spotted Hyena, n=30; Striped Hyena, n=30; African Lion, n=30; North American Brown Bear, n=28 (from Denver Zoo)

Captive feeding observations of African wild dog (*Lycaeon pictus*), spotted hyena (*Crocota crocuta*), striped hyena (*Hyaena hyaena*), African lion (*Panthera leo*), and North

American brown bear (*Ursus arctos*), were conducted at the Denver Zoo. Animals were fed moderately fleshed humeri from size 3 bovids on fasting days on a bi-weekly basis. Feeding behavior was occasionally, but not always observed during the active phase of the feeding episode and bones were collected from the enclosure after 20-24 hours. A total of 26 bones for all species from the Denver Zoo feeding trials were included in this thesis: six from the African wild dogs, six from the spotted hyena, six from the striped hyena, four from the African lion, and six from the North American brown bear feeding trials.

3.4 Archaeological Sample

Fossil trace marks are from faunal remains excavated from a Middle Bed II site in Olduvai Gorge, Tanzania, dating to approximately 1.7 million years. A total of 25 bones, totaling 29 trace marks are included within this thesis. All trace marks were initially analyzed by Dr. Michael Pante, the zooarchaeologist for the Olduvai Gorge Archaeology Project (OGAP) with a 10x hand lens under 100w incandescent light following the protocol set forth by Blumenshine et al. (1996). Fossil trace marks included in this thesis were chosen based on their initial analysis and condition of the bone. Replicas of the trace marks were molded using 3M ESPE Express Vinyl Polysiloxane Impression Material Putty Base and Catalyst following the method and protocol established in Bello (2011) for ease of transport to Colorado State University's zooarchaeology lab for analysis. Molding was done by mixing the putty base and catalyst together until they formed a uniform color, pressing the putty mixture into the tooth mark, and leaving to set until the putty was dry (2-3 minutes).

3.5 Preparation of Sample for Analysis

3.5.1 Bone collection

Carnivore consumed bones were collected from both the W.O.L.F Sanctuary and Denver Zoo within 24 hours of feeding. Animals were not allowed access to the bones for longer periods of time to minimize unique behaviors such as gnawing seen in captive animals, but uncharacteristic and not observed in the wild (Faith 2007; Gidna et al. 2013; Dominguez-Rodrigo et al. 2015). This behavior is largely believed to occur due to the boredom experienced by captive animals (Faith 2007). At both the W.O.L.F Sanctuary and Denver Zoo, caretakers and on occasion myself entered the animal enclosures the following morning to remove the bones and set them aside for collection. Denver Zoo caretakers placed individual bones in bags labelled according to which carnivore taxa that had fed upon them.

3.5.2 Cleaning

All bones from Blumenschine (1988), Njau & Blumenschine (2006), and Pobiner (2007) were cleaned following the same methodology. Bones were placed in a simmering solution of water and laundry detergent until bones were adequately defleshed. Following this, bones were cleaned with wooden or plastic tools as to not leave cut mark traces from the tools on the bone surface. Bones were then placed in a hydrogen peroxide solution for bleaching and sterilization and were left in open-air environments to dry.

Due to the biohazard risk, carnivore consumed bones from the Denver Zoo, could not be cleaned following the methodology of the published samples (Blumenschine 1988, Njau & Blumenschine 2006; Pobiner 2007). A large boiler was available from the Zoology department; however, the temperature was very high and not adjustable. When used with one sample, the high temperature led to drastic exfoliation of the bone surface and the altering of the carnivore

trace marks. Due to these limitations, flesh eating dermestid beetles (*Dermestes maculatus*) were used to clean the bone. Bones were fed to dermestid beetles for approximately three weeks depending on the amount of flesh left on the bone post carnivore feeding. Bones were labeled and placed into separate containers organized by the carnivore species that had fed on them to ensure no bones were wrongly identified at later stages of this project. Following this, bones were cleaned of remaining flesh and ligament with a soft bristle brush under warm water with care not to leave any traces on the bone and placed in an 18% hydrogen peroxide solution for 8-12 hours for further degreasing, bleaching, and sterilization. Bones were then transported to the zooarchaeology lab and set under 100w incandescent lights to dry. This cleaning process took significantly longer and required more effort than simmering in hot water, but had the added benefit of ensuring the cleaning process would not alter any of the tooth marks.

3.6 Profilometer – Scanning Procedure

This section briefly describes the systematic and replicable protocol for the collection and analysis of carnivore feeding traces left on bone using a high-resolution 3D scanner. A detailed overview of the methodology, justification of the methodology, as well as research citing the accuracy, precision, and replicability between observers can be found in Pante et al. (2017).

3.6.1 Profilometer & Software

All trace marks were scanned using a Nanovea ST400 white-light non-contact confocal profilometer equipped with a 3 mm optical pen (Figure 1). Scanning was done at a resolution of 40 nm on the z-axis. All scans were analyzed using Nanovea's expert 3D software, a customized version of Digital Surf's Mountains software (2015).

3.6.2 Scanning & Analysis Protocol

The resolution of the scanner was set at 5 nm along the x-axis and 10 nm along the y-axis. A dual frequency of 300 Hz and 1000 Hz was chosen for the optical pen. Bones were placed underneath the optical pen, leveled along the x and y-axis and with the marks oriented perpendicular along the long axis of the mark. Only marks on the midshaft were included in this study in order to keep variation caused by bone density to a minimum (Braun et al. 2016). Once trace marks were scanned, files were processed in the expert 3D following the processing and measurement protocols outlined below.

3.6.3 3D data processing

Prior to any analysis, the bone surface surrounding the tooth mark was digitally leveled in order to clearly define the mark edges and shoulders, and to minimize the underlying shape of the bone from affecting measurements. This was accomplished by manually selecting an area surrounding the mark and removing unnecessary profiles around the mark through a polynomial function. The process from initial scan to cleaned and processed scan can be seen in Figure 2.

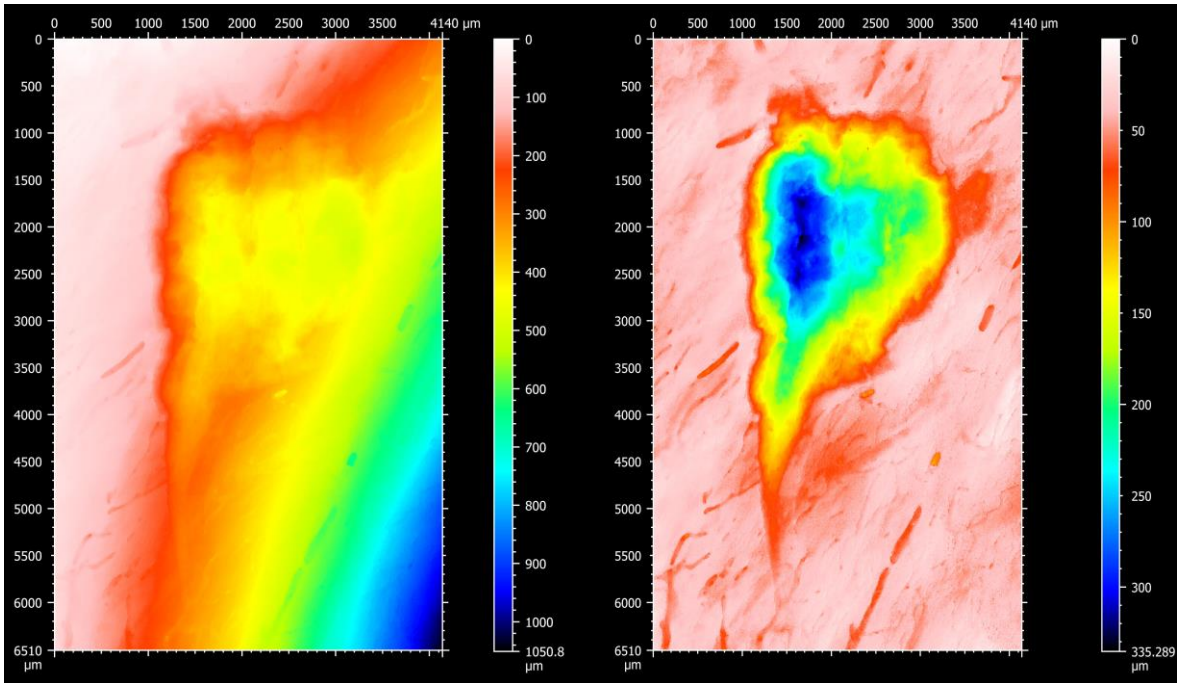


Figure 1 - Two studiabiles from a single spotted hyena tooth mark. The image on the left displays the unprocessed scan, the image on the right is created by removing the form of the bone and filling missing data points through a polynomial function. Scales on the right represent the relationship between color and depth.

3.6.4 3D data measurement

Once the scans were processed and cleaned, 3D measurements of the trace marks were taken. Three-dimensional measurement metrics used in this thesis included surface area, volume, maximum depth, mean depth, maximum length, and maximum width. Description of each metric and how it was taken is described below.

Surface area, volume, maximum depth, and mean depth are all measured using the “volume of a hole” function with the least squares setting. The measurements are taken after manually selecting the borders of the tooth mark from the bone surface (Figure 3). Surface area represents the entire 2D surface of the mark, manually defined by the user. Volume represents the entire 3D area of the tooth mark that has been displaced by the carnivore tooth, and is taken from the deepest point to the shoulder of the mark. Maximum depth is the lowest point found

within the tooth mark and mean depth is the average depth of the entire floor surface of the mark. Maximum length and width along the x and y-axes are defined with the distance tool.

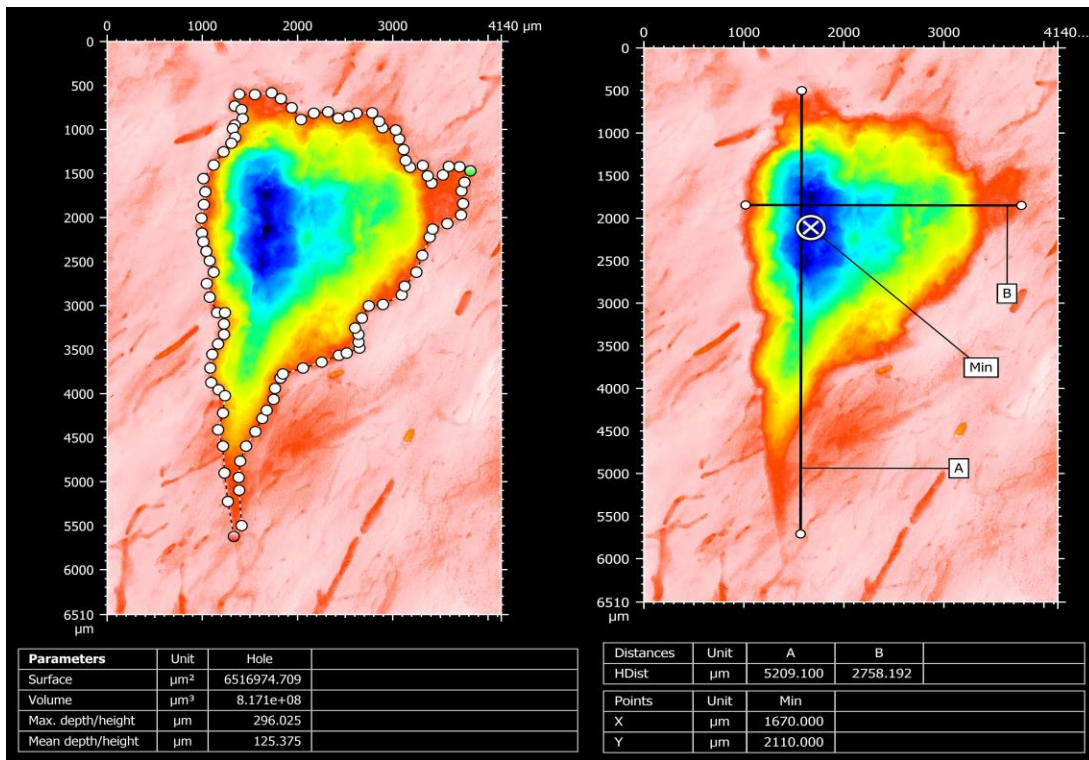


Figure 2 - Measurements taken during 3D analysis. The figure to the left displays the outline manually created in order to produce surface, volume, max depth, and mean depth values. The figure to the right displays the distance measurements manually created in order to produce length and width values.

3.6.5 Profile extraction

A single 2D profile was taken from the tooth mark at the deepest point of the mark along the x-axis (Figure 4). A profile is a cross-section from the tooth mark and represents a single pass of the optical pen over the tooth mark during scanning. The deepest point of the mark was chosen for profile location as it was easily defined by the program and therefore can be precisely replicated between observers and accurately compared to other tooth marks. The “area of a hole” function was used on the 2D profile to define the coordinates of the tooth mark edges and to exclude the remaining bone surface from analysis. The area is defined by the software using the “under the waterline” option or manually defined for tooth marks that are very shallow,

referencing the 3D image of the mark when this cannot be accurately accomplished by the software.

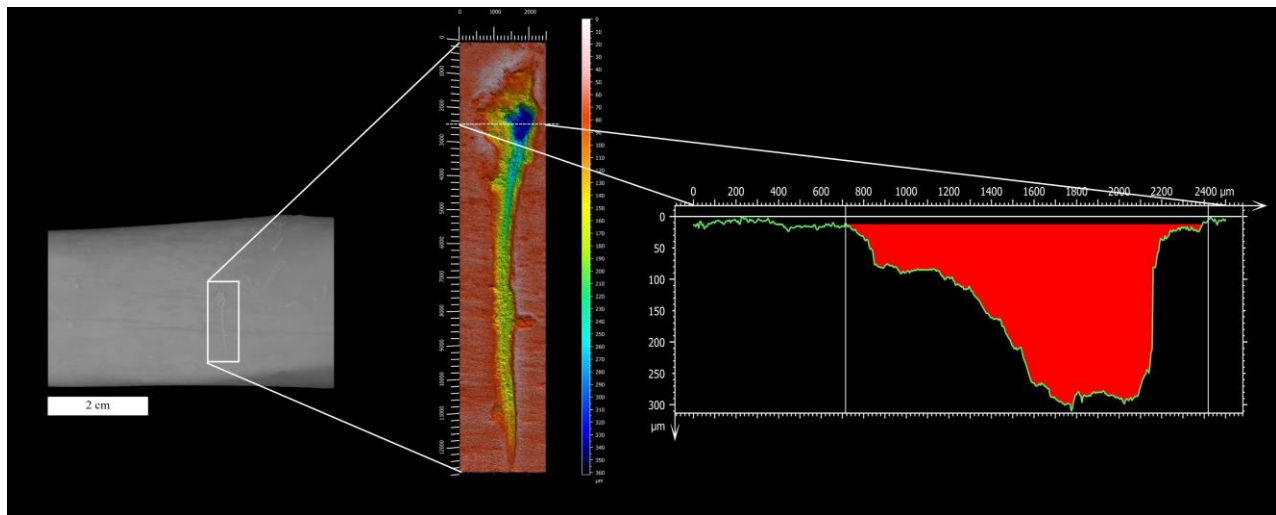


Figure 3 - Sample image of a crocodile tooth marked bone, extracted scanning surface, and cross-sectional profile taken across the deepest profile of the mark.

3.6.6 Profile measurement

Two-dimensional measurement metrics taken from a profile along the deepest point of the tooth mark are maximum depth, area, maximum width, roughness, opening angle, and floor radius. Maximum depth and area of the mark are calculated from the entire profile of the mark, maximum depth represents the deepest point in the profile (Figure 5). Maximum width, roughness, opening angle, and floor radius are measured from only the tooth mark profile, the user manually removes the surrounding bone outside the mark prior to analysis. Maximum width represents the width of the mark at its widest point from shoulder to shoulder. Roughness is measured using the “parameters table” function and represents the arithmetic mean deviation of the mark’s surface area. Opening angle and floor radius are calculated using the “contour analysis” function (Figure 6). Opening angle is measured from drawing two points, one from the first point to the deepest point along the profile and one from the last point to the deepest point

along the profile. Radius is measured by drawing an arc from the first and last points in the profile.

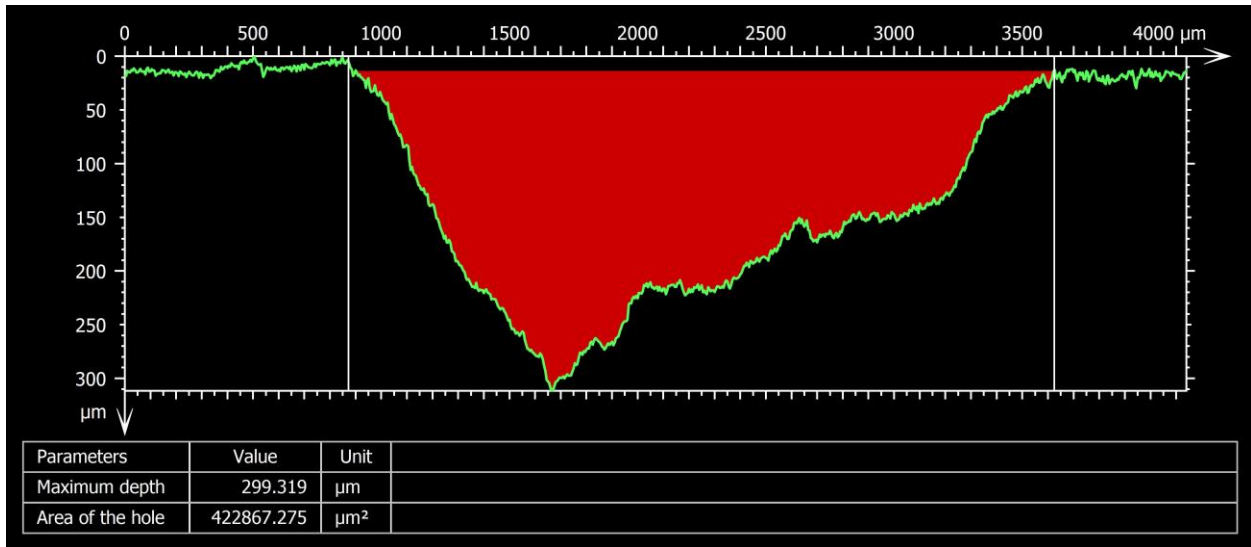


Figure 4 - Area of a hole from the profile extracted from the deepest profile.

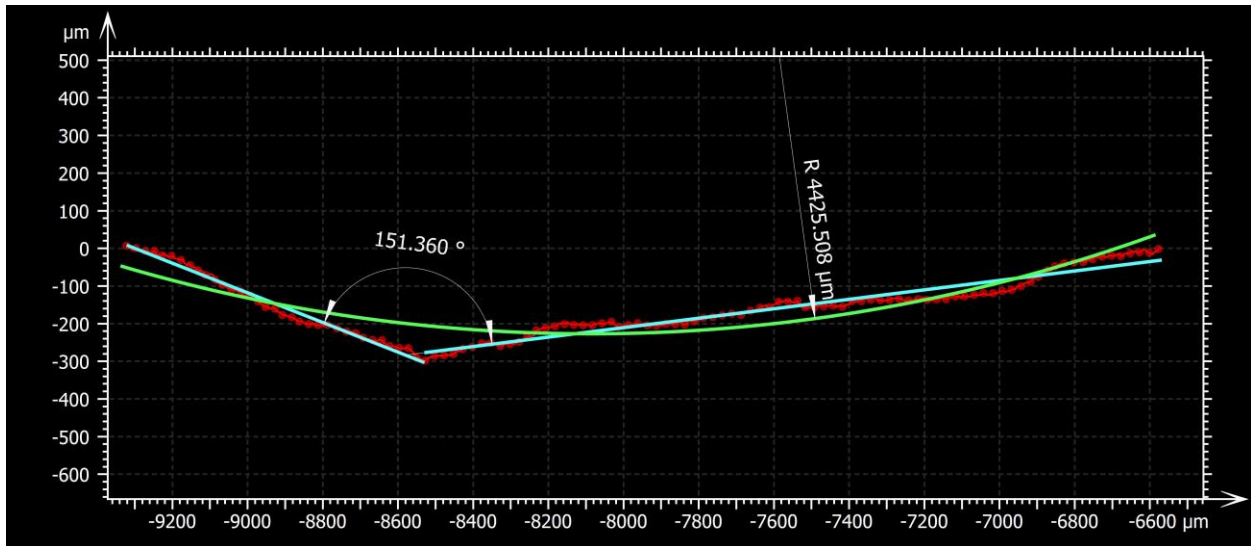


Figure 5 – Contour analysis showing opening angle and floor radius of the tooth mark with the remaining bone outside of the mark removed.

3.7 Statistical Methods – Treatment of Results

Statistical analyses were done in Microsoft Excel and Paleontological Statistics Software 3.11 PAST (Hammer et al. 2001). Paired *t*-tests were used to test the ability of the molding material to accurately replicate the micromorphological characteristics of the original tooth

marks. Analysis of variance (ANOVA) tests were completed for each individual measurement metric in order to test the accuracy of the recorded variable to differentiate between carnivore actors. When distributions were not parametric a Kruskal-Wallis test was used in place of the ANOVA. Both tests were followed with Mann-Whitney U tests to further examine the accuracy of each variable between each carnivore species.

Multivariate limited discriminant analyses were used to determine how accurate the recorded variables were at classifying the tooth marks. Coefficient of correlation tests were computed to ensure that variables were not highly correlated and incorrectly increasing the reported accuracy of the multivariate analysis. All measured variables were significant at the $r=0.1$ to -0.1 level and therefore considered simultaneously in the analysis. Discriminant analyses were conducted with carnivores organized by several groupings based on geological location, family level classification, and biomechanical classification. Fossil trace marks were computed in several discriminant analyses to determine how they would be classified within the actualistic sample.

CHAPTER 4 RESULTS

4.1 Testing the Applicability of Replicas

Scans of spotted hyena (*Crocuta crocuta*) tooth marks were taken from the bone surface and from replica molds of the same tooth marks and compared using a paired *t*-test. Marks were statistically indistinguishable at a *p*-value of 0.05 for nine of twelve measurement metrics (Figure 6, Table 5). Maximum depth (3D), maximum depth (profile), and area (profile) reported statistically were significantly higher for the original marks when compared with the replicas.

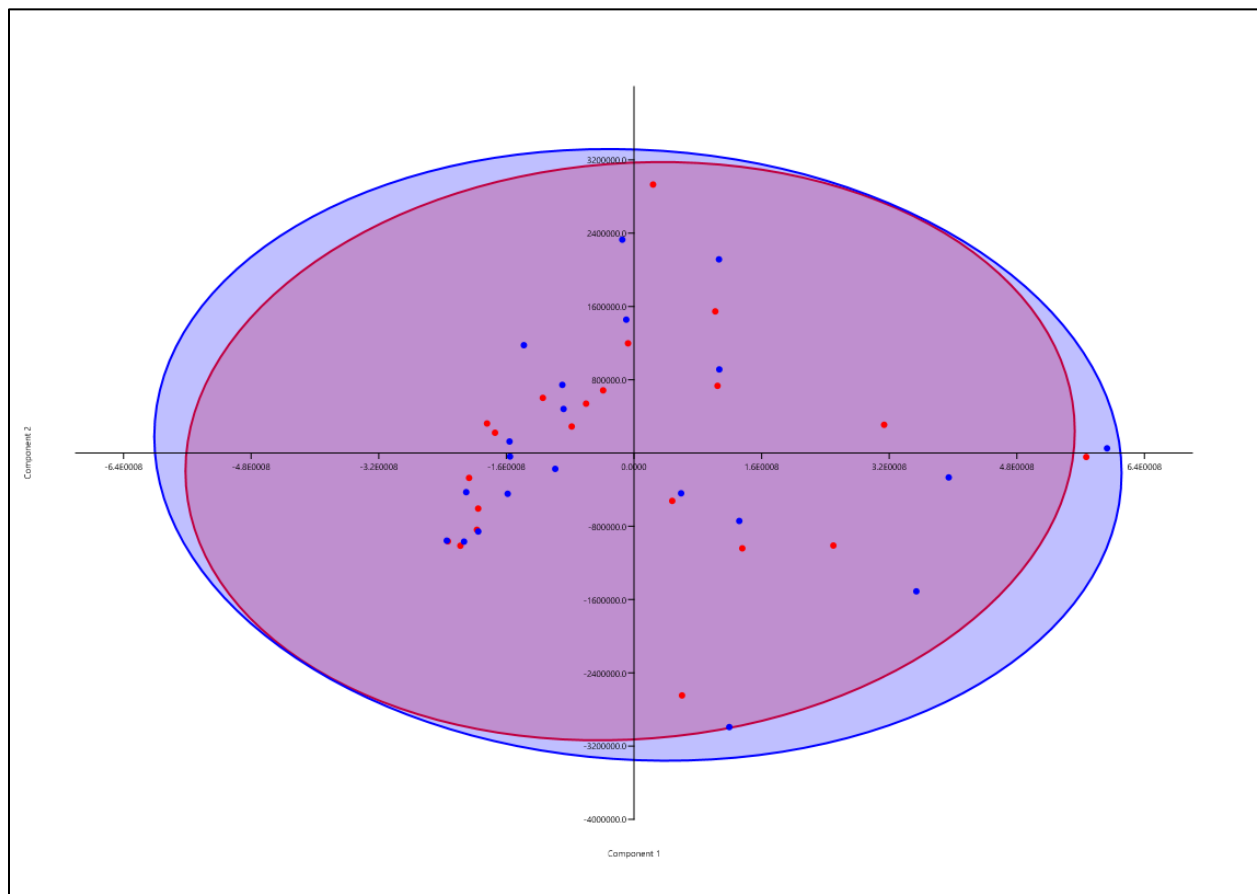


Figure 6 - Principal Component Analysis between original and replica scans. Based on variables shown in Appendix C. Original tooth marks are represented by blue dots and shaded blue area. Replicas are represented by the red dots and shaded red area.

Table 5 - Summary statistics of tooth marks between original and replica. Statistically significant differences between values at the 0.05 level of probability are in italics.

		3-D Measurements					
		Surface Area (μm^2)	Volume (μm^3)	Maximum Depth (μm)	Mean Depth (μm)	Maximum Length (μm)	Maximum Width (μm)
ORIGINAL	Mean	2862825.6	245218095.2	192.5	72.7	3181.6	1553.1
	Median	2716349.9	211400000.0	181.0	63.9	3555.3	1377.2
	Standard Deviation	1824411.5	204730592.3	77.5	33.9	1479.0	672.0
REPLICA	Mean	2886420.1	254989523.8	205.7	74.1	3129.6	1564.6
	Median	2819924.9	161800000.0	187.1	62.8	3110.8	1372.4
	Standard Deviation	1840852.2	222692887.3	83.3	35.5	1491.7	702.7
<i>p</i>-value		0.852	0.294	<i>0.010</i>	0.517	0.439	0.847

		Profile Measurements					
		Maximum Depth (μm)	Area (μm^2)	Width (μm)	Roughness (R_a)	Angle ($^\circ$)	Radius (μm)
ORIGINAL	Mean	186.1	143354.8	1432.4	5.9	144.9	2535.3
	Median	174.8	95485.8	1205.0	5.0	147.0	1055.4
	Standard Deviation	74.3	113926.7	755.0	3.0	20.0	3863.2
REPLICA	Mean	204.9	163361.7	1429.0	7.1	144.0	2176.1
	Median	186.7	127493.9	1115.0	6.4	143.9	962.6
	Standard Deviation	83.6	121432.4	697.3	3.0	17.0	2220.1
<i>p</i>-value		<i>0.003</i>	<i>0.002</i>	0.938	0.073	0.791	0.418

4.2 Comparison of Inter-Carnivore Samples

Two of the carnivores included in this study, the African lion and spotted hyena, have data from captive as well as naturalistic feeding trials. These samples were compared using an unpaired t-test to assess the validity of combining two distinct samples of the same animal together within a discriminant analysis. The lion sample is very distinct between the wild and controlled feeding trials. Only three of the twelve measurement metrics are statistically indistinguishable between wild and captive; therefore, the lions are broken up into two categories

for analysis of individual measurement metrics but combined for multivariate analysis, justification for this is discussed in chapter 5. Overall, wild lions produced significantly larger tooth marks (Table 6).

Table 6 - Summary statistics for tooth marks produced by wild and captive African lions. Statistically significant differences between values at the 0.05 level of probability are in italics.

3-D Measurements							
		Surface Area (μm^2)	Volume (μm^3)	Maximum Depth (μm)	Mean Depth (μm)	Maximum Length (μm)	Maximum Width (μm)
Wild African Lion	Mean	3567511.93	253382068.97	139.18	48.43	5080.15	995.64
	Median	2690874.88	90260000.00	105.37	35.99	5479.61	953.56
	St. Dev	2597528.05	451434045.32	86.57	41.27	2383.47	445.52
Captive African Lion	Mean	927210.44	36554832.47	88.14	34.39	2191.37	549.77
	Median	598074.97	15070000.00	73.38	28.49	1886.76	536.82
	St.Dev	953546.50	53591213.92	48.89	21.28	1586.38	258.79
Difference Between Means		2640301.48	216827236.50	51.03	14.04	2888.78	445.87
p-value		<i>0.000010</i>	<i>0.015670</i>	<i>0.008292</i>	0.110896	<i>0.000002</i>	<i>0.000028</i>
Profile Measurements							
		Maximum Depth (μm)	Area (μm^2)	Width (μm)	Roughness (R_a)	Angle ($^\circ$)	Radius (μm)
Wild African Lion	Mean	134.68	79830.90	1120.34	4.41	152.88	1475.83
	Median	96.91	37943.11	975.00	3.67	150.24	1121.40
	St. Dev	85.40	88484.72	840.57	3.20	9.58	1126.80
Captive African Lion	Mean	81.70	24918.13	552.93	2.93	147.37	1265.59
	Median	70.38	18769.68	565.00	2.16	147.70	526.25
	St.Dev	46.30	24996.78	230.49	2.28	15.11	3215.33
Difference Between Means		52.98	54912.77	567.41	1.48	5.51	210.24
p-value		<i>0.005303</i>	<i>0.002941</i>	<i>0.001364</i>	<i>0.047648</i>	0.103851	0.741652

The spotted hyena sample is more similar between wild and captive animals, where nine out of twelve measurement metrics are statistically indistinguishable between samples (Table 7), therefore, samples are combined for all remaining analysis, justification for this is discussed in chapter 5. The primary difference between these samples is that captive hyenas have a slightly

larger area and width in their tooth mark morphology compared to their wild counterparts. Interestingly, when spotted and striped hyenas are compared, they are statistically indistinguishable on all metrics except mean depth (3D), where striped hyenas have a slightly greater mean depth (3D) (Table 8).

Table 7 - Summary statistics for tooth marks produced by wild and captive spotted hyenas. Statistically significant differences between values at the 0.05 level of probability are in italics.

		3-D Measurements					
		Surface Area (μm^2)	Volume (μm^3)	Maximum Depth (μm)	Mean Depth (μm)	Maximum Length (μm)	Maximum Width (μm)
Wild Spotted Hyena	Mean	2965728.84	267906028.04	197.64	74.66	3118.89	1490.19
	Median	2716349.88	190000000.00	172.26	62.96	3349.72	1370.79
	St. Dev	2282294.45	273051871.30	111.70	44.93	1494.96	681.62
Captive Spotted Hyena	Mean	5619070.69	28667834000	249.12	99.80	3523.23	1669.99
	Median	3521412.34	310250000.00	211.08	84.61	3218.25	1363.01
	St.Dev	4859562.64	152990229670	152.42	59.26	2309.49	843.21
Difference Between Means		2653341.85	28399927972	51.47	25.14	404.34	179.80
p-value		<i>0.0100</i>	0.3177	0.1440	0.0713	0.4270	0.3709
		Profile Measurements					
		Maximum Depth (μm)	Area (μm^2)	Width (μm)	Roughness (R_a)	Angle ($^\circ$)	Radius (μm)
Wild Spotted Hyena	Mean	191.72	147449.39	1373.62	6.22	144.24	2226.40
	Median	170.16	90763.81	1205.00	5.09	146.73	1055.39
	St. Dev	109.24	133083.00	753.29	3.87	18.90	3376.81
Captive Spotted Hyena	Mean	234.76	264001.44	1869.00	11.80	149.98	2945.20
	Median	197.21	148058.59	1602.50	6.47	150.58	2279.63
	St.Dev	138.03	270113.06	829.15	23.99	12.04	2122.52
Difference Between Means		43.03	116552.06	495.38	5.57	5.74	718.80
p-value		0.1890	<i>0.0405</i>	<i>0.0195</i>	0.2187	0.1725	0.3345

Table 8 - Summary statistics for tooth marks produced by spotted hyenas and striped hyenas. Statistically significant differences between values at the 0.05 level of probability are in italics.

3-D Measurements							
		Surface Area (μm^2)	Volume (μm^3)	Maximum Depth (μm)	Mean Depth (μm)	Maximum Length (μm)	Maximum Width (μm)
Spotted Hyena	Mean	4314885.72	14708547370	223.82	87.44	3324.48	1581.62
	Median	3164149.86	242400000	191.53	67.74	3288.04	1370.79
	St. Dev	4013998.96	109124230890	135.32	53.77	1946.11	766.82
Striped Hyena	Mean	8942596.54	758524667	190.77	71.47	5384.16	1589.08
	Median	4388062.30	215450000	172.74	64.16	3530.50	1354.68
	St.Dev	12728985.41	1511473295	101.63	42.96	4126.91	798.45
Difference Between Means		4627710.82	-13950022703	33.05	15.98	2059.67	7.46
<i>p-value</i>		0.0609	0.3303	0.2005	0.1331	<i>0.0138</i>	0.9665
Profile Measurements							
		Maximum Depth (μm)	Area (μm^2)	Width (μm)	Roughness (R_a)	Angle ($^\circ$)	Radius (μm)
Spotted Hyena	Mean	213.60	206713.14	1625.51	9.06	147.16	2591.89
	Median	181.47	116809.97	1455.00	5.99	149.70	1655.59
	St. Dev	125.53	220191.66	824.67	17.40	15.91	2808.69
Striped Hyena	Mean	191.22	173820.80	1627.50	7.47	157.31	2929.94
	Median	172.96	101752.23	1405.00	6.25	158.14	2403.63
	St.Dev	109.20	245191.37	831.58	4.08	8.74	1852.79
Difference Between Means		22.38	32892.34	1.99	1.58	10.16	338.05
<i>p-value</i>		0.3884	0.5387	0.9915	0.5094	0.2006	0.4993

4.3 Analysis of Individual Measurement Metrics

Analysis was conducted between all carnivore species for one measurement metric at a time to identify the strength of each metric to distinguish between carnivore actors. Non-parametric Kruskal Wallis tests were used due to the sample not being normally distributed. All variables reported significant values at the 0.05 level of probability. Post-hoc Mann-Whitney U tests identify which carnivores cannot be differentiated for each individual variable. There are a total of 28 possible pairings between carnivore taxa. Comparisons between sets of carnivores

identify a range of accuracy for each measurement metric from 4 of 28 pairings for maximum width to 13 of 28 pairings for opening angle where the measurement metric does not differentiate between carnivore species at the 0.05 level of probability. Results for the post-hoc Mann-Whitney U tests are displayed in Table 9-20, and box and whisker plots displaying the range of each sample for each measurement metric are shown in Figure 7-18

Table 9 – Kruskal-Wallis and Mann-Whitney U tests for Surface Area (3D) measurements between all carnivore species tooth marks. Carnivores that cannot be differentiated with this measurement metric are highlighted in yellow.

	One-way Anova		Kruskal-Wallis						
Surface 3D	3.83E-26		1.795E-24						
Mann-Whitney Pairwise	African Wild Dog	Grey Wolf	Spotted Hyena	Striped Hyena	Lion (Wild)	Lion (Captive)	Nile Crocodile	Grizzly Bear	
African Wild Dog		0.0508600000	0.0000001052	0.0000000404	0.0000012220	0.4418000000	0.0000000430	0.0000000001	
Grey Wolf	0.0508600000		0.0001142000	0.0000079990	0.0003916000	0.0089850000	0.0000194500	0.0000000007	
Spotted Hyena	0.0000001052	0.0001142000		0.1101000000	0.6300000000	0.0000000284	0.1685000000	0.0000000110	
Striped Hyena	0.0000000404	0.0000079990	0.1101000000		0.0852700000	0.0000000125	0.7922000000	0.0002633000	
Lion (Wild)	0.0000012220	0.0003916000	0.6300000000	0.0852700000		0.0000002236	0.1239000000	0.0000001213	
Lion (Captive)	0.4418000000	0.0089850000	0.0000000284	0.0000000125	0.0000002236		0.0000000116	0.0000000002	
Nile Crocodile	0.0000000430	0.0000194500	0.1685000000	0.7922000000	0.1239000000	0.0000000116		0.0000044620	
Grizzly Bear	0.0000000001	0.0000000007	0.0000000110	0.0002633000	0.0000001213	0.0000000002	0.0000044620		

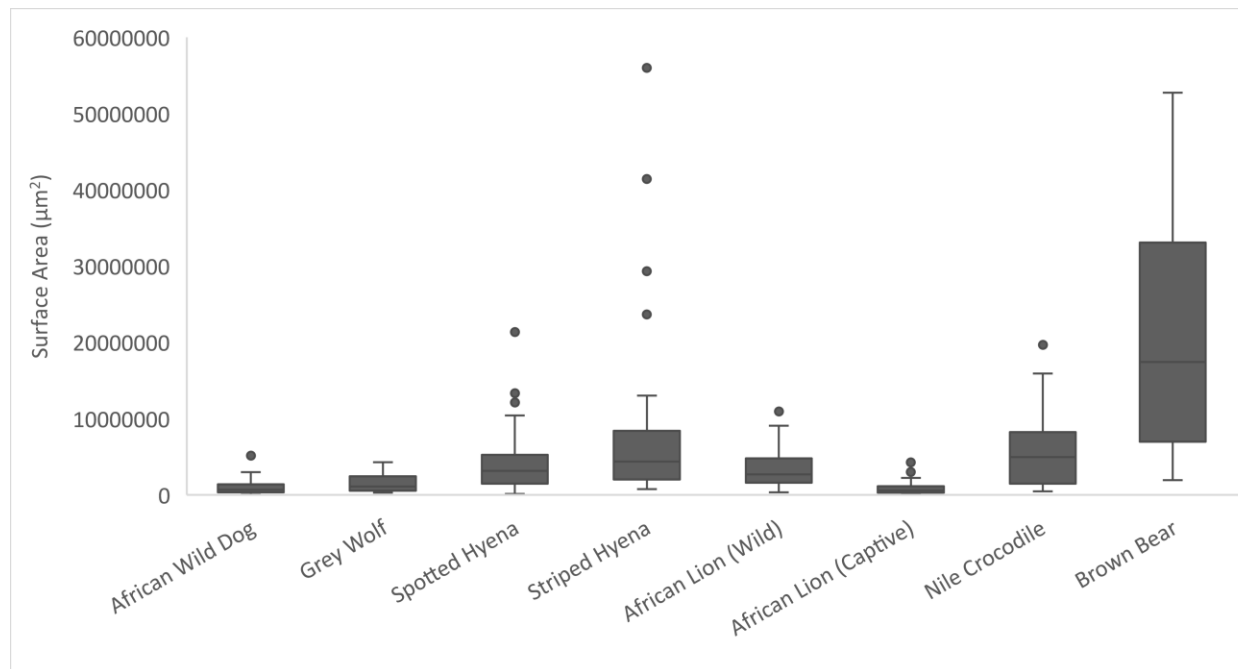


Figure 7 – Box and whisker plots for Surface Area (3D) measurements between all carnivore species tooth marks.

Table 10 - Kruskal-Wallis and Mann-Whitney U tests for Volume (3D) measurements between all carnivore species tooth marks. Carnivores that cannot be differentiated with this measurement metric are highlighted in yellow.

	One-way Anova	Kruskal-Wallis						
Volume 3D	1.04E-15	1.21E-22						
Mann-Whitney Pairwise	African Wild Dog	Grey Wolf	Spotted Hyena	Striped Hyena	Lion (Wild)	Lion (Captive)	Nile Crocodile	Grizzly Bear
African Wild Dog		0.0889100000	0.0000002610	0.0000012070	0.0003157000	0.1807000000	0.0000004403	0.0000000004
Grey Wolf	0.0889100000		0.0001229000	0.0003170000	0.0519100000	0.0010620000	0.0000764000	0.0000000025
Spotted Hyena	0.0000002610	0.0001229000		0.7714000000	0.0405200000	0.0000000012	0.2307000000	0.0000006170
Striped Hyena	0.0000012070	0.0003170000	0.7714000000		0.0357300000	0.0000000114	0.5943000000	0.0000539200
Lion (Wild)	0.0003157000	0.0519100000	0.0405200000	0.0357300000		0.0000013220	0.0113500000	0.0000000892
Lion (Captive)	0.1807000000	0.0010620000	0.0000000012	0.0000000114	0.0000013220		0.0000000032	0.0000000001
Nile Crocodile	0.0000004403	0.0000764000	0.2307000000	0.5943000000	0.0113500000	0.0000000032		0.0002531000
Grizzly Bear	0.0000000004	0.0000000025	0.0000006170	0.0000539200	0.0000000892	0.0000000001	0.0002531000	

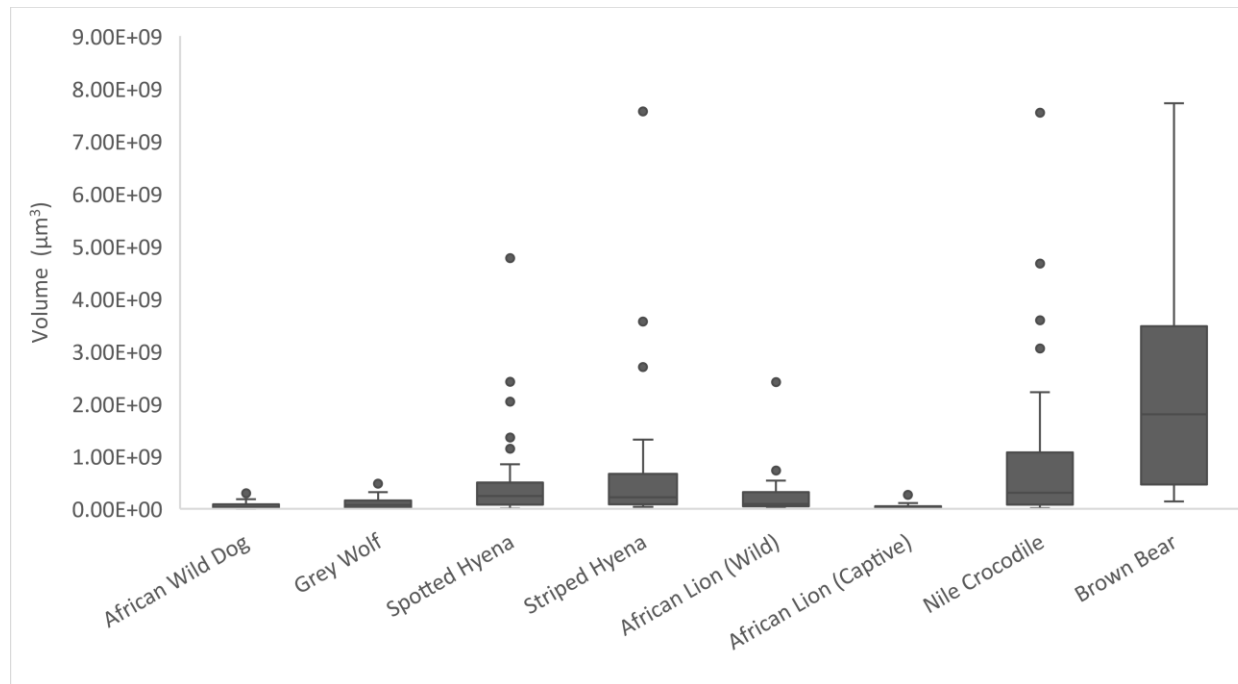


Figure 8 - Box and whisker plots for Volume (3D) measurements between all carnivore species tooth marks.

Table 11 - Kruskal-Wallis and Mann-Whitney U tests for Maximum Depth (3D) measurements between all carnivore species tooth marks. Carnivores that cannot be differentiated with this measurement metric are highlighted in yellow.

	One-way Anova		Kruskal-Wallis					
Max Depth 3D	6.82E-13		6.06E-17					
Mann-Whitney Pairwise	African Wild Dog	Grey Wolf	Spotted Hyena	Striped Hyena	Lion (Wild)	Lion (Captive)	Nile Crocodile	Grizzly Bear
African Wild Dog		0.0835000000	0.0000013290	0.0002153000	0.2086000000	0.0458200000	0.0000100900	0.0000000049
Grey Wolf	0.0835000000		0.0012870000	0.0331500000	0.6297000000	0.0004949000	0.0020910000	0.0000018910
Spotted Hyena	0.0000013290	0.0012870000		0.2543000000	0.0005361000	0.0000000026	0.3556000000	0.0085100000
Striped Hyena	0.0002153000	0.0331500000	0.2543000000		0.0111000000	0.0000003943	0.1404000000	0.0010550000
Lion (Wild)	0.2086000000	0.6297000000	0.0005361000	0.0111000000		0.0029750000	0.0007367000	0.0000009180
Lion (Captive)	0.0458200000	0.0004949000	0.0000000026	0.0000003943	0.0029750000		0.0000000434	0.0000000014
Nile Crocodile	0.0000100900	0.0020910000	0.3556000000	0.1404000000	0.0007367000	0.0000000434		0.3807000000
Grizzly Bear	0.0000000049	0.0000018910	0.0085100000	0.0010550000	0.0000009180	0.0000000014	0.3807000000	

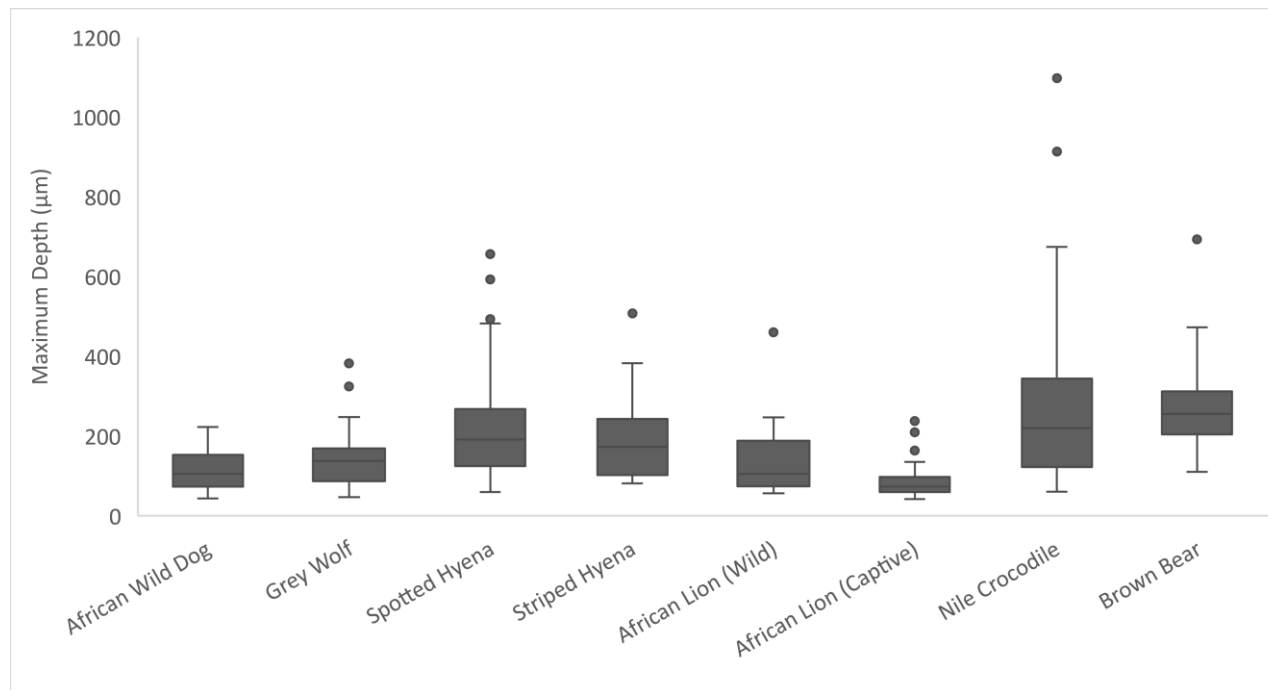


Figure 9 - Box and whisker plots for Maximum Depth (3D) measurements between all carnivore species tooth marks.

Table 12 - Kruskal-Wallis and Mann-Whitney U tests for Mean Depth (3D) measurements between all carnivore species tooth marks. Carnivores that cannot be differentiated with this measurement metric are highlighted in yellow.

	One-way Anova		Kruskal-Wallis					
Mean Depth 3D	7.80E-11		3.89E-13					
Mann-Whitney Pairwise	African Wild Dog	Grey Wolf	Spotted Hyena	Striped Hyena	Lion (Wild)	Lion (Captive)	Nile Crocodile	Grizzly Bear
African Wild Dog		0.2868000000	0.0002025000	0.0321700000	0.5540000000	0.0370000000	0.0004191000	0.000026270
Grey Wolf	0.2868000000		0.0073910000	0.2166000000	0.0815500000	0.0002907000	0.0104600000	0.0000728900
Spotted Hyena	0.0002025000	0.0073910000		0.1766000000	0.0000479700	0.0000000047	0.5252000000	0.0620100000
Striped Hyena	0.0321700000	0.2166000000	0.1766000000		0.0121000000	0.0000337200	0.1152000000	0.0045140000
Lion (Wild)	0.5540000000	0.0815500000	0.0000479700	0.0121000000		0.2628000000	0.0001092000	0.0000014890
Lion (Captive)	0.0370000000	0.0002907000	0.0000000047	0.0000337200	0.2628000000		0.0000012650	0.000000139
Nile Crocodile	0.0004191000	0.0104600000	0.5252000000	0.1152000000	0.0001092000	0.0000012650		0.4479000000
Grizzly Bear	0.0000026270	0.0000728900	0.0620100000	0.0045140000	0.0000014890	0.0000000139	0.4479000000	

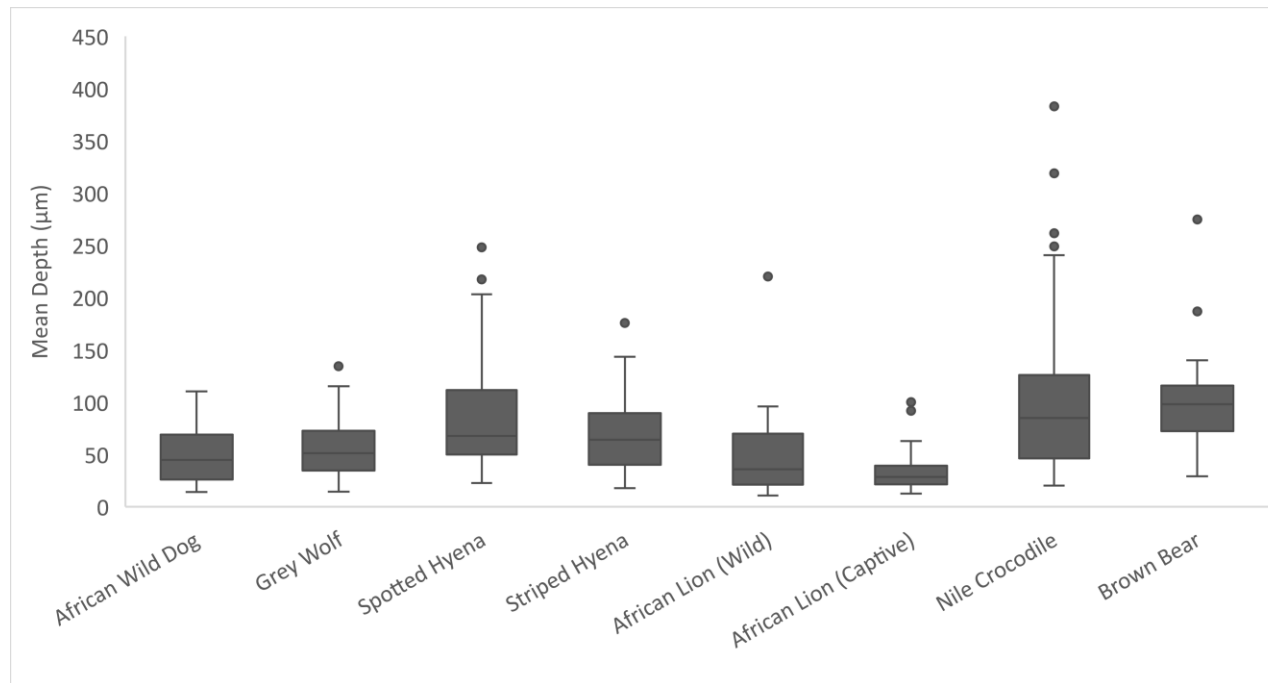


Figure 10 - Box and whisker plots for Mean Depth (3D) measurements between all carnivore species tooth marks.

Table 13 – Kruskal-Wallis and Mann-Whitney U tests for Maximum Length (3D) measurements between all carnivore species tooth marks. Carnivores that cannot be differentiated with this measurement metric are highlighted in yellow.

	One-way Anova		Kruskal-Wallis					
Max Length 3D	7.62E-21		3.81E-18					
Mann-Whitney Pairwise	African Wild Dog	Grey Wolf	Spotted Hyena	Striped Hyena	Lion (Wild)	Lion (Captive)	Nile Crocodile	Grizzly Bear
African Wild Dog		0.3748000000	0.0000065420	0.0000012070	0.0000002078	0.4075000000	0.000000035	0.000000143
Grey Wolf	0.3748000000		0.0002704000	0.0000410800	0.0000015450	0.9504000000	0.0000011270	0.000000547
Spotted Hyena	0.0000065420	0.0002704000		0.0790600000	0.0010310000	0.0028370000	0.0324000000	0.0000009226
Striped Hyena	0.0000012070	0.0000410800	0.0790600000		0.6767000000	0.0001750000	0.9776000000	0.0169200000
Lion (Wild)	0.0000002078	0.0000015450	0.0010310000	0.6767000000		0.0000107700	0.3829000000	0.0053450000
Lion (Captive)	0.4075000000	0.9504000000	0.0028370000	0.0001750000	0.0000107700		0.0000158200	0.0000001871
Nile Crocodile	0.000000035	0.0000011270	0.0324000000	0.9776000000	0.3829000000	0.0000158200		0.0037290000
Grizzly Bear	0.000000143	0.000000547	0.0000009226	0.0169200000	0.0053450000	0.0000001871	0.0037290000	

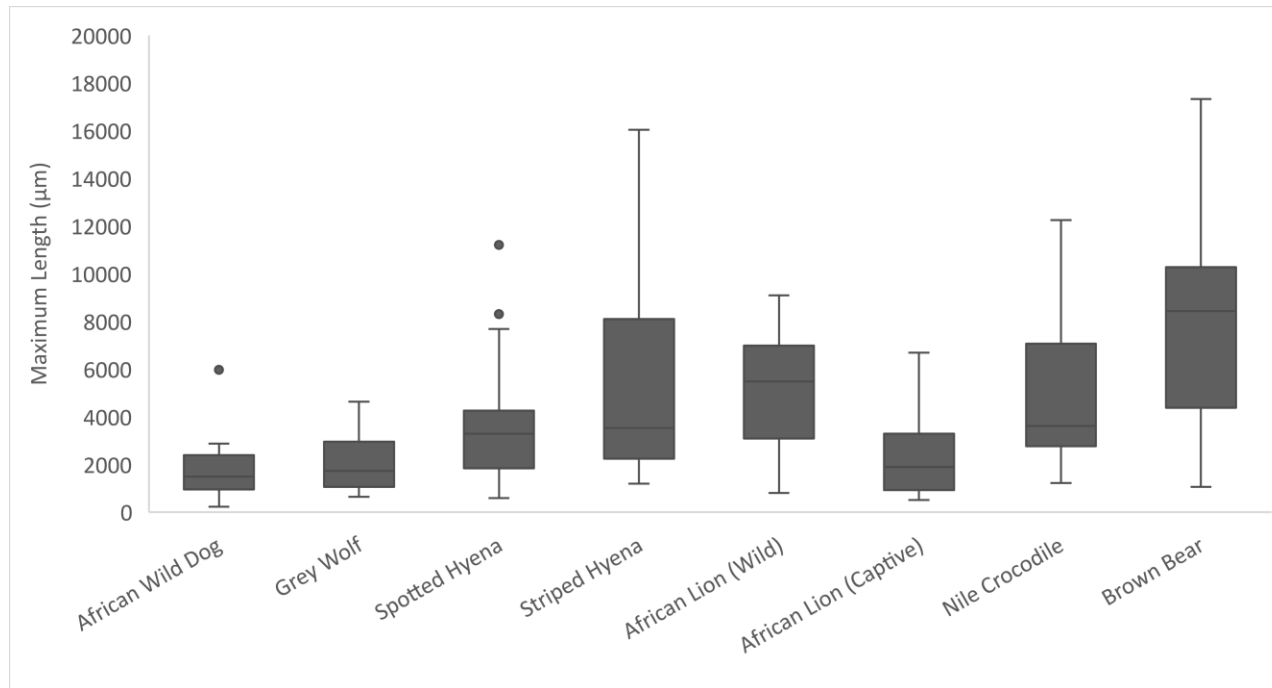


Figure 11 - Box and whisker plots for Maximum Length (3D) measurements between all carnivore species tooth marks.

Table 14 - Kruskal-Wallis and Mann-Whitney U tests for Maximum Width (3D) measurements between all carnivore species tooth marks. Carnivores that cannot be differentiated with this measurement metric are highlighted in yellow.

	One-way Anova		Kruskal-Wallis						
Max Width 3D	5.52E-33		8.22E-25						
Mann-Whitney Pairwise	African Wild Dog	Grey Wolf	Spotted Hyena	Striped Hyena	Lion (Wild)	Lion (Captive)	Nile Crocodile	Grizzly Bear	
African Wild Dog		0.0051770000	0.0000000122	0.0000005355	0.0100600000	0.0427000000	0.0000002069	0.0000000003	
Grey Wolf	0.0051770000		0.0013280000	0.0049150000	0.6078000000	0.0000086810	0.0015920000	0.0000000096	
Spotted Hyena	0.0000000122	0.0013280000		0.9474000000	0.0001767000	0.0000000000	0.3775000000	0.0000001612	
Striped Hyena	0.0000005355	0.0049150000	0.9474000000		0.0004232000	0.0000000029	0.5561000000	0.0000057360	
Lion (Wild)	0.0100600000	0.6078000000	0.0001767000	0.0004232000		0.0000165000	0.0003885000	0.0000000054	
Lion (Captive)	0.0427000000	0.0000086810	0.0000000000	0.0000000029	0.0000165000		0.0000000015	0.0000000001	
Nile Crocodile	0.0000002069	0.0015920000	0.3775000000	0.5561000000	0.0003885000	0.0000000015		0.0000480400	
Grizzly Bear	0.0000000003	0.0000000096	0.0000001612	0.0000057360	0.0000000054	0.0000000001	0.0000480400		

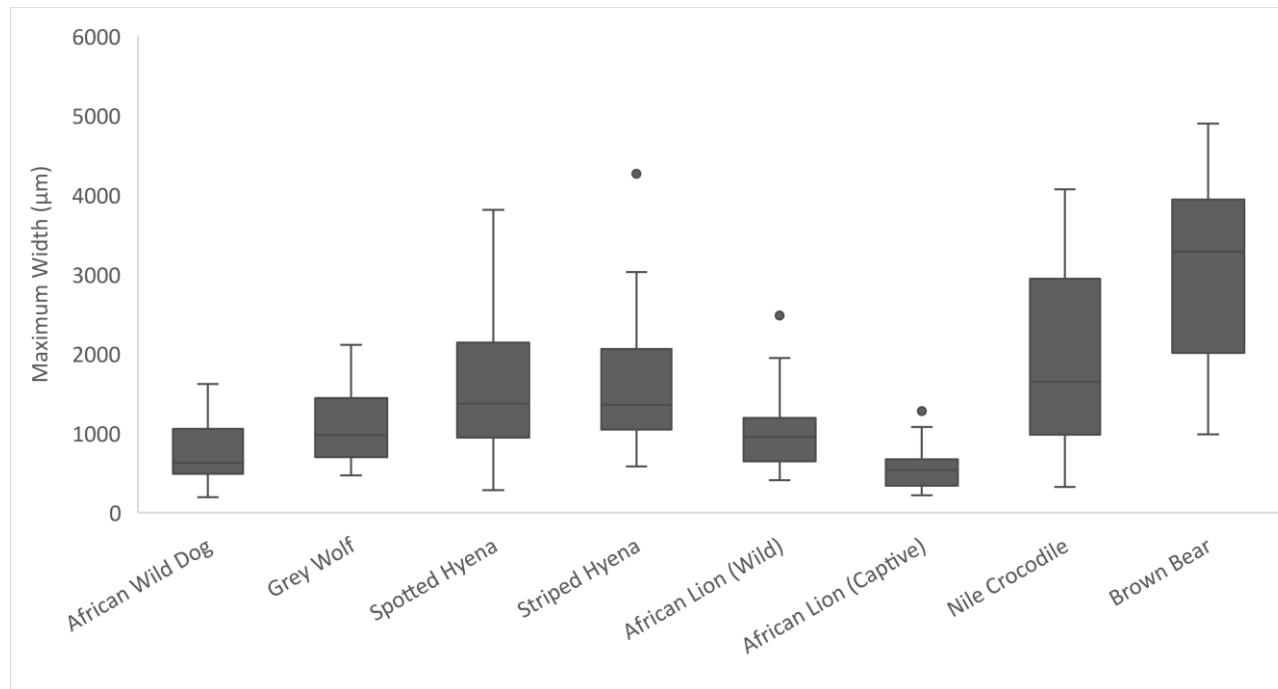


Figure 12 - Box and whisker plots for Maximum Width (3D) measurements between all carnivore species tooth marks.

Table 15 – Kruskal-Wallis and Mann-Whitney U tests for Maximum Depth (Profile) measurements between all carnivore species tooth marks. Carnivores that cannot be differentiated with this measurement metric are highlighted in yellow.

	One-way Anova		Kruskal-Wallis					
Max Depth Profile	1.62E-13		1.18E-17					
Mann-Whitney Pairwise	African Wild Dog	Grey Wolf	Spotted Hyena	Striped Hyena	Lion (Wild)	Lion (Captive)	Nile Crocodile	Grizzly Bear
African Wild Dog		0.0096340000	0.0000002222	0.0000296200	0.1644000000	0.1204000000	0.0000015120	0.0000000037
Grey Wolf	0.0096340000		0.0048970000	0.0429600000	0.3754000000	0.0000642400	0.0042510000	0.0000048030
Spotted Hyena	0.0000002222	0.0048970000		0.4570000000	0.0005925000	0.0000000018	0.3078000000	0.0078420000
Striped Hyena	0.0000296200	0.0429600000	0.4570000000		0.0077930000	0.0000000985	0.1767000000	0.0014620000
Lion (Wild)	0.1644000000	0.3754000000	0.0005925000	0.0077930000		0.0059130000	0.0005255000	0.0000038170
Lion (Captive)	0.1204000000	0.0000642400	0.0000000018	0.0000000985	0.0059130000		0.0000000225	0.0000000010
Nile Crocodile	0.0000015120	0.0042510000	0.3078000000	0.1767000000	0.0005255000	0.0000000225		0.2817000000
Grizzly Bear	0.0000000037	0.0000048030	0.0078420000	0.0014620000	0.0000038170	0.0000000010	0.2817000000	

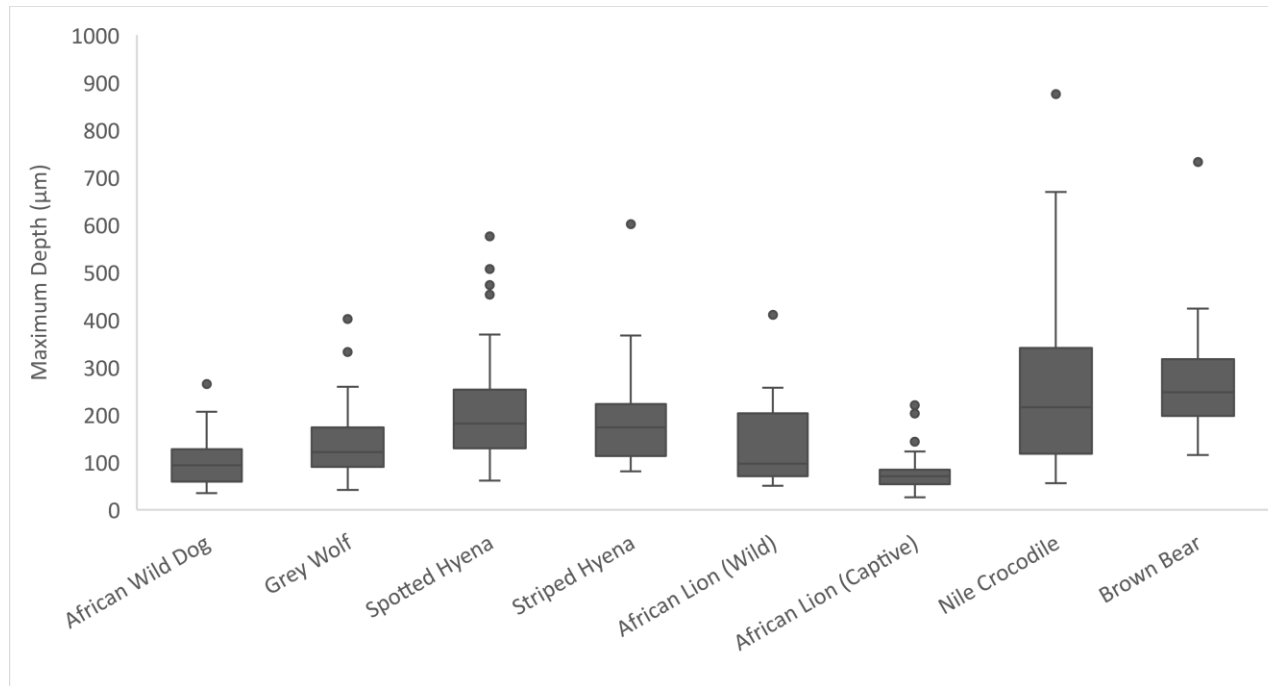


Figure 13 - Box and whisker plots for Maximum Depth (Profile) measurements between all carnivore species tooth marks.

Table 16 - Kruskal-Wallis and Mann-Whitney U tests for Area (Profile) measurements between all carnivore species tooth marks. Carnivores that cannot be differentiated with this measurement metric are highlighted in yellow.

	One-way Anova		Kruskal-Wallis					
Area Profile	1.91E-11		4.09E-21					
Mann-Whitney Pairwise	African Wild Dog	Grey Wolf	Spotted Hyena	Striped Hyena	Lion (Wild)	Lion (Captive)	Nile Crocodile	Grizzly Bear
African Wild Dog		0.0039200000	0.0000000622	0.0000053270	0.0474600000	0.0544700000	0.0000009719	0.000000013
Grey Wolf	0.0039200000		0.0039040000	0.0478600000	0.3047000000	0.0000041610	0.0029420000	0.000005609
Spotted Hyena	0.000000622	0.0039040000		0.3051000000	0.0003002000	0.000000001	0.4197000000	0.0003813000
Striped Hyena	0.0000053270	0.0478600000	0.3051000000		0.0027490000	0.000000125	0.1877000000	0.0000657200
Lion (Wild)	0.0474600000	0.3047000000	0.0003002000	0.0027490000		0.0000833800	0.0002085000	0.000001213
Lion (Captive)	0.0544700000	0.0000041610	0.000000001	0.000000125	0.0000833800		0.000000025	0.000000002
Nile Crocodile	0.0000009719	0.0029420000	0.4197000000	0.1877000000	0.0002085000	0.000000025		0.0400600000
Grizzly Bear	0.000000013	0.000005609	0.0003813000	0.0000657200	0.000001213	0.000000002	0.0400600000	

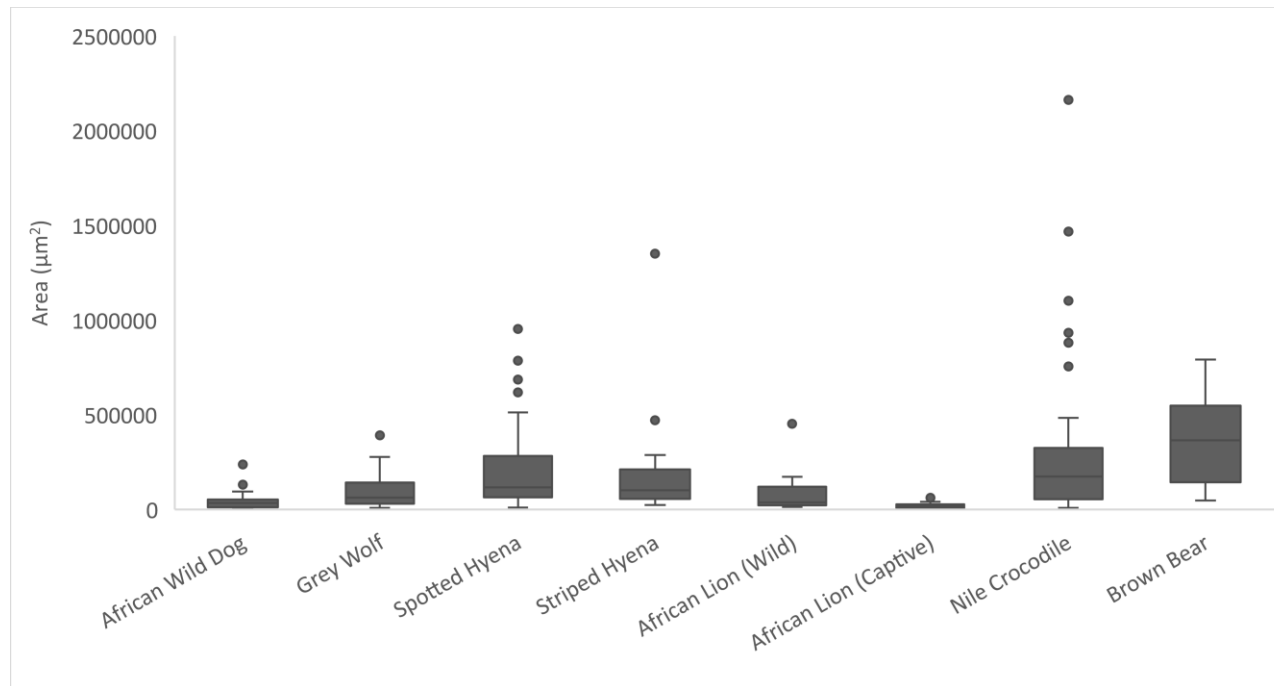


Figure 14 - Box and whisker plots for Area (Profile) measurements between all carnivore species tooth marks.

Table 17 - Kruskal-Wallis and Mann-Whitney U tests for Width (Profile) measurements between all carnivore species tooth marks. Carnivores that cannot be differentiated with this measurement metric are highlighted in yellow.

	One-way Anova		Kruskal-Wallis					
Width Profile	2.78E-26		6.90E-23					
Mann-Whitney Pairwise	African Wild Dog	Grey Wolf	Spotted Hyena	Striped Hyena	Lion (Wild)	Lion (Captive)	Nile Crocodile	Grizzly Bear
African Wild Dog		0.0008280000	0.0000001930	0.0000004266	0.0236000000	0.0313500000	0.0000004935	0.0000000007
Grey Wolf	0.0008280000		0.0162100000	0.0159100000	0.2729000000	0.0000010820	0.0057560000	0.0000000654
Spotted Hyena	0.0000001930	0.0162100000		0.9754000000	0.0006328000	0.0000000001	0.4137000000	0.0000030430
Striped Hyena	0.0000004266	0.0159100000	0.9754000000		0.0015700000	0.0000000006	0.5338000000	0.0000127200
Lion (Wild)	0.0236000000	0.2729000000	0.0006328000	0.0015700000		0.0000115500	0.0006359000	0.0000000815
Lion (Captive)	0.0313500000	0.0000010820	0.0000000001	0.0000000006	0.0000115500		0.0000000017	0.0000000002
Nile Crocodile	0.0000004935	0.0057560000	0.4137000000	0.5338000000	0.0006359000	0.0000000017		0.0002473000
Grizzly Bear	0.0000000007	0.0000000654	0.0000030430	0.0000127200	0.0000000815	0.0000000002	0.0002473000	

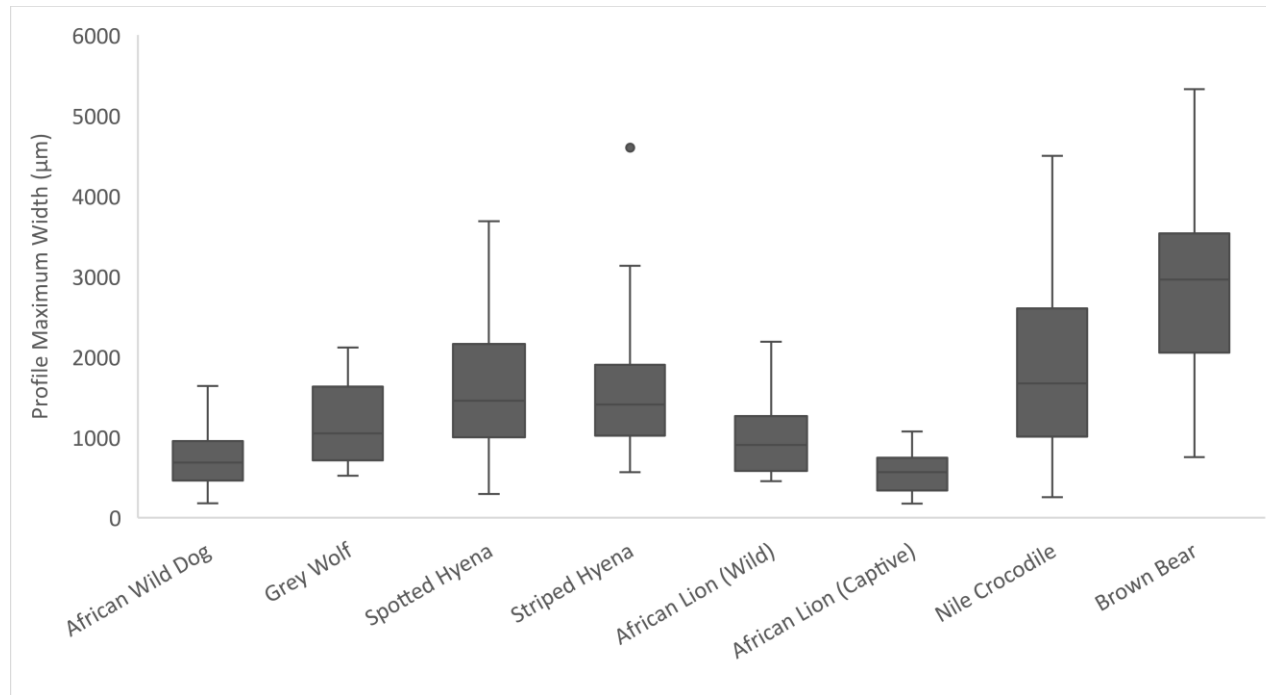


Figure 15 - Box and whisker plots for Width (Profile) measurements between all carnivore species tooth marks.

Table 18 - Kruskal-Wallis and Mann-Whitney U tests for Roughness (Profile) measurements between all carnivore species tooth marks. Carnivores that cannot be differentiated with this measurement metric are highlighted in yellow.

	One-way Anova		Kruskal-Wallis					
Roughness Profile	1.51E-14		3.90E-17					
Mann-Whitney Pairwise	African Wild Dog	Grey Wolf	Spotted Hyena	Striped Hyena	Lion (Wild)	Lion (Captive)	Nile Crocodile	Grizzly Bear
African Wild Dog		0.0202100000	0.0000076900	0.0000074870	0.1556000000	0.0370000000	0.0000080240	0.000000222
Grey Wolf	0.0202100000		0.1182000000	0.0370900000	0.1199000000	0.0001389000	0.0039540000	0.0000195500
Spotted Hyena	0.0000076900	0.1182000000		0.3485000000	0.0008095000	0.000000498	0.0341000000	0.0002115000
Striped Hyena	0.0000074870	0.0370900000	0.3485000000		0.0001550000	0.0000001758	0.2281000000	0.0069390000
Lion (Wild)	0.1556000000	0.1199000000	0.0008095000	0.0001550000		0.0028270000	0.0001585000	0.000000333
Lion (Captive)	0.0370000000	0.0001389000	0.000000498	0.0000001758	0.0028270000		0.0000000773	0.000000023
Nile Crocodile	0.0000080240	0.0039540000	0.0341000000	0.2281000000	0.0001585000	0.0000000773		0.4002000000
Grizzly Bear	0.000000222	0.0000195500	0.0002115000	0.0069390000	0.000000333	0.000000023	0.4002000000	

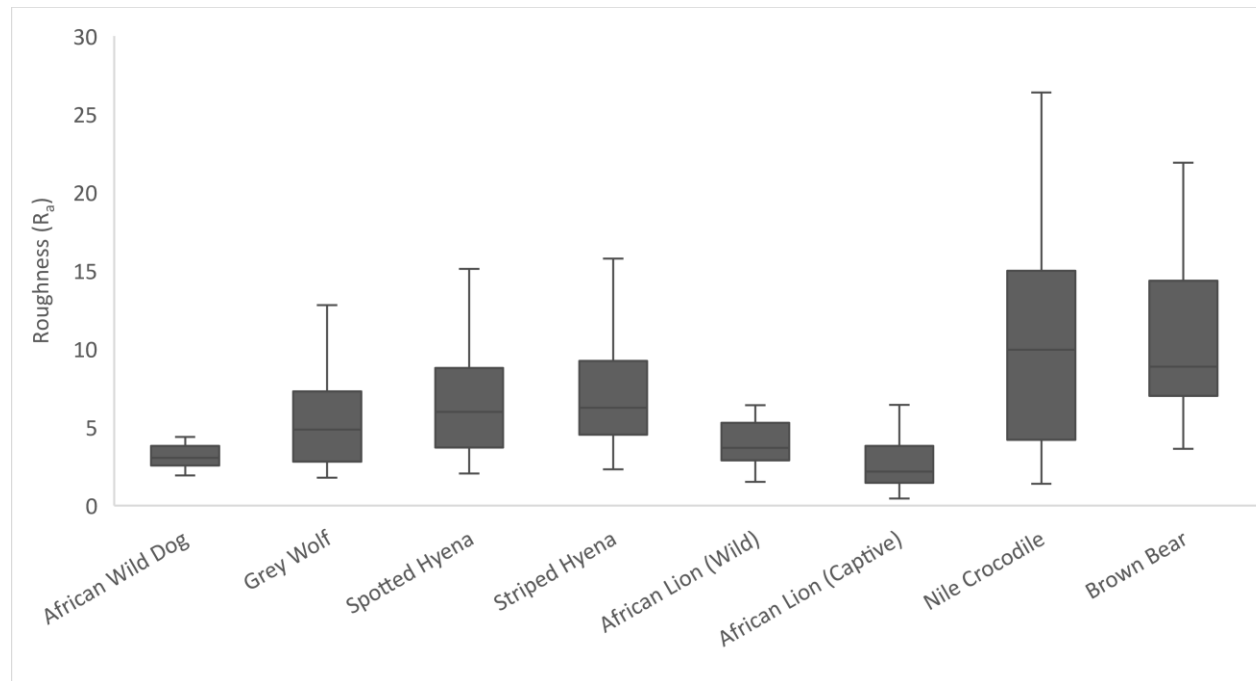


Figure 16 - Box and whisker plots for Roughness (Profile) measurements between all carnivore species tooth marks.

Table 19 - Kruskal-Wallis and Mann-Whitney U tests for Opening Angle (Profile) measurements between all carnivore species tooth marks. Carnivores that cannot be differentiated with this measurement metric are highlighted in yellow.

	One-way Anova		Kruskal-Wallis					
Opening Angle Profile	0.04474		6.66E-06					
Mann-Whitney Pairwise	African Wild Dog	Grey Wolf	Spotted Hyena	Striped Hyena	Lion (Wild)	Lion (Captive)	Nile Crocodile	Grizzly Bear
African Wild Dog		0.7787000000	0.0739600000	0.0702200000	0.6046000000	0.0808900000	0.0097220000	0.0061460000
Grey Wolf	0.7787000000		0.1995000000	0.0357300000	0.9504000000	0.1355000000	0.0169300000	0.0052150000
Spotted Hyena	0.0739600000	0.1995000000		0.0006470000	0.2157000000	0.7020000000	0.1352000000	0.0003312000
Striped Hyena	0.0702200000	0.0357300000	0.0006470000		0.0414200000	0.0014910000	0.0001230000	0.0472600000
Lion (Wild)	0.6046000000	0.9504000000	0.2157000000	0.0414200000		0.1355000000	0.0101200000	0.0109000000
Lion (Captive)	0.0808900000	0.1355000000	0.7020000000	0.0014910000	0.1355000000		0.3465000000	0.0016180000
Nile Crocodile	0.0097220000	0.0169300000	0.1352000000	0.0001230000	0.0101200000	0.3465000000		0.0003108000
Grizzly Bear	0.0061460000	0.0052150000	0.0003312000	0.0472600000	0.0109000000	0.0016180000	0.0003108000	

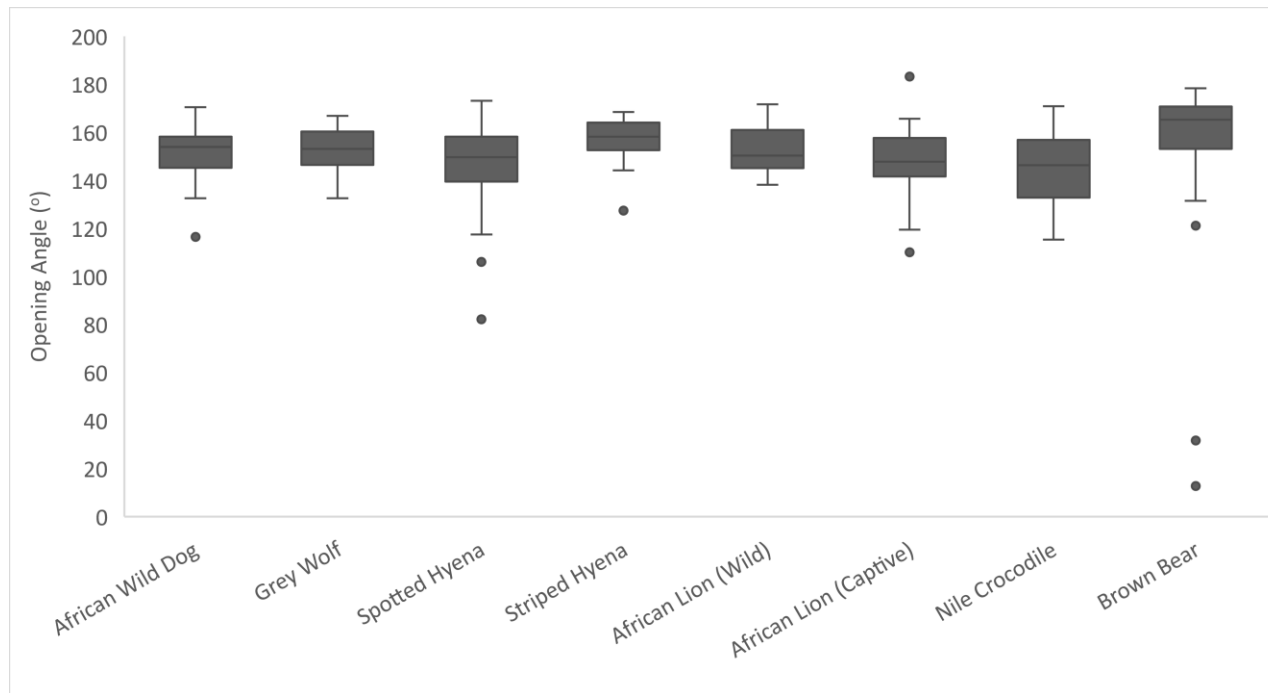


Figure 17 - Box and whisker plots for Opening Angle (Profile) measurements between all carnivore species tooth marks.

Table 20 - Kruskal-Wallis and Mann-Whitney U tests for Floor Radius (Profile) measurements between all carnivore species tooth marks. Carnivores that cannot be differentiated with this measurement metric are highlighted in yellow.

	One-way Anova		Kruskal-Wallis					
Floor Radius Profile	2.48E-17		1.25E-16					
Mann-Whitney Pairwise	African Wild Dog	Grey Wolf	Spotted Hyena	Striped Hyena	Lion (Wild)	Lion (Captive)	Nile Crocodile	Grizzly Bear
African Wild Dog		0.0623400000	0.0035570000	0.0000215200	0.2486000000	0.0179400000	0.0048680000	0.0000000315
Grey Wolf	0.0623400000		0.3026000000	0.0064970000	0.3838000000	0.0000833800	0.2754000000	0.0000006617
Spotted Hyena	0.0035570000	0.3026000000		0.0533300000	0.0317600000	0.0000009897	0.8718000000	0.0000002398
Striped Hyena	0.0000215200	0.0064970000	0.0533300000		0.0000211000	0.0000000177	0.0684600000	0.0000412800
Lion (Wild)	0.2486000000	0.3838000000	0.0317600000	0.0000211000		0.0002907000	0.0185900000	0.0000000221
Lion (Captive)	0.0179400000	0.0000833800	0.0000009897	0.0000000177	0.0002907000		0.0000023720	0.0000000059
Nile Crocodile	0.0048680000	0.2754000000	0.8718000000	0.0684600000	0.0185900000	0.0000023720		0.0000005900
Grizzly Bear	0.0000000315	0.0000006617	0.0000002398	0.0000412800	0.0000000221	0.0000000059	0.0000005900	

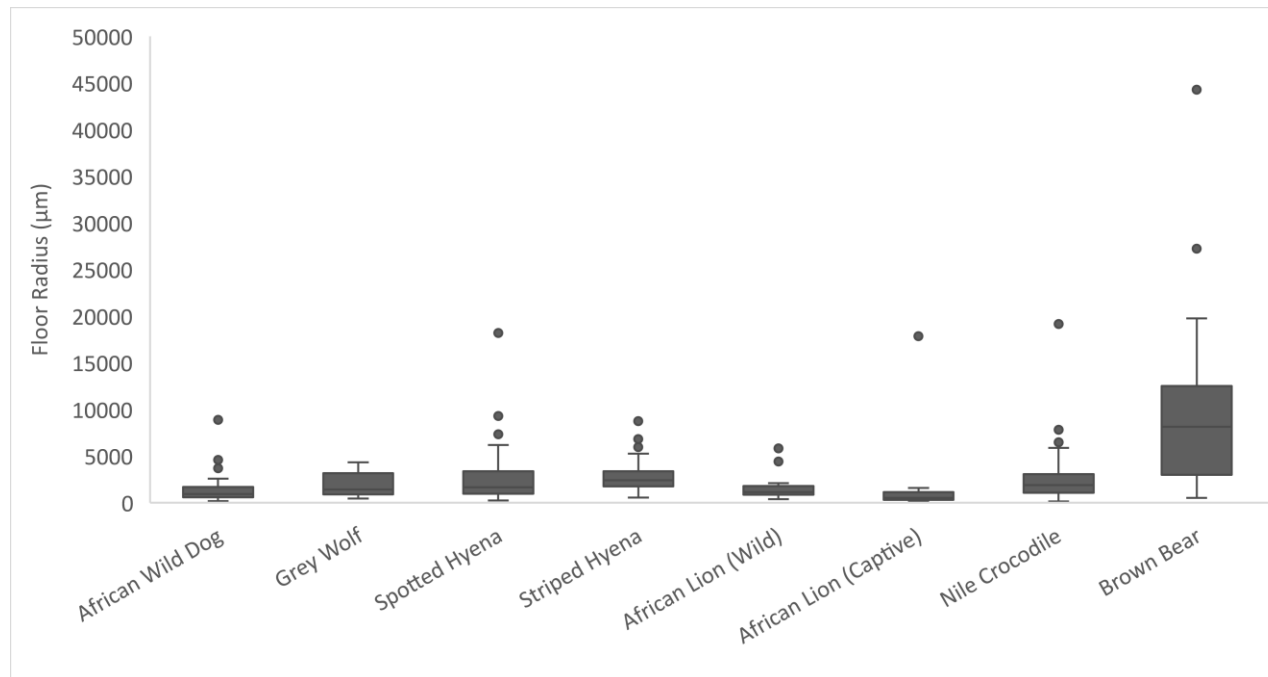


Figure 18 - Box and whisker plots for Floor Radius (Profile) measurements between all carnivore species tooth marks.

4.4 Multivariate Linear Discriminate Analysis

4.4.1 Potential to Discriminate Between Actors

Linear discriminant analyses were used to determine how accurate the recorded variables were at classifying the tooth marks of different carnivore species. Seven models were computed, grouping the carnivores by different ecological, biological, and biomechanical characteristics. Descriptions of the groupings and results of the linear discriminant analyses are displayed in Table 21. A confusion matrix shows that marks are classified correctly to their carnivore agent from a range of 49.93% for analysis of every species included in this study as a distinct group to 76.33% for analysis of species when grouped by their biomechanical capabilities related to maximum bite force. Confusion matrices for these results are displayed in Tables 22-28 and graphs displaying the results as 95% confidence intervals are displayed in Figures 19-25.

Table 21 - Summary and descriptions of linear discriminant analyses. Family level classifications are Canidae consisting of African wild dog and grey wolf, Felidae consisting of African lion, Hyaenidae consisting of spotted hyena and striped hyena, Crocodylidae consisting of Nile crocodile, and Ursidae consisting of brown bear. Biomechanical grouping is related to gross bone damage capabilities as either bone cruncher (capable of breaking size 3 bone) or flesh slicer. Species within the bone cruncher grouping include spotted hyena, striped hyena, Nile crocodile and brown bear; species within the flesh slicer grouping include African wild dog, grey wolf, and African lion.

Carnivore Grouping	Accuracy of Discriminant Analysis
All Species	49.93%
All Species, Family Level	53.62%
African Species Only	52.45%
African Species Only, Family Level	56.09%
Biomechanical, All Species	75.29%
Biomechanical, African Species Only	76.33%
Species Class, Reptilia vs. Mammalia	75.00%

Table 22 - Confusion matrix for linear discriminant analysis between all species. Accuracy of predictions is 49.93%.

	Predicted Groups							Total	
	African Wild Dog	Grey Wolf	Spotted Hyena	Striped Hyena	African Lion	Nile Crocodile	Brown Bear		
Given Groups	African Wild Dog	25	1	2	0	2	1	0	31
	Grey Wolf	9	11	4	0	4	1	0	29
	Spotted Hyena	6	9	26	4	5	6	2	58
	Striped Hyena	2	8	5	9	1	1	4	30
	African Lion	16	4	5	4	24	5	0	58
	Nile Crocodile	1	4	7	3	7	18	3	43
	Brown Bear	0	1	2	5	1	2	17	28
	Total	59	38	51	25	44	34	26	277

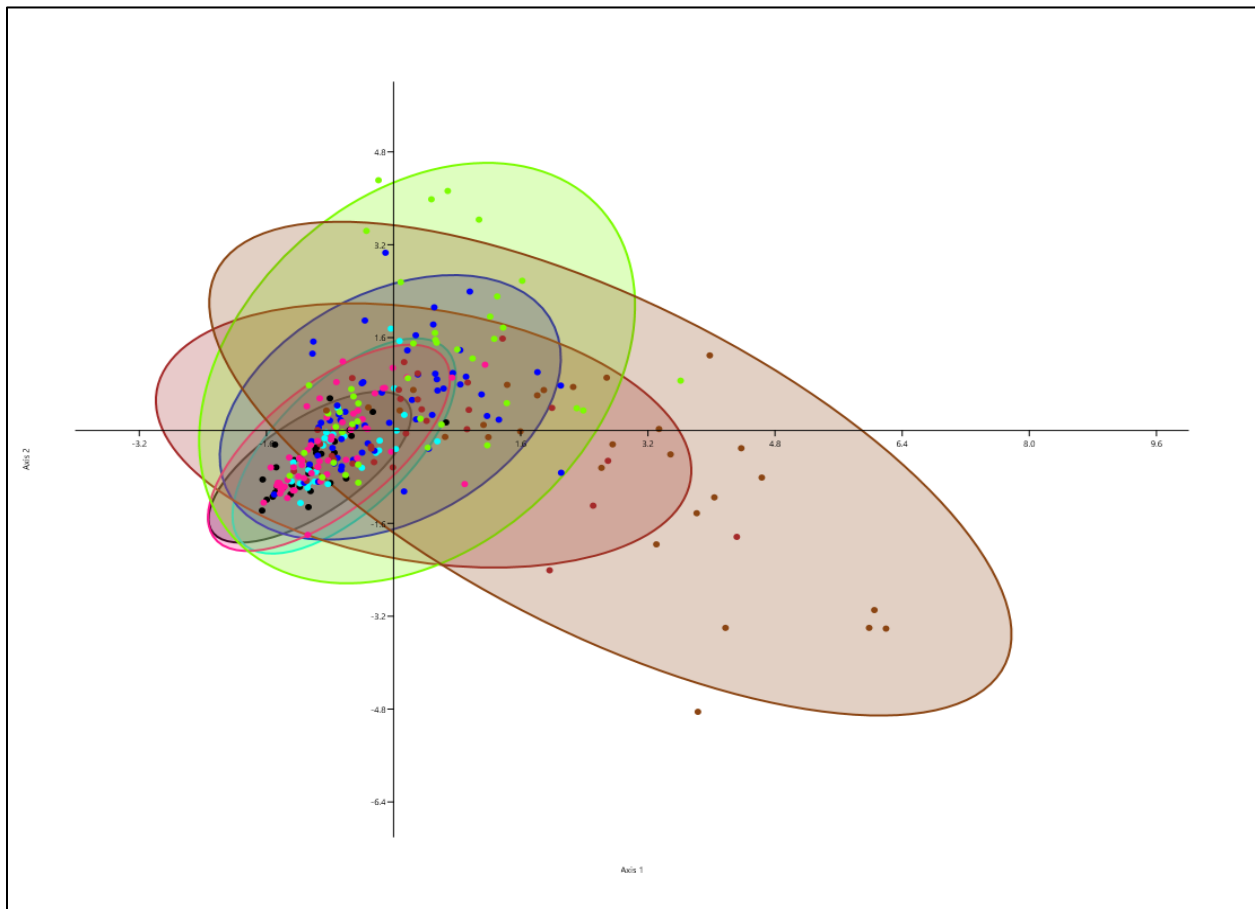


Figure 19 - Graph showing results of linear discriminant analysis between all species as 95% confidence intervals. Results are based on measured variables shown in Appendix A. Shaded areas represent 95% confidence intervals for samples. Brown dots represent brown bears, green dots represent Nile crocodiles, blue dots represent spotted hyena, red dots represent striped hyena, pink dots represent African lions, teal dots represent grey wolf, and black dots represent African wild dogs.

Table 23 - Confusion matrix for linear discriminant analysis between all species at the family level. Accuracy of predictions is 53.62%. Canidae consists of African wild dog and grey wolf, Hyaenidae consist of striped hyena and spotted hyena, Felidae consist of African lion, Crocodylidae consist of Nile crocodile, and Ursidae consist of brown bear.

		Predicted Groups					Total
		Canidae	Hyaenidae	Felidae	Crocodylidae	Ursidae	
Given Groups	Canidae	42	11	5	2	0	60
	Hyaenidae	23	37	10	12	6	88
	Felidae	17	9	28	4	0	58
	Crocodylidae	3	7	11	19	3	43
	Ursidae	0	5	2	4	17	28
Total		85	69	56	41	26	277

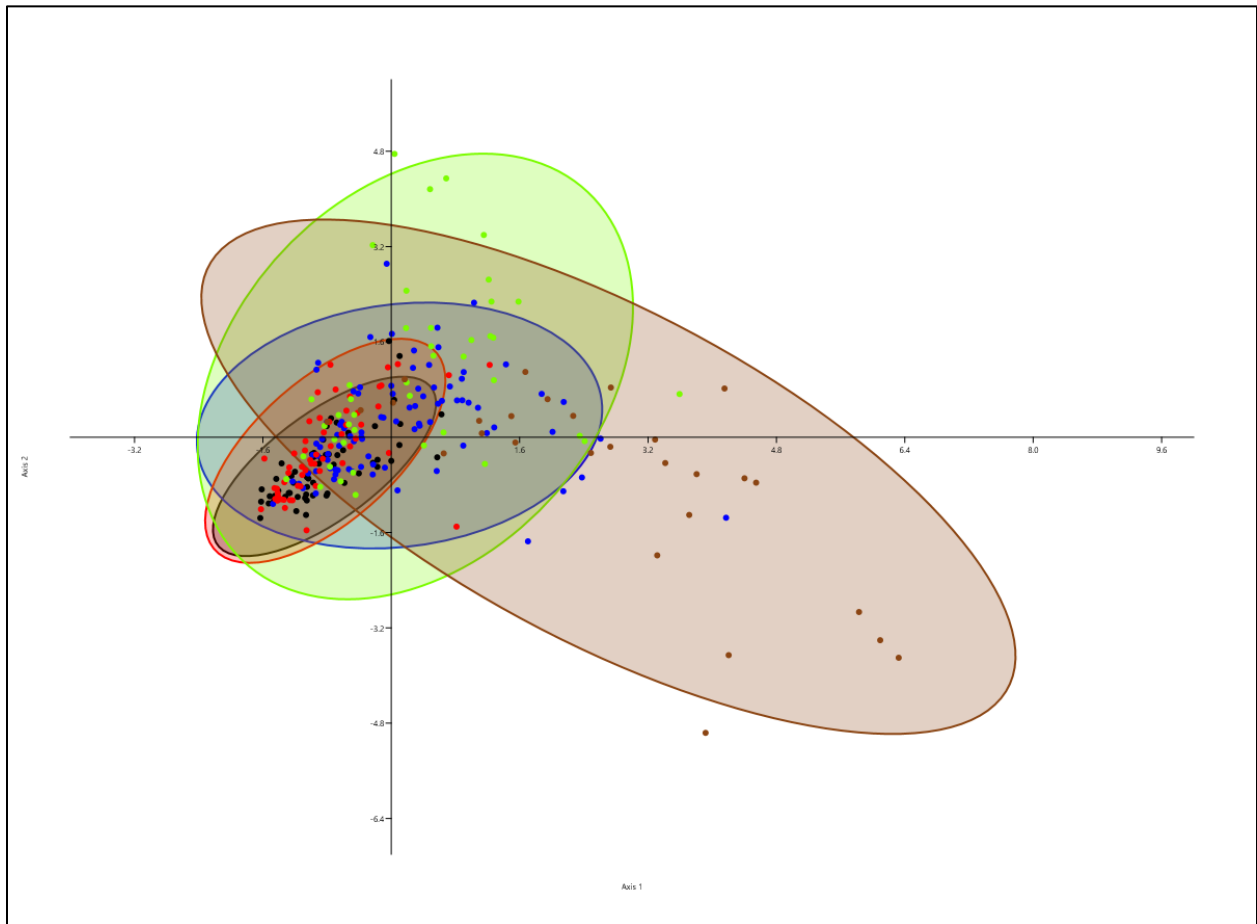


Figure 20 - Graph showing results of linear discriminant analysis between all species at the family level as 95% confidence intervals. Results are based on measured variables shown in Appendix A. Shaded areas represent 95% confidence intervals for samples. Brown dots represent ursids (brown bear), green dots represent crocodylids (Nile crocodile), blue dots represent hyaenids (striped hyena and spotted hyena), red dots represent felids (African lion), and black dots represent canids (African wild dog and grey wolf).

Table 24 - Confusion matrix for linear discriminant analysis between all African species. Accuracy of predictions is 52.45%.

		Predicted Groups					Total
		African Wild Dog	Spotted Hyena	Striped Hyena	African Lion	Nile Crocodile	
Given Groups	African Wild Dog	25	2	0	2	2	31
	Spotted Hyena	11	27	4	6	10	58
	Striped Hyena	9	6	12	1	2	30
	African Lion	17	6	2	28	5	58
	Nile Crocodile	3	9	2	10	19	43
Total		65	50	20	47	38	220

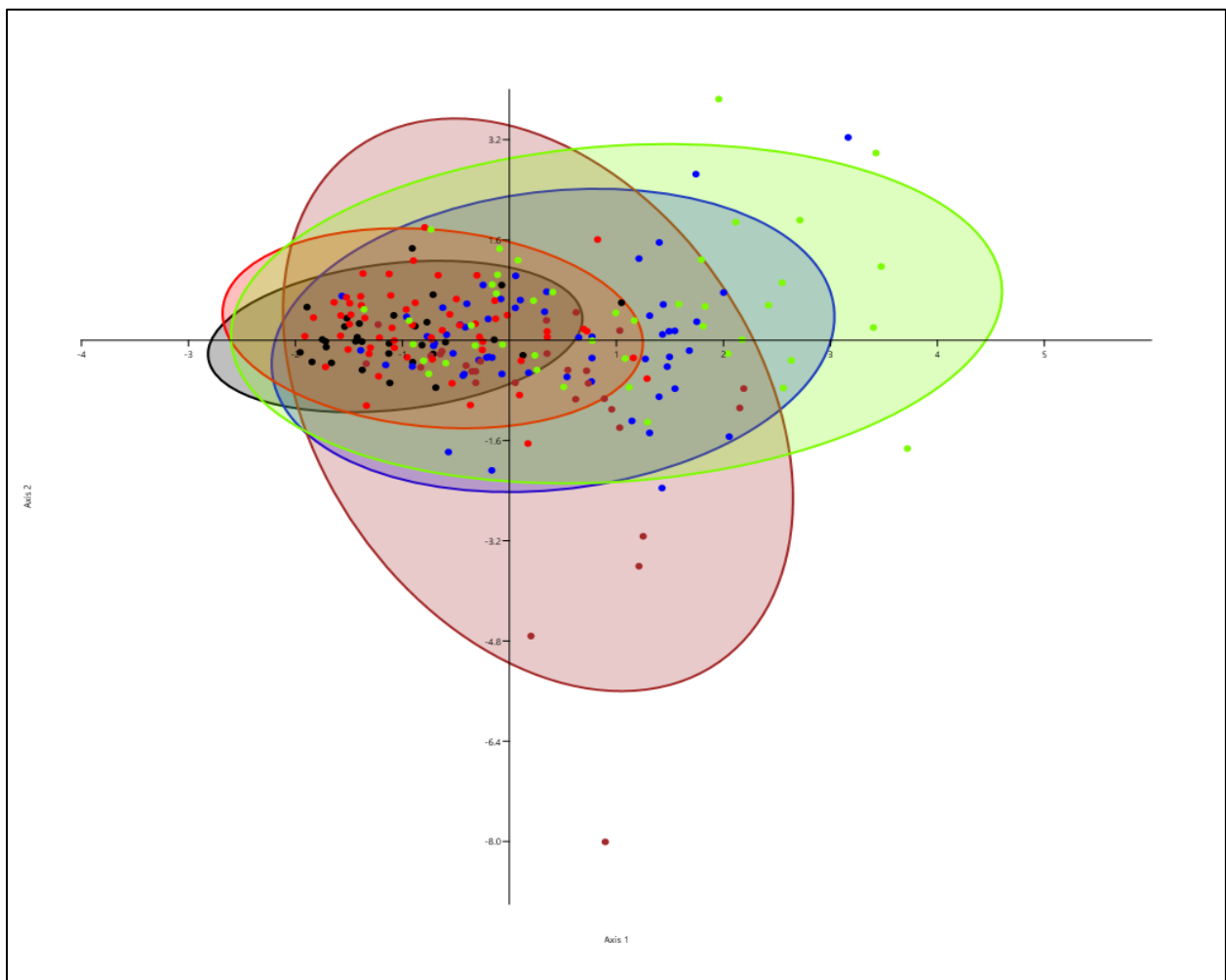


Figure 21 - Graph showing results of linear discriminant analysis between all African species as 95% confidence intervals. Results are based on measured variables shown in Appendix A. Shaded areas represent 95% confidence intervals for samples. Green dots represent Nile crocodile, brown dots represent striped hyena, blue dots represent spotted hyena, red dots represent African lion, and black dots represent African wild dog.

Table 25 - Confusion matrix for linear discriminant analysis between all African species at the family level. Accuracy of predictions is 56.09%. Canidae consists of African wild dog, Hyaenidae consists of striped hyena and spotted hyena, Felidae consists of African lion, and Crocodylidae consists of Nile crocodile.

		Predicted Groups				Total
		Canidae	Hyaenidae	Felidae	Crocodylidae	
Given Groups	Canidae	25	2	2	2	31
	Hyaenidae	21	42	12	13	88
	Felidae	17	7	30	4	58
	Crocodylidae	3	7	11	22	43
Total		66	58	55	41	220

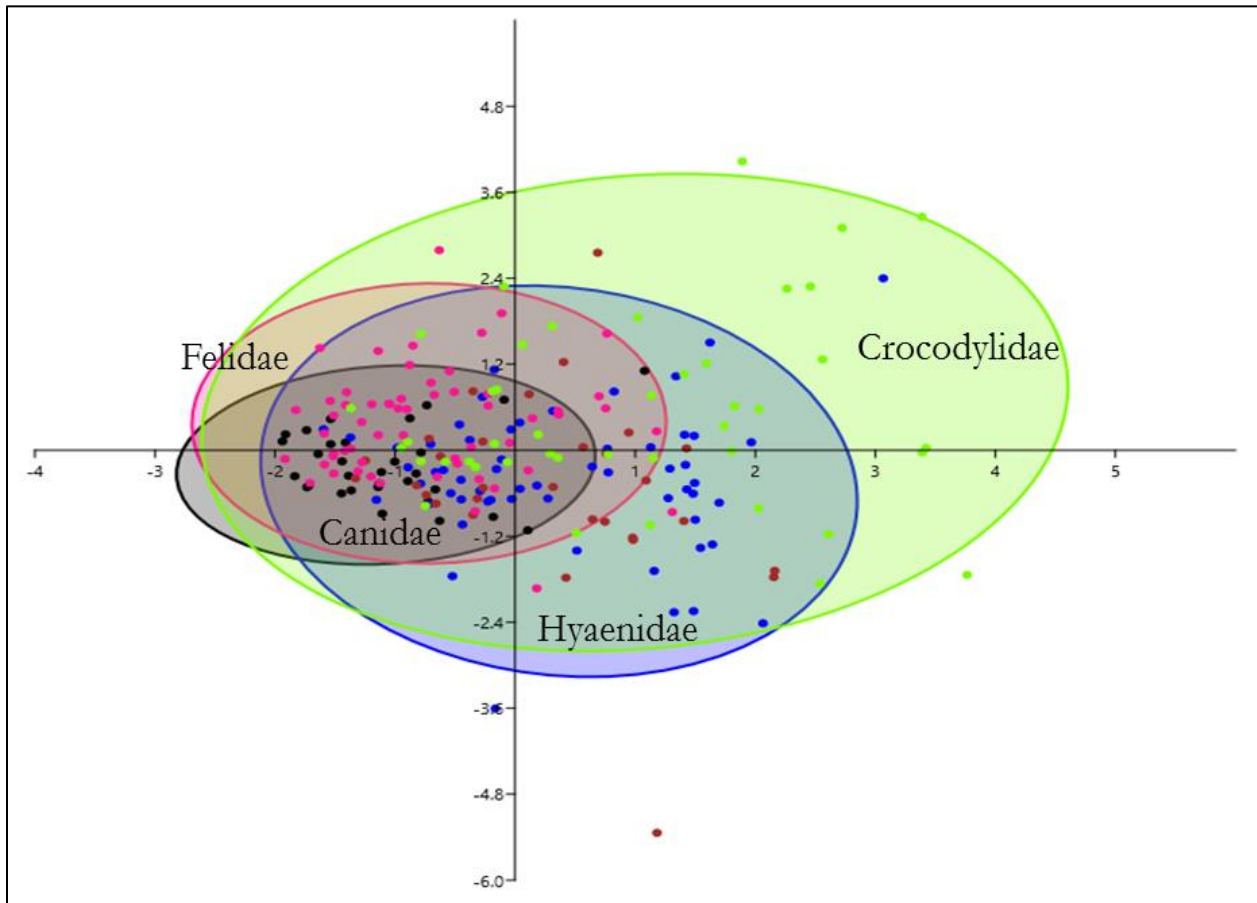


Figure 22 - Graph showing results of linear discriminant analysis between all African species at the family level as 95% confidence intervals. Results are based on measured variables shown in Appendix A. Shaded areas represent 95% confidence intervals for samples. Green dots represent crocodylian (Nile crocodile), blue dots represent hyaenids (striped hyena and spotted hyena), pink dots represent felids (African lion), and black dots represent Canids (African wild dog).

Table 26 - Confusion matrix for linear discriminant analysis between all species grouped biomechanically. Accuracy of predictions is 75.29%. Flesh slicers consist of African wild dog, grey wolf, and African lion. Bone crunchers consist of striped hyena, spotted hyena, brown bear, and Nile Crocodile.

		Predicted Groups		
		Flesh Slicer	Bone Cruncher	Total
Given Groups	Flesh Slicer	97	21	118
	Bone Cruncher	53	106	159
Total		150	127	277

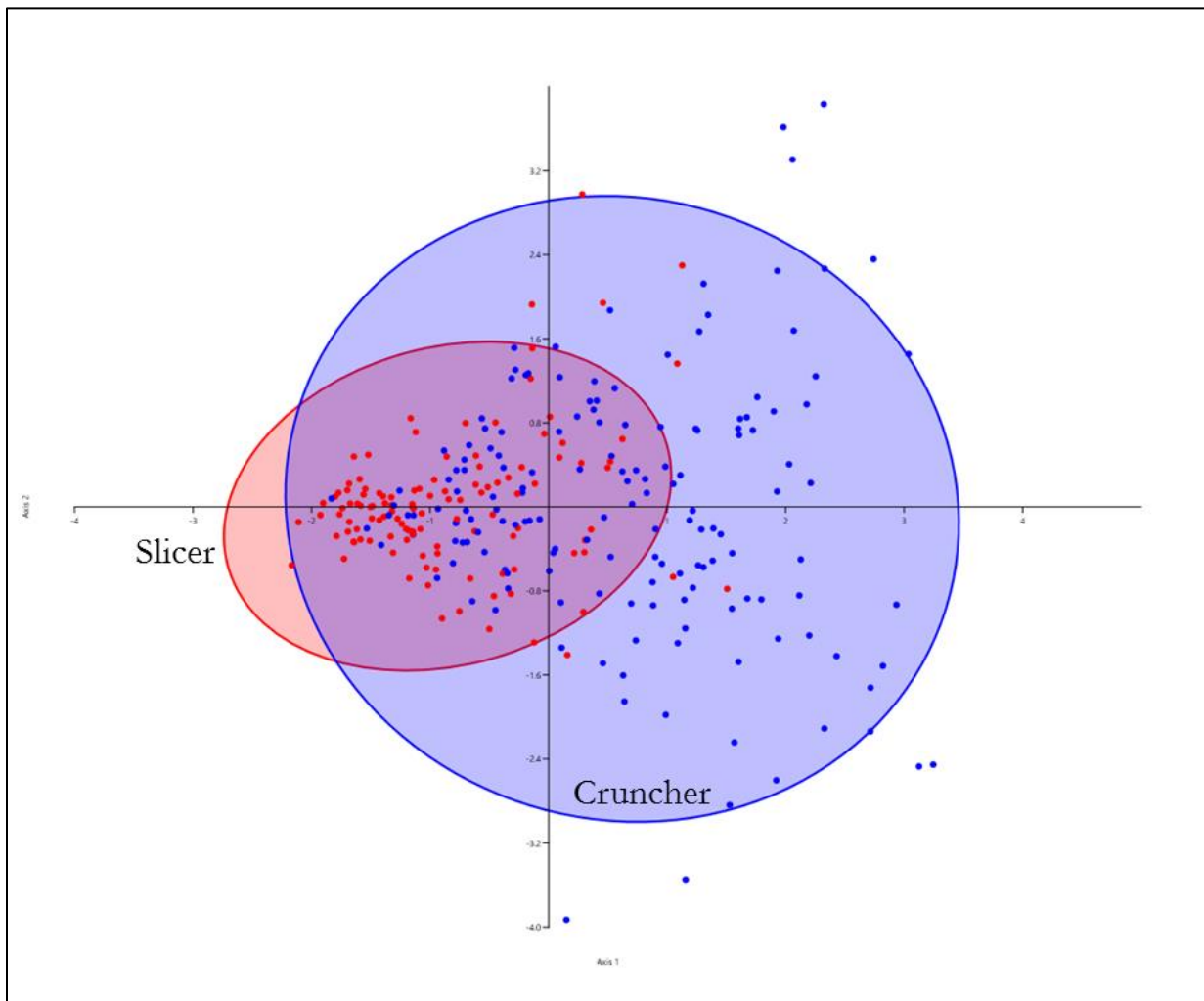


Figure 23 - Graph showing results of linear discriminant analysis between all species grouped biomechanically as 95% confidence intervals. Results are based on measured variables shown in Appendix A. Shaded areas represent 95% confidence intervals for samples. Blue dots represent bone crunchers and red dots represent flesh slicers.

Table 27 - Confusion matrix for linear discriminant analysis between all African species grouped biomechanically. Accuracy of predictions is 76.33%. Flesh slicers consist of African wild dog and African lion. Bone crunchers consists of striped hyena, spotted hyena, and Nile crocodile.

		Predicted Groups		
		Flesh Slicer	Bone Cruncher	Total
Given Groups	Flesh Slicer	73	16	89
	Bone Cruncher	42	89	131
Total		115	105	220

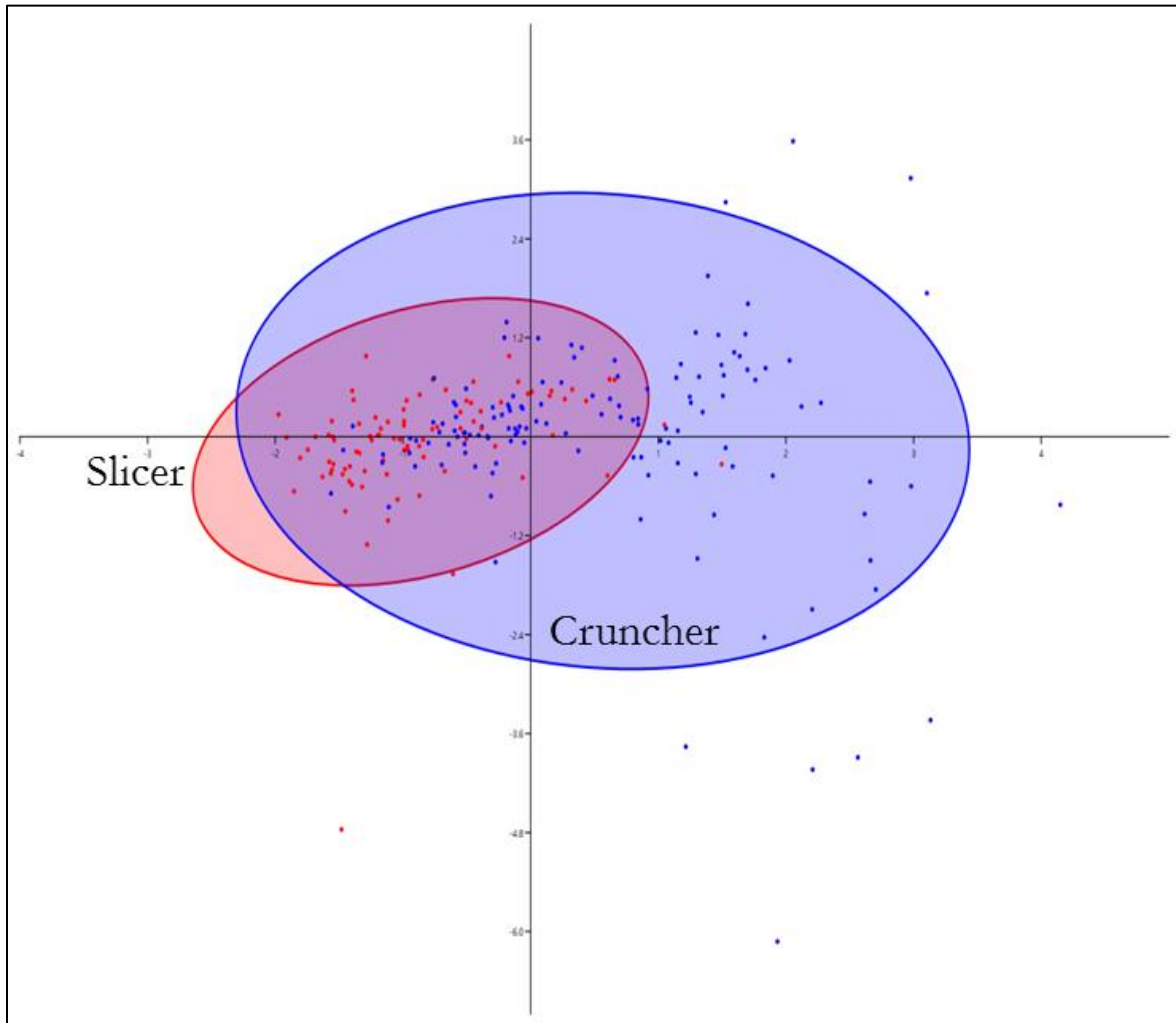


Figure 24 - Graph showing results of linear discriminant analysis between all African species grouped biomechanically as 95% confidence intervals. Results are based on measured variables shown in Appendix A. Shaded areas represent 95% confidence intervals for samples. Blue dots represent bone crunchers (striped hyena, spotted hyena, and Nile Crocodile) and red dots represent flesh slicers (African wild dog and African lion).

Table 28 - Confusion matrix for linear discriminant analysis between Reptilia and Mammalia species classes. Accuracy of predictions is 75%. Reptilia consist of Nile crocodile. Mammalia consist of African wild dog, African lion, striped hyena, and spotted hyena.

		Predicted Groups		
		Mammalia	Reptilia	Total
Given Groups	Mammalia	139	38	177
	Reptilia	17	26	43
Total		156	64	220

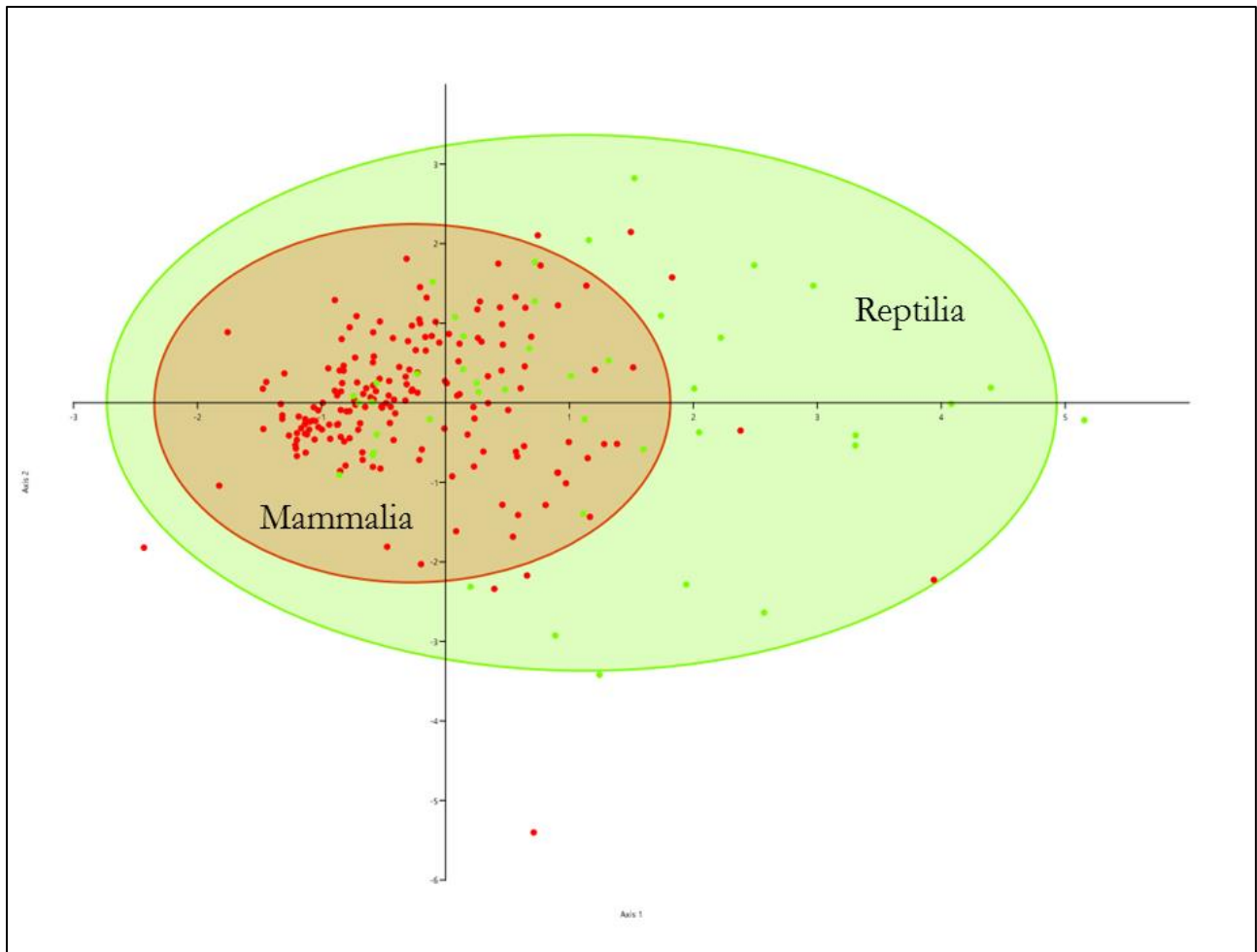


Figure 25 - Graph showing results of linear discriminant analysis between Reptilia and Mammalia species class as 95% confidence intervals. Results are based on measured variables shown in Appendix A. Shaded areas represent 95% confidence intervals for samples. Green dots represent Reptilia (Nile crocodile) and red dots represent Mammalia (African wild dog, African lion, striped hyena, and spotted hyena) species classes.

4.4.2 Comparisons Between Animal Pairs

Analysis was conducted between each animal pairing to determine how distinguishable they are by their tooth mark morphology on an individual basis. Multivariate linear discriminant analysis demonstrates the accuracy of this method for distinguishing specific carnivore actors by their tooth mark morphology. A confusion matrix shows that marks are classified correctly from a range of 69.61% for spotted hyena and Nile crocodile to 97.19% accuracy for African lion and brown bear; results for all species comparisons are displayed in Table 29. Notable species comparisons between the African lion and the hyenas (86.23% accuracy), hyenas and Nile crocodile (74.70% accuracy), African wild dog and African lion (79.28% accuracy), and grey wolf and brown bear (96.49% accuracy) are examined with further detail in chapter 5.

Table 29 - Species Comparisons between every carnivore included in this study.

Species Comparison	Accuracy of Discriminant Analysis
African Wild Dog & Grey Wolf	83.33%
African Wild Dog & Spotted Hyena	82.22%
African Wild Dog & Striped Hyena	91.80%
African Wild Dog & African Lion	79.28%
African Wild Dog & Nile Crocodile	87.84%
African Wild Dog & Brown Bear	98.31%
Grey Wolf & Spotted Hyena	76.45%
Grey Wolf & Striped Hyena	79.66%
Grey Wolf & African Lion	85.76%
Grey Wolf & Nile Crocodile	80.56%
Grey Wolf & Brown Bear	96.49%
Spotted Hyena & Striped Hyena	70.79%
Spotted Hyena & African Lion	83.34%
Spotted Hyena & Nile Crocodile	69.61%
Spotted Hyena & Brown Bear	89.66%
Striped Hyena & African Lion	90.50%
Striped Hyena & Nile Crocodile	79.45%
Striped Hyena & Brown Bear	81.03%
All Hyena & Nile Crocodile	74.70%
All Hyena & African Lion	86.23%
All Hyena & African Wild Dog	79.17%
African Lion & Nile Crocodile	83.20%
African Lion & Brown Bear	97.19%
Nile Crocodile & Brown Bear	85.92%

4.4.3 Inferred fossil trace marks

Fossil trace marks were computed in the African family level and biomechanical discriminant analyses (56.09% and 76.33% accuracy). Fossil trace marks are shown as the large red X's in Figure 26 and classifications can be seen in Table 30. There is a wide distribution of actors present in this fossil assemblage. All fossil trace marks match between models except for one trace mark shown as a large yellow x in Figure 26. Four archaeological trace marks do not classify with any carnivore from the actualistic sample, these four trace marks do not fall outside of the models but rather between multiple actors.

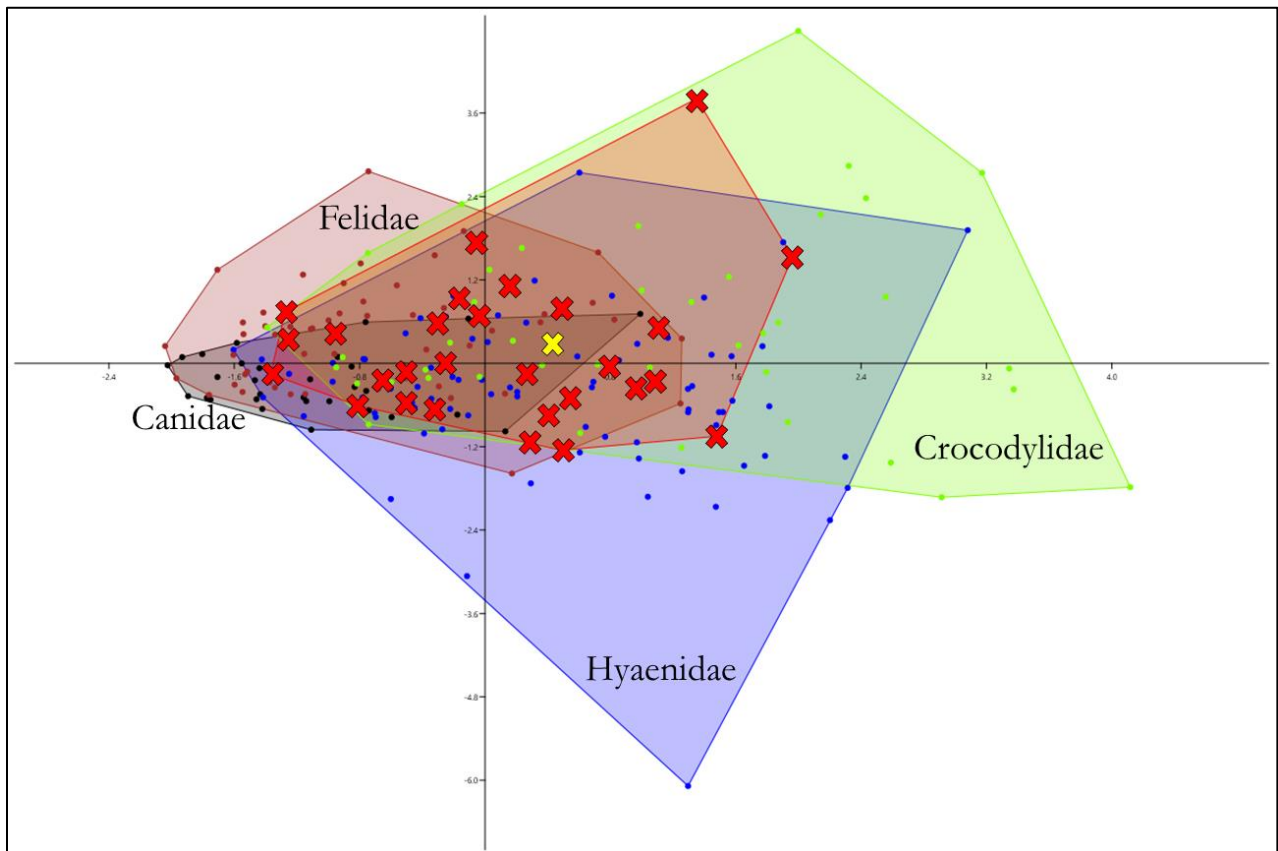


Figure 26 - Graph showing results of limited discriminant analysis as convex hulls with fossil trace marks within the African family level discriminant analysis. Results are based on measured variables shown in Appendix A. Shaded areas represent absolute ranges for the samples. Green dots represent Crocodylian, blue dots represent Hyaenids, pink dots represent Felids, and black dots represent Canids. Fossil trace marks are represented by a red X, the yellow X represents the dual classified fossil trace mark.

Table 30 – Classifications for fossil trace marks. Results are based on measured variables shown in Appendix B. See Bunn (1982) for prey size (Size 1 <23kg; Size 2, 23-114kg; Size 3, 114-341kg).

Identification Number	Skeletal Element	Tooth Mark Location	Prey Taxon, Body Size	Family Level Classification	Biomechanical Classification
1652	Radius	Near Epiphysis	Bovid, 3	Felidae	Flesh Slicer
4242	Metacarpal	Epiphysis	Bovid, 3	Felidae	Flesh Slicer
4268	Femur	Midshaft	Indeterminate, 3	Felidae	Bone Cruncher
2743	Long Bone	Midshaft	Indeterminate, 3	Felidae	Flesh Slicer
4168	Humerus	Epiphysis	Indeterminate, 3	Felidae	Flesh Slicer
4176B1	Radius	Midshaft	Bovid, 3	Felidae	Flesh Slicer
4176B2	Radius	Midshaft	Bovid, 3	Felidae	Flesh Slicer
1886A	Scapula	Blade	Indeterminate, 3	Felidae	Flesh Slicer
60275	Rib	Head	Indeterminate, 3	Felidae	Flesh Slicer
4176B3	Radius	Midshaft	Bovid, 3	Canidae	Flesh Slicer
1886B	Scapula	Blade	Indeterminate, 3	Canidae	Flesh Slicer
60021A	Metapodial	Midshaft	Indeterminate, 3	Canidae	Flesh Slicer
60021B	Metapodial	Midshaft	Indeterminate, 3	Canidae	Flesh Slicer
4107	Metapodial	Midshaft	Bovid, 3	Hyaenidae	Bone Cruncher
1975	Long Bone	Near Epiphysis	Indeterminate, 3	Hyaenidae	Bone Cruncher
677A	Humerus	Head	Indeterminate, 3	Hyaenidae	Bone Cruncher
677B	Humerus	Head	Indeterminate, 3	Hyaenidae	Bone Cruncher
60050	Long Bone	Midshaft	Indeterminate, 3	Hyaenidae	Bone Cruncher
2908B	Calcaneum	Body	Bovid, 3	Crocodylidae	Bone Cruncher
4176A	Radius	Midshaft	Bovid, 3	Crocodylidae	Bone Cruncher
1045A	Humerus	Midshaft	Indeterminate, 3	Crocodylidae	Bone Cruncher
1045B	Humerus	Midshaft	Indeterminate, 3	Crocodylidae	Bone Cruncher
1045C	Humerus	Midshaft	Indeterminate, 3	Crocodylidae	Bone Cruncher
3969	Cervical Vertebra	Zygopophysis	Indeterminate, 3	Crocodylidae	Bone Cruncher
60025	Long Bone	Midshaft	Indeterminate, 3	N/A	N/A
356	Tibia	Midshaft	Indeterminate, 3	N/A	N/A
3833A	Tibia	Midshaft	Indeterminate, 3	N/A	N/A
3833B	Tibia	Midshaft	Indeterminate, 3	N/A	N/A

CHAPTER 5 DISCUSSION

Due to the paucity of carnivore remains in the archeological record, linking specific carnivores to feeding traces found on fossil bones is critical to reconstructing the ecological and behavioral contexts of Early Stone Age archaeological sites. Archaeological sites from the Early Stone Age often have dual-patterned faunal assemblages that bear both hominin butchery marks and carnivore tooth marks, but few body fossils of hominins or carnivores. Analysis of these feeding traces can refine our knowledge of past hominin and carnivore interactions as hominins began encroaching on the carnivore guild by regularly consuming flesh and marrow.

The application of high-resolution 3D scanning to the analysis of carnivore tooth mark morphology has provided a level of inference and confidence unattainable with previous methods and a higher level of confidence compared to recently employed micro photogrammetry (Mate-Gonzalez et al 2016; Arriaza et al. 2017). Although results are not 100% accurate in distinguishing between the tooth marks of different carnivore species, this project has greatly improved upon previous research which displayed only weak correlations between body size and tooth mark size (Dominguez-Rodrigo & Piqueras 2003; Delaney-Rivera et al. 2009). For example, within this thesis, when African carnivores are examined at the family level in a limited discriminate analysis, taxa can be discriminated with 56.09% accuracy and increased to 76.33% accuracy when examined by their biomechanical feeding classification. Furthermore, when carnivores are compared in pairs, accuracy increases to the 80th and 90th percentiles depending on taxa examined. Ultimately, high-resolution 3D scanning provides an accurate and precise method with which to identify specific carnivore actors from their feeding traces. Building upon this dataset will continue to enhance our ecological reconstructions of Early Stone Age archeological sites and early hominin behavior.

5.1 Interpretation of Results

5.1.1 Potential and Accuracy of Molding Materials

Previous research tested the comparative accuracy of cut mark replicas (Bello 2011). However, this study was limited in sample size (n of 3) and did not examine carnivore tooth marks. For these reasons, a larger sample of carnivore tooth marks (n of 30) was compared between scans of the original marks and replicas of the same marks, ensuring confidence in the use of replicas in this thesis.

The results of this comparison demonstrated that the mold replicas provided accurate representations and were statistically indistinguishable from the original marks for nine out of twelve measurements. Discrepancy between these measurements and the results of previous research that analyzed cut mark morphology (Bello 2011) is likely due to the molding material not capturing the entire curvature of the bone as tooth marks are significantly deeper and wider than cut marks. Furthermore, Bello (2011) did not have a sufficient sample size and their reported results cannot be reliably compared against. Various scanning and processing procedures such as rescanning along the opposite axis and adjusting the polynomial degree when isolating the mark during initial processing (Figure 1) were tested to confirm that these discrepancies were not due to methodology or user error. However, these changes did not improve the results. This discrepancy is a concern for the lion sample due to the wild lion tooth mark sample being scanned from replicas of the original tooth marks. However, when analyzed with a *t*-test, the replicas of the wild lion sample shows significantly greater values for nine of twelve measurements rather than an expected decrease, suggesting the discrepancy is likely due to other variables such as carnivore body size, bone type, flesh availability, body size, or level of competition, which are all variables that can affect tooth mark morphology (Blumenschine 1988;

Lam 1992; Blumenschine & Marean 1993; Pobiner 2007; Faith 2007; Gidna et al. 2013; Nascou & Mori 2014).

5.1.2 Sources of Variation between wild and captive animals

Previous research has cautioned against the use of captive animals to characterize the behavior and patterns of feeding traces left by carnivore species (Faith 2007; Gidna 2013; Dominguez-Rodrigo et al. 2015). However, difference between wild and captive animals are not as likely to impact tooth mark morphology, which is more directly related to tooth size and biomechanical constraints. Furthermore, utilization of captive animals allows for control over variables such as carnivore age, body size, prey size, and bone type which have been shown to affect tooth mark morphology (Blumenschine 1988; Lam 1992; Blumenschine & Marean 1993; Pobiner 2007; Faith 2007; Gidna et al. 2013; Nascou & Mori 2014). Nevertheless, the cause of the discrepancy between wild and captive lions must be examined.

The age and body size of a carnivore can affect the size and morphology of tooth marks. Previous research has shown a correlation between carnivore body size and tooth mark size (Delaney-Rivera et al. 2009). The captive lions included in this study were relatively young and not yet at their adult body weight (see Table 3 in Chapter 3). Conversely, there is no difference between the captive hyena and the wild hyena samples. Captive hyenas included within this study are at their adult body weight and similar to the African lions were fed prey they are known to feed on in the wild (Blumenschine 1988; Dominguez-Rodrigo 1999; Pobiner 2007). The similarity between the captive and wild hyena samples indicates differences in body size between the captive and wild African lions is likely the main variable responsible for the incongruity between samples; unfortunately, the body weight of the wild African lions is

unknown. Nevertheless, combining these distinct samples provides a more complete characterization of the diversity of tooth mark morphology for one carnivore taxa.

5.1.3 Potential to discriminated between actors

Due to the similarities between carnivore tooth size and morphology, the results are wide ranging and produce variable levels of accuracy between models. Analysis of individual measurement metrics showed that each metric was suitable for differentiating between carnivores; however, no metric was 100% accurate and all metrics could not differentiate between at least two carnivore pairs. These findings indicate the need for a multivariate approach where all measured variables are analyzed simultaneously for each carnivore tooth mark.

If all tooth marks and their measured variables are computed into a limited discriminant analysis without further grouping, the level of accuracy is only 49.93%. However, the application of high-resolution 3D scanning to taphonomy is not intended to dismiss previous methods; rather, this approach provides a novel and significant aid to biomechanical, behavioral, and ecological interpretations of a carnivore's taphonomic imprint. These additional methods can inform our analysis and allow for further classification and realistic grouping of carnivores for statistical analysis.

Grouping carnivore actors where appropriate can produce higher accuracy and effectively increase the 49.93% accuracy to the 80-90% range. Examination of the confusion matrices and post-hoc Mann-Whitney U tests show the majority of the overlap is present between carnivores with lower bite force - the grey wolf, African wild dog, and African lion. Additionally, there is overlap between the larger bone crunching spotted hyena, striped hyena, Nile crocodile, and brown bear which produce small tooth marks that misclassify with the tooth marks of smaller

carnivores. Once this overlap is eliminated through further classification and grouping, the discriminatory power of 3D scanning methods is substantially increased.

Limiting analysis to African carnivores at the family level provides a higher level of accuracy (56.09%). However, the data still presents large overlap between the African wild dog, African lion, and some of the spotted hyena sample, as all three of these animals produce small pits and scores that even at our degree of analysis are difficult to differentiate. Therefore, low accuracy in this model is likely due to all carnivores producing small tooth marks which misclassify in other groupings. Hyenas have a wide distribution as they have small tooth pits that classify with canids and larger tooth pits that classify with crocodiles. Most felid tooth marks are accurately grouped but a portion of their shorter shallower tooth scores classify with canids. Smaller marks produced by crocodiles classify with the felids and some of their mid-sized tooth marks classify with hyenas. The African wild dog has the lowest bite force and smallest tooth marks with very narrow and short scores and shallow pits, allowing African wild dog tooth marks to classify with the highest accuracy.

When carnivores are grouped by the biomechanical capabilities of their mandible and cranial vault in relation to gross bone damage, accuracy increases to 76.33%. The biomechanical groupings are split between obligate flesh slicing carnivores with low bite force and carnivores with high bite force that are capable of breaking bone. Flesh slicers in this model consist of the African wild dog and lion; bone crunchers in this model are the spotted hyena, striped hyena, and Nile crocodile. Accuracy in this model is still limited by bone crunchers, who although possessing an extremely high bite force also produce small tooth marks that misclassify with the tooth marks of flesh slicers.

Accuracy of these models increases greatly when comparing one species to another, which could be justified with an understanding of ecological contexts, and an analysis of skeletal element profiles related to gross bone damage capabilities of certain carnivores. For example, the discriminant analysis is able to distinguish between hyenas and lions with 86.23% accuracy. African lions produce long, narrow, and shallow tooth scores; whereas hyenas produce long, wide, and extremely deep tooth marks comparatively (Figure 27). The ability to distinguish between these two actors by their feeding traces is critical to understanding hominin behavior, carcass acquisition sequences, and furthering the hunting vs. scavenging debate, as these actors would be the prominent carnivores with whom hominins would likely be interacting with. For instance, Early Stone Age sites such as FLK *Zinjanthropus* in Olduvai Gorge, Tanzania have been the center of debates regarding timing of access of carcasses for hominins as this site bears abundant dual-patterned bones with stone tool cut marks and what is thought to be felid tooth marks (Dominguez-Rodrigo & Barba 2006; Blumenschine et al. 2007; Dominguez-Rodrigo et al. 2014; Pante et al. 2012; 2015; Parkinson et al. 2015). There would be a stark difference in flesh availability for scavenging hominins after each of these actors had fed on the carcass as lions would provide substantially more flesh for secondary consumers than would hyenas, who tend to consume not only the majority of flesh but also delete marrow rich bones from the carcass before hominins would have had access to it (Pobiner 2007, 2015). The ability to distinguish between these two carnivore actors will be significant for understanding the context and timing of dual patterned bones in the archaeological record.

In similar analysis, utilizing microphotogrammetry for the comparison of African lion and spotted hyena tooth marks, Arriaza et al. (2017) report the ability to differentiate between these carnivore actors with 76% accuracy. This coincides with accuracy reported here between

these two species (83.34%). Furthermore, between striped hyenas and African lions, accuracy increases to 90.5%, and as mentioned above when hyaenid species are pooled, 86.23%. The differences between results reported here and in Arrizia et al. (2017), although not major, are likely due to the limitations of their methodology, as their analysis was limited to 2D profiles of tooth marks taken from cross-sections along the mark.

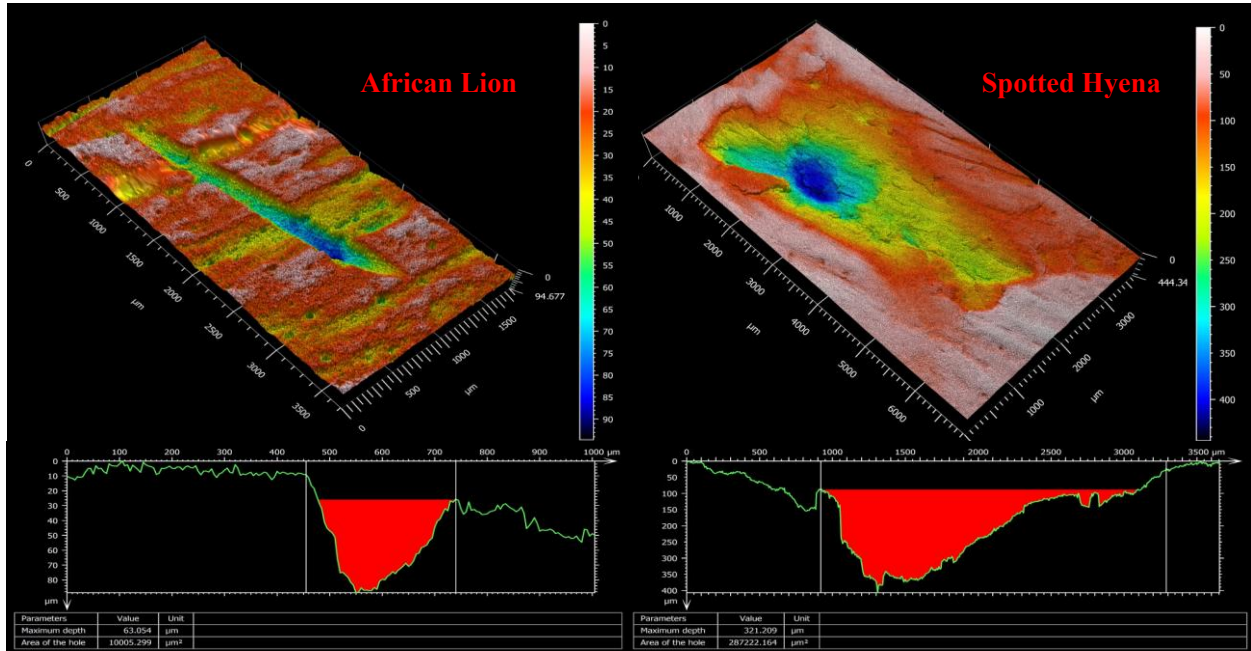


Figure 27 - Sample tooth marks of African lion (left) and spotted hyena (right).

Between hyenas and crocodiles, the African taxa that have the largest bite force, the discriminant analysis is able to identify marks with 74.70% accuracy. This lower accuracy is due to both of these actors leaving very deep tooth mark profiles, which isn't surprising as they both regularly completely destroy limb bones (Blumenschine 1988; Njau & Blumenschine 2006; Yirga et al. 2012; Pobiner 2015). Hyena and crocodile pits are very similar in terms of depth, although crocodiles produce wider tooth pits. Tooth scores are similar in depth but very distinct in 3D and profile measurements as crocodiles often produce tooth marks with v-shaped profiles that are more similar to cut marks than mammalian carnivore tooth marks (Figure 28).

Crocodiles also produce much wider and longer scores as they roll their prey during submersion (Njau & Blumenschine 2006). Tooth scores in this case are much more reliable for classification and useful for analysis of dense and highly fragmented assemblages.

The analysis of crocodile feeding traces has been limited (Njau & Blumenschine 2006; Baquedano et al. 2012; Njau & Blumenschine 2012). Previous research has examined unique qualitative features of crocodile feeding traces such as the bisected pits their unique tooth shape produces; however, identification of these features provides only 10% accuracy for differentiating carnivore tooth marks (Njau & Blumenschine 2006). Precise and accurate identification of crocodile feeding traces is required as many trace marks thought to be evidence of the earliest hominin butchery action and tool use are likely crocodile tooth marks that bear strong similarity to stone tool cut marks; such as the trace marks found in the Dikika assemblages (Ethiopia, 3.4mya), that have been the center of high-profile and unresolved disagreements (Dominguez-Rodrigo et al. 2010, 2011, 2012; McPherron et al. 2011; Thompson et al. 2015). Comparison of these controversial marks within the actualistic sample generated in this thesis would provide a more definitive assessment of the actor responsible for these archaeological traces.

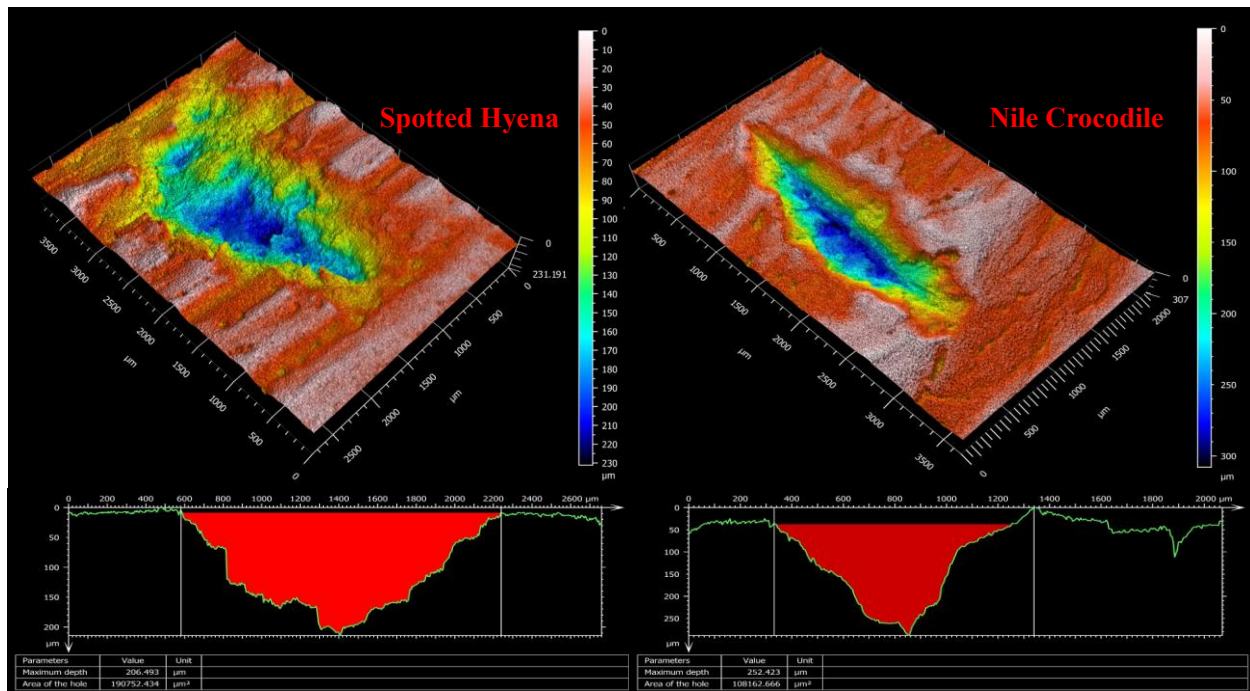


Figure 28 – Sample tooth marks of spotted hyena (left) and Nile crocodile (right).

Between species with smaller bite force included in this project, the African wild dog and African lion, the discriminant analysis classifies marks with 79% accuracy. In the confusion matrices, African wild dogs do not misclassify as African lions as the tooth marks of African wild dogs are extremely small; however, smaller pits and scores produced by the African lions fall within the range of African wild dogs. Overall, African wild dogs produce low frequencies of very short and shallow scores compared to the longer scores produced by lions (Figure 29); depth values are similar among the smaller lion pits but generally African lions produce deeper and wider pits.

These findings coincide with previous research that claims African wild dogs exhibit feeding behavior involving less contact between the predator's dentition and prey bone due to weak carnassial teeth, and therefore, produce minimal and very small tooth marks on the bone surface (Harstone-Ross 2008). Furthermore, the low incidences of extremely small tooth marks found on the bone surface reported here have also been observed and described by previous

actualistic research of African wild dogs (Yravedra et al. 2014). This indicates that African wild dog carcass-processing behavior seems to be oriented towards meat rather than bone consumption, making identification of African wild dogs in the archaeological record by their feeding traces very difficult.

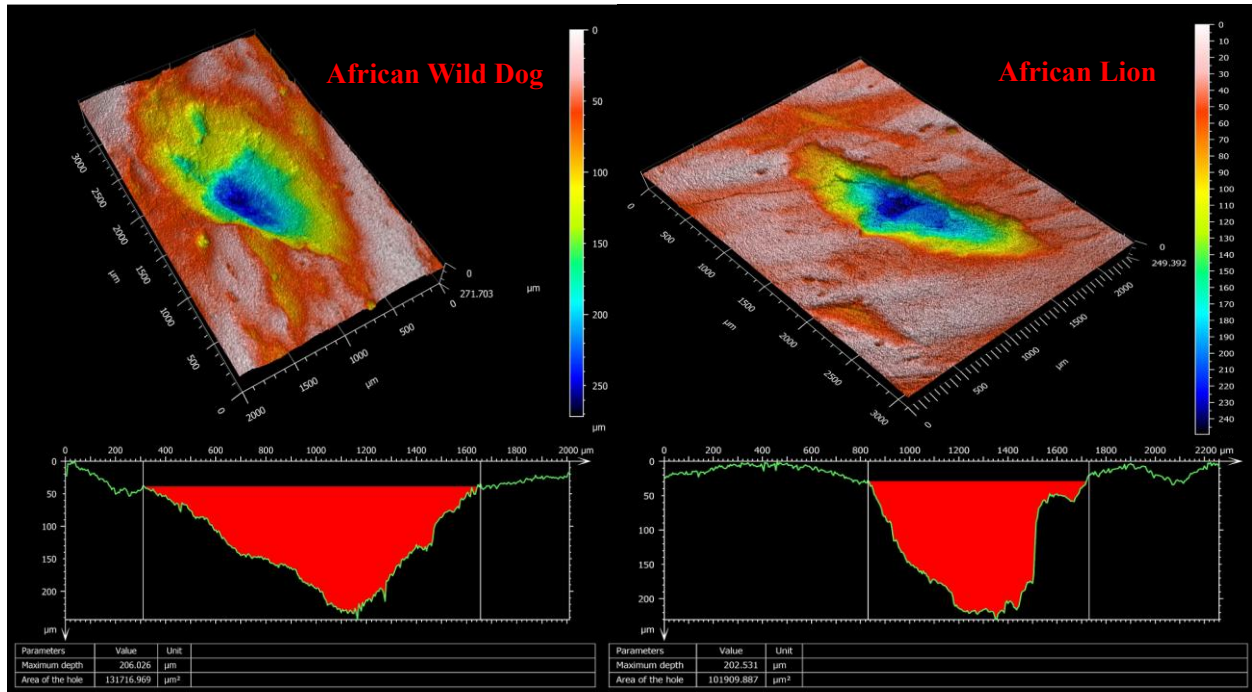


Figure 29 – Sample tooth marks of African wild dog (left) and African lion (right).

Between the North American carnivores included in this study, the grey wolf and brown bear, the discriminant analysis is able to identify marks with 96.49% accuracy. This is an excellent result but is not all together surprising since the brown bear has the most distinct tooth mark morphology in this study with extremely wide and shallow marks (Figure 30).

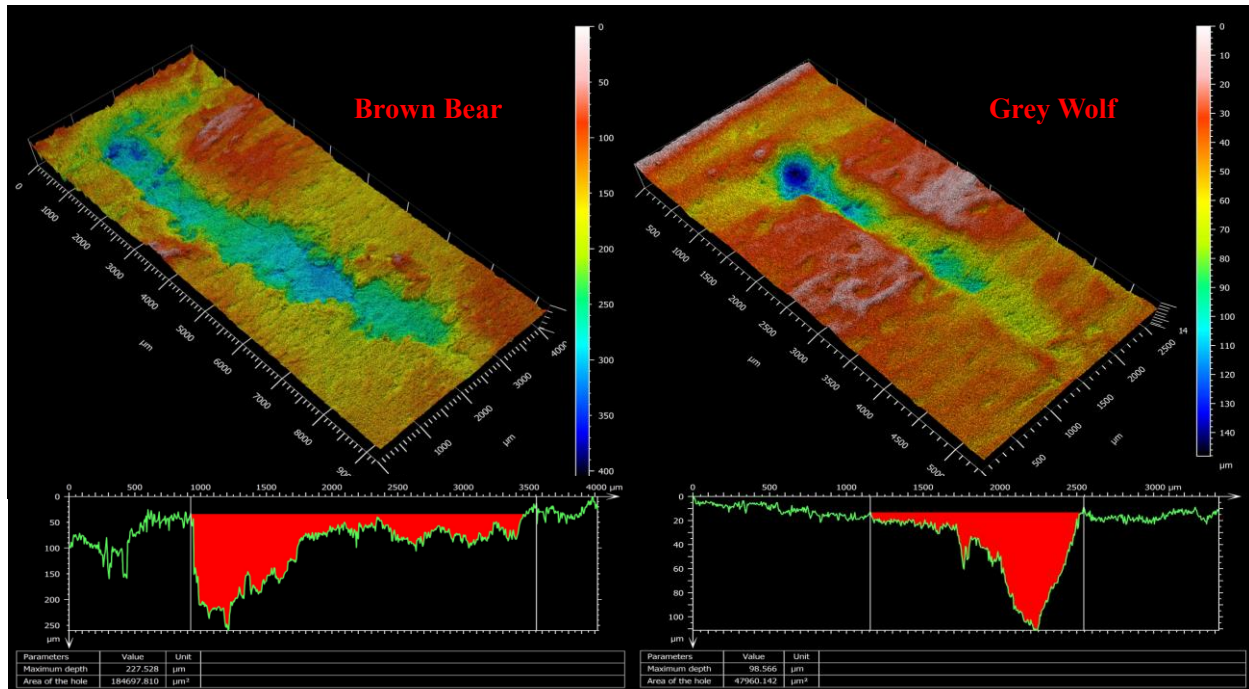


Figure 30 – Sample tooth marks of North American brown bear (left) and grey wolf (right).

5.1.4 Inferred Fossil Trace Marks

Fossil trace marks were computed into the family level and biomechanical discriminant analysis to determine how they would be classified within our actualistic sample. The fossil trace marks are shown as the large red x's in the discriminant analysis in Figure 26 and their classifications are reported in Table 30. The analyses suggest there is a wide distribution of actors present in this fossil assemblage.

All fossil trace marks match between models except for one trace mark (4268), which dual classifies as a felid in the family level discriminant analysis and a bone cruncher in the biomechanical discriminant analysis due to its deep profile. This dual classification could belong to a felid with higher bite force, compared to the African lion such as *Dinofelis*, which has fossil remains at this archaeological site. However, given the higher accuracy of our biomechanical model compared to the family level model, this is likely a smaller tooth mark produced by a bone cruncher.

Four of the archaeological marks do not classify with any carnivore. This may be due to taphonomic processes that have abraded the bone surface and altered the tooth marks morphology (Behrensmeyer 1978; Shipman & Rose 1983). Alternatively, these tooth marks may belong to species that are extinct and have not been modeled. However, limitations of the samples used in this comparison cannot be ruled out; for example, leopards and cheetahs are not represented in this study. Tooth marks that do not classify, are not outliers falling outside of the carnivore groupings but rather fall within multiple ranges, and likely are too similar to multiple actors for accurate classification. Furthermore, the archaeological trace marks also fall within the area that smaller felids such as leopards and cheetahs would likely classify based on average body size and biomechanics (Van Valkenburgh 1996). It has been argued that scavenging from tree-store leopard kills may have been an important food source for early hominins, and as such, these species should be included in future work (Cavallo & Blumenschine 1989; Van Valkenburgh et al. 2002; Pobiner 2007; Van Valkenburgh 2007).

Furthermore, analyzing the archaeological trace marks that do not classify by skeletal element does not provide an alternative explanation for why these traces do not classify. These trace marks are found on the midshaft of size 3 long bones and are therefore comparable to the bones used in the actualistic feeding trials. This indicates that the inability of the discriminant analysis to classify these marks is due either the lower accuracy of the models or the lack of carnivores represented in this study.

5.2 Weaknesses, Limitations, & Future Work

High-resolution 3D scanning techniques have the ability to revolutionize quantitative methods of analysis and strengthen our interpretations by limiting observer bias, analyzing metrics not possible through traditional means, and by providing a quantitative assessment for

marks with debated origins (Dominguez-Rodrigo & Barba 2006; Blumenschine et al. 2007; Dominguez-Rodrigo et al. 2010, 2011, 2012; McPherron et al. 2011; Pante et al. 2015; Thompson et al. 2015). High-resolution 3D scanning methods are well equipped to answer zooarchaeological and taphonomic questions previously unknown due to traditional methodological limitations such as differentiating carnivore taxa by their feeding trace marks. Additionally, high-resolution confocal profilometers are significantly less expensive than traditional SEMs, and require less training and maintenance. Therefore, the significant benefits of this technology and methodology greatly outweigh upfront costs of the technology. As shown in Bello (2011) and in this project, low-cost molding materials can confidently be used in analysis and be accurately compared to other samples, allowing for collaboration between labs if costs prohibit the use of this expensive technology.

Variables such as prey size and feeding trial duration were controlled for in this experiment in order to maintain consistency between results, allowing for researchers to easily replicate, compare, and expand upon this research. The use of captive animals was critical to this quantitative approach; however, as stated above, captive animals are not completely analogous to wild animals in terms of behavior; how much this would affect quantitative features is unknown but the impact is likely minimal. Other variables such as bone type, prey size, and the amount of flesh present would likely have a much larger effect on tooth mark morphology. Further development of this research would likely see interesting results if prey type and size were varied. Lastly, further expanding the sample size, both in carnivores studied and number of feeding trials would be beneficial; this would likely result in lower accuracy and lower confidence levels; however, it would provide an opportunity to classify tooth marks by their type and anatomical location on bone.

The largest issue restricting the accuracy of the approach utilized in this thesis is that smaller tooth marks produced by large carnivores misclassify with the tooth marks of smaller carnivores. These smaller tooth marks were not removed from analysis as they are important in characterizing the diversity of tooth mark morphology for any one taxa. Future work will focus on the analysis of shape and remove size from consideration.

When archaeological trace marks were compared in the multivariate analysis, some of them did not classify with any carnivore species or grouping. There are several possibilities for the ineffectiveness of the models when applied to these marks. Foremost, there are many other carnivore types that need to be analyzed such as leopards and cheetahs. There are also tooth marks which do not classify within our samples, and could be indicative of species that do not have a direct modern analog requiring future research to analyze biomechanical characteristics of tooth shape and predicted bite force to infer tooth mark morphology.

The misclassification or lack of classification for archaeological traces can also be due to taphonomic processes such as soil abrasion, weathering, and fluvial transport, all of which alter bone surfaces and trace marks found on those surfaces. This is problematic as the actualistic sample of tooth marks has not undergone any of these post-depositional taphonomic processes and is essentially fresh bone, not wholly comparable to the weathered and abraded archaeological trace marks. Current research is testing the effects of fluvial abrasion on experimentally created cut and tooth marks and has shown these processes to have a minimal effect on cut and tooth mark morphology (Gumrukcu et al. 2017). Therefore, the most parsimonious explanation for why certain archaeological trace marks do not classify within the actualistic sample is the limitations of sample size and carnivore actors represented in this study.

High-resolution 3D scanning provides a quantitative approach to further strengthen the analysis and our understanding of archaeological remains. Further actualistic studies will be beneficial to developing a means to differentiate carnivores by their tooth mark morphology as demonstrated within this thesis, leading to a more holistic understanding of early hominin subsistence strategies.

CHAPTER 6 CONCLUSION

This study represents the first systematic analysis of carnivore tooth mark micromorphology. The results of this study are broadly consistent with previous attempts but with a significant contribution to accuracy and efficacy. These conclusions describe for the first time a quantifiable difference between multiple carnivores and their feeding traces. The significance of these results lies not only in the analysis of Bed II fossil assemblages reported here but in the application and demonstration of the methodology, which is broadly applicable to archaeological assemblages regardless of age or geographic location.

Although this study was limited in the number of carnivore species included, the results demonstrate that this method is accurate and applicable for the identification of carnivore species from their feeding traces. Expansion of this project is required to establish a broader database, allowing for improved accuracy and confidence in this methodology.

This thesis contributes new avenues for understanding the feeding behaviors of early hominins through the development of new methods for analysis of hominin-carnivore interactions. These interactions are critical to understanding meat acquisition strategies of early hominins as they encroached upon the larger carnivore guild, regularly consuming flesh and marrow from carcasses, leading to rapid encephalization evolution of the genus *Homo*. Future research will seek to expand this exploration, to increase the accuracy of carnivore identification, and to better understand the specific carnivores early hominins interacted with. Ultimately, we seek to illuminate the relationship between early hominins and carnivores at the time when animal source foods were introduced into hominin diet as it corresponds to the morphological and technological adaptations seen in the genus *Homo*. As it is through this research that seeks to better understand the precursors of our evolutions, shifting social organization, and the

technological advancement of our ancestors that we will better guide the future of our planet and the future of humanity today.

REFERENCES

- Agudo, R., Rico, C., Vilà, C., Hiraldo, F., & Donazar, J. A. (2010). The role of humans in the diversification of a threatened island raptor. *Evolutionary Biology*, 10(1), 384.
- Aiello, L.C., Wheeler, P., 1995. The expensive-tissue hypothesis: The brain and digestive system in human and primate evolution. *Current Anthropology*, 36, 199-221.
- Aiello, L.C. and Wells, J.C., 2002. Energetics and the evolution of the genus *Homo*. *Annual Review of Anthropology*, pp.323-338.
- Andrés, M., Gidna, A. O., Yravedra, J., & Domínguez-Rodrigo, M. (2012). A study of dimensional differences of tooth marks (pits and scores) on bones modified by small and large carnivores. *Archaeological and Anthropological Sciences*, 4(3), 209-219.
- Anton, S.C., and J.J. Snodgrass. 2012. Origins and the evolution of the genus *Homo* new perspectives. *Current Anthropology* 53: S479-S496.
- Anyonge, W., 1996. Microwear on canines and killing behavior in large carnivores: Saber function in *Smilodon fatalis*. *Journal of Mammalogy* 77(4), 1059-1067.
- Arriaza, M. C., Yravedra, J., Domínguez-Rodrigo, M., Mate-González, M. Á., Vargas, E. G., Palomeque-González, J. F., Baquedano, E. (2017). On applications of micro-photogrammetry and geometric morphometrics to studies of tooth mark morphology: The modern Olduvai Carnivore Site (Tanzania). *Palaeogeography, Palaeoclimatology, Palaeoecology*.
- Arribas, A., Palmqvist, P., 1998. Taphonomy and paleoecology of an assemblage of large mammals: hyaenid activity in the Lower Pleistocene site at Venta Micena (Orce, Guadix-Baza Basin, Granada, Spain). *Geobios*, 31(3), 3-47.
- Arribas, A., Palmqvist, P., 1999. On the ecological connection between sabre-teeth and hominids: faunal dispersal events in the Lower Pleistocene and a review of the evidence for the first human arrival in Europe. *Journal of Archaeological Science*, 26, 571-585.
- Attard M.R.G., Chamoli U., Ferrara T.L., Rogers T.L., Wroe S. 2010. Skull mechanics and implications for feeding behavior in a large marsupial carnivore guild: the thylacine, Tasmanian devil and spotted-tailed quoll *Journal of Zoology* 285:292-300
- Barash, A., Bastir, M., & Been, E. (2015). 3D Morphometric Study of the Mandibular Fossa and Its Implication for Species Recognition in *Homo erectus*. *Advances in Anthropology*, 5(03), 152.
- Bartelink, E. J., Wiersema, J. M., & Demaree, R. S. (2001). Quantitative analysis of sharp-force trauma: an application of scanning electron microscopy in forensic anthropology. *Journal of Forensic Science*, 46(6), 1288-1293.
- Bartram, L.E.Jr., Marean, C.W., 1999. Explaining the “Klasies Pattern”: Jua enthoarchaeology, the Die Kelders Middle Stone Age archaeofaunal, long bone fragmentation and carnivore ravaging. *Journal of Archaeological Science*, 26, 9-29.

- Baquedano, E., Dominguez-Rodrigo, M., Musiba, C. 2012. An experimental study of large mammal bone modification by crocodiles and its bearing on the interpretation of crocodile predation at FLK Zinj and FLK NN3. *Journal of Archaeological Science*, 39: 1728-1737.
- Behrensmeyer, A. K. (1978). Taphonomic and ecologic information from bone weathering. *Paleobiology*, 4(02), 150-162.
- Behrensmeyer, A. K., Gordon, K. D., & Yanagi, G. T. (1986). Trampling as a cause of bone surface damage and pseudo-cutmarks. *Nature*, 319(6056), 768-771.
- Behrensmeyer, A. K. (1991). Terrestrial vertebrate accumulations. *Taphonomy: releasing the data locked in the fossil record*, 9, 291-335.
- Bello, S. M., & Soligo, C. (2008). A new method for the quantitative analysis of cutmark micromorphology. *Journal of Archaeological Science*, 35(6), 1542-1552.
- Bello, S. M., Parfitt, S. A., & Stringer, C. (2009). Quantitative micromorphological analyses of cut marks produced by ancient and modern handaxes. *Journal of Archaeological Science*, 36(9), 1869-1880.
- Bello, S. M., Vervenioutou, E., Cornish, L., & Parfitt, S. A. (2011). 3-dimensional microscope analysis of bone and tooth surface modifications: comparisons of fossil specimens and replicas. *Scanning*, 33(5), 316-324.
- Bello, S. M. (2011). New results from the examination of cut-marks using three-dimensional imaging. In *The Ancient Human Occupation of Britain, Amsterdam: The Netherlands* (pp. 249-262).
- Bello, S. M., De Groote, I., & Delbarre, G. (2013). Application of 3-dimensional microscopy and micro-CT scanning to the analysis of Magdalenian portable art on bone and antler. *Journal of Archaeological Science*, 40(5), 2464-2476.
- Bello, S. M., Parfitt, S. A., De Groote, I., & Kennaway, G. (2013). Investigating experimental knapping damage on an antler hammer: a pilot-study using high-resolution imaging and analytical techniques. *Journal of Archaeological Science*, 40(12), 4528-4537
- Bello, S. M., Wallduck, R., Dimitrijević, V., Živaljević, I., & Stringer, C. B. (2016). Cannibalism versus funerary defleshing and disarticulation after a period of decay: comparisons of bone modifications from four prehistoric sites. *American Journal of Physical Anthropology*, 161(4), 722-743.
- Biknevicius, A.R., Van Valkenburgh, B., 1996. Design for killing: craniodental adaptations of predators. In Gittleman, J., (Ed.), *Carnivore Behavior, Ecology and Evolution*. Cornell University Press, New York, pp. 393-428.
- Biknevicius, A.R., Van Valkenburgh, B., Walker, J., 1996. Incisor size and shape: implications for feeding behaviors in saber-toothed "cats". *Journal of Vertebrate Paleontology* 16(3), 510-521.
- Binder W.J., Thompson E.N., Van Valkenburgh B. 2002. Temporal variation in tooth fracture among Rancho La Brea dire wolves. *Journal of Vertebrate Paleontology* 22(2):423-428.
- Binford, L.R., 1981. *Bones: Ancient Men and Modern Myths*. Academic Press, New York.
- Binford, L.R., 1984. *Faunal Remains from Klasies River Mouth*. Academic Press, New York.

- Binford, L.R., Mills, M.G.L., Stone, N. M., 1988. Hyaena scavenging behavior and its implications for the interpretation of faunal assemblages from FLK 22 (the Zinj floor) at Olduvai Gorge. *Journal of Anthropological Archaeology* 7, 99-135.
- Blumenschine, R.J., 1986. Carcass consumption sequences and the archaeological distinction of hunting and scavenging. *Journal of Human Evolution*, 15, 639-659.
- Blumenschine, R.J., 1988. An experimental model of the timing of hominid and carnivore influence on archaeological bone assemblages. *Journal of Archaeological Science*, 15, 483-502.
- Blumenschine, R.J., Selvaggio, M.M., 1988. Percussion marks on bone surfaces as a new diagnostic of hominid behavior. *Nature*, 333, 763-765.
- Blumenschine, R.J., Cavallo, J.A., 1992. Scavenging and human evolution. *Scientific American*, 267, 90-96.
- Blumenschine, R.J., Marean, C. W., 1993. A carnivore's view of archaeological bone assemblages. In Hudson, J. (Ed.), *From Bones to Behavior: Ethnoarchaeological and Experimental Contributions to the Interpretation of Faunal Remains*. Center for Archaeological Investigations, University of Southern Illinois, Carbondale, pp. 273-300.
- Blumenschine, R. J. (1995). Percussion marks, tooth marks, and experimental determinations of the timing of hominid and carnivore access to long bones at FLK Zinjanthropus, Olduvai Gorge, Tanzania. *Journal of Human Evolution*, 29(1), 21-51.
- Blumenschine, R. J., Marean, C. W., & Capaldo, S. D. (1996). Blind tests of inter-analyst correspondence and accuracy in the identification of cut marks, percussion marks, and carnivore tooth marks on bone surfaces. *Journal of Archaeological Science*, 23(4), 493-507.
- Blumenschine, R.J., Prassack, K.A., Kreger, C.D., Pante, M.C., 2007. Carnivore toothmarks, microbial bioerosion, and the invalidation of Dominguez-Rodrigo and Barba's (2006) test of Oldowan hominin scavenging behavior. *J. Hum. Evol.* 53, 420-426.
- Bocaege, E., Humphrey, L. T., & Hillson, S. (2010). Technical note: A new three-dimensional technique for high resolution quantitative recording of perikymata. *American journal of physical anthropology*, 141(3), 498-503.
- Boschin, F., & Crezzini, J. (2012). Morphometrical analysis on cut marks using a 3D digital microscope. *International Journal of Osteoarchaeology*, 22(5), 549-562.
- Brain, C.K., 1981. *The Hunters or the Hunted? An Introduction to African Cave Taphonomy*. University of Chicago Press, Chicago.
- Braun, D., Pante, M.C., Acher, W. 2016. Cut marks on bone surfaces: influences on variation in the form of traces of ancient behavior. *Interface Focus*. 6(3), 20160006.
- Bretzke, K., & Conard, N. J. (2012). Evaluating morphological variability in lithic assemblages using 3D models of stone artifacts. *Journal of Archaeological Science*, 39(12), 3741-3749.
- Bunn, H. T. (1981). Archaeological evidence for meat-eating by Plio-Pleistocene hominids from Koobi Fora and Olduvai Gorge. *Nature* 291:574-577

- Bunn, H.T., 1982. Meat-eating and human evolution: studies on the diet and subsistence practices of Plio-Pleistocene hominids in East Africa. Ph.D. dissertation, University of California, Berkley.
- Bunn, H.T., 1983. Comparative analysis of modern bone assemblages from a San hunter-gatherer camp in the Kalahari Desert, Botswana, and from a spotted hyaena den near Nairobi, Kenya. In Clutton-Brock, J., Grigson, C. (Eds.), *Animals and Archaeology, Volume 1: Hunters and Their Prey*. British Archaeological Reports International Series 163, Oxford, pp. 143-148.
- Bunn, H.T., 1986. Patterns of skeletal representation and hominid subsistence activities at Olduvai Gorge, Tanzania and Koobi Fora, Kenya. *Journal of Human Evolution*, 15, 673-690.
- Bunn, H.T., Kroll, E.M., 1986. Systematic butchery by Plio/Pleistocene hominids at Olduvai Gorge, Tanzania. *Current Anthropology*, 27, 431-452
- Bunn, H.T., Kroll, E.M., 1988. Fact and fiction about the Zinjanthropus floor: data, arguments, and interpretations. *Curr. Anthropol.* 29, 135-149.
- Bunn, H.T., Ezzo J. 1993. Hunting and scavenging by Plio-Pleistocene hominids: Nutritional constraints, archaeological patterns, and behavioural implications. *Journal of Archaeological Science* 20:365-398.
- Bunn, H.T., 2001. Hunting, power scavenging, and butchering by Hadza foragers and by Plio-Pleistocene *Homo*. In Stanford, C.B., Bunn, H.T. (Eds), *Meat-Eating and Human Evolution*. Oxford University Press, New York, pp. 199-218.
- Burke, C.C., Neotaphonomic analysis of the feeding behaviors and modification marks produced by North American carnivores. *Journal of Taphonomy*, 11(1), 1-20
- Calvin, W.H., 1982. Did throwing stones shape hominid brain evolution?. *Ethology and Sociobiology*, 3(3), pp.115-124.
- Camarós, E., Cueto, M., Lorenzo, C., Villaverde, V., & Rivals, F. (2016). Large carnivore attacks on hominins during the Pleistocene: a forensic approach with a Neanderthal example. *Archaeological and anthropological sciences*, 8(3), 635-646.
- Capaldo, S.D., 1998. Simulating the formation of dual-patterned archaeofaunal assemblages with experimental control samples. *Journal of Archaeological Science*, 25, 311-330.
- Capaldo, S.D., 1997. Experimental determinations of carcass processing by Plio-Pleistocene hominids and carnivores at FLK 22 (*Zinjanthropus*), Olduvai Gorge, Tanzania. *J. Hum. Evol.* 33, 555-597.
- Capaldo, S.D., Blumenschine, R.J. 1994. A quantitative diagnosis of notches made by hammerstone percussion and carnivore gnawing on bovid long bones. *American Antiquity*, 59, 724-748.
- Caruana, M. V., Carvalho, S., Braun, D. R., Presnyakova, D., Haslam, M., Archer, W., ... & Harris, J. W. (2014). Quantifying traces of tool use: a novel morphometric analysis of damage patterns on percussive tools. *PloS one*, 9(11), e113856.
- Cassini, G.H., Vizcaíno, S.F. and Bargo, M.S., 2012. Body mass estimation in Early Miocene native South American ungulates: a predictive equation based on 3D landmarks. *Journal of Zoology*, 287(1), pp.53-64.

- Cavallo, J.A. and Blumenschine, R.J., 1989. Tree-stored leopard kills: expanding the hominid scavenging niche. *Journal of Human Evolution*, 18(4), pp.393-399.
- Christiansen, P. and Wroe, S., 2007. Bite forces and evolutionary adaptations to feeding ecology in carnivores. *Ecology*, 88(2), pp.347-358.
- Clark, J.D., Kurashina, H., 1979. Hominid occupation of the east-central highlands of Ethiopia in the Plio-Pleistocene. *Nature*, 282, 33-39.
- Clarkson, C., Vinicius, L., & Lahr, M. M. (2006). Quantifying flake scar patterning on cores using 3D recording techniques. *Journal of Archaeological Science*, 33(1), 132-142.
- Coard, R. (2007). Ascertaining an agent: using tooth pit data to determine the carnivore/s responsible for predation in cases of suspected big cat kills in an upland area of Britain. *Journal of archaeological science*, 34(10), 1677-1684.
- Collinson, M.E., Hooker, J.J., 2000. Gnaw marks on Eocene seeds: evidence for early rodent behavior. *Palaeogeography, Palaeoclimatology, Palaeoecology* 157, 127-149.
- Crowder, C., Rainwater, C. W., & Fridie, J. S. (2013). Microscopic analysis of sharp force trauma in bone and cartilage: a validation study. *Journal of forensic sciences*, 58(5), 1119-1126.
- Crezzini, J., Boschin, F., Boscato, P., & Wierer, U. (2014). Wild cats and cut marks: Exploitation of *Felis silvestris* in the Mesolithic of Galgenbühel/Dos de la Forca (South Tyrol, Italy). *Quaternary International*, 330, 52-60.
- Cruz-Uribe, K., 1991. Distinguishing hyaena from hominid bone accumulations. *Journal of Field Archaeology* 18, 467-486.
- Curtis A.A., Van Valkenburgh B. 2014. Beyond the Sniffer: Frontal Sinuses in Carnivora *The Anatomical Record* 297:2047-2064
- Dart, R.A., 1949. The predatory implement technique of *Australopithecus*. *American Journal of Physical Anthropology*, 7, 1-38.
- Delaney-Rivera C., Plummer T.W., Hodgson J.A., Forrest F., Hertel F., Oliver J.S. 2009. Pits and pitfalls: taxonomic variability and patterning in tooth mark dimensions *Journal of Archaeological Science* 26:2597-2608
- Denys, C. (2002). Taphonomy and experimentation. *Archaeometry*, 44(3), 469-484. Mountains surface imaging & metrology software 'Digital Surf: MountainsMap Premium'. 2015. <http://www.digitalsurf.fr/en/mntkey.html>
- Domínguez-Rodrigo, M., 1997. Meat-eating by early hominids at the FLK 22 Zinjanthropus site, Olduvai Gorge (Tanzania): an experimental approach using cut-mark data. *Journal of Human Evolution* 33, 669-690.
- Domínguez-Rodrigo, M., 1999. Flesh availability and bone modifications in carcasses consumed by lions: palaeoecological relevance in hominid foraging patterns. *Palaeogeography, Palaeoclimatology, and Palaeoecology* 149, 373-388.

- Domínguez-Rodrigo, M., 2001. A study of carnivore competition in riparian and open habitats of modern savannas and its implications for hominid behavioral modelling. *Journal of Human Evolution*, 40, 77-98.
- Domínguez-Rodrigo, M. and Piqueras, A., 2003. The use of tooth pits to identify carnivore taxa in tooth-marked archaeofaunas and their relevance to reconstruct hominid carcass processing behaviours. *Journal of Archaeological Science*, 30(11), pp.1385-1391.
- Domínguez-Rodrigo M, Pickering TR. 2003. Early hominid hunting and scavenging: A zooarcheological review. *Evolutionary Anthropology*, 12: 275–282.
- Domínguez-Rodrigo, M., Barba, R., 2006. New estimates of tooth mark and percussion mark frequencies at the FLK Zinj site: the carnivore-hominid-carnivore hypothesis falsified. *J. Hum. Evol.* 50, 170-194.
- Domínguez-Rodrigo, M., Pickering, T.R., Bunn, H.T., 2010. Configurational approach to identifying the earliest hominin butchers. *Proc. Natl. Acad. Sci.* 107, 20929-20934.
- Domínguez-Rodrigo, M., Pickering, T.R., Bunn, H.T., 2011. Reply to McPherron et al.: Doubting Dikika is about data, not paradigms. *Proc. Natl. Acad. Sci.* 108.
- Domínguez-Rodrigo, M., Pickering, T., Bunn, H.T., 2012. Experimental study of cut marks made with rocks unmodified by human flaking and its bearing on claims of ~3.4-million-year-old butchery evidence from Dikika, Ethiopia. *J. Archaeol. Sci.* 39, 205.
- Domínguez-Rodrigo, M., Diez-Martin, F., Yravedra, J., Barba, R., Mabulla, A., Baquedano, E., Uribealarea, D., Sánchez, Policarpo., Eren, M.I., 2014. Study of the SHK Main Site faunal assemblage, Olduvai Gorge, Tanzania: Implications for Bed II taphonomy, paleoecology, and hominin utilization of megafauna. *Quat. Int.* 322-323, 153-166.
- Domínguez-Rodrigo, M., Bunn, H.T. and Yravedra, J., 2015. A critical re-evaluation of bone surface modification models for inferring fossil hominin and carnivore interactions through a multivariate approach: application to the FLK Zinj archaeofaunal assemblage (Olduvai Gorge, Tanzania). *Quaternary International*, 322, pp.32-43.
- Dunbar, R. I., & Shultz, S. (2007). Evolution in the social brain. *science*, 317(5843), 1344-1347.
- Egeland, C.P., Pickering, T.R., Domínguez-Rodrigo, M., Brain, C.K., 2004. Disentangling Early Stone Age palimpsests: determining the functional independence of hominid- and carnivore-derived portions of archaeofaunas. *Journal of Human Evolution* 47: 343-357.
- Erickson, G.M., Olson, K.H., 1996. Bite marks attributable to *Tyrannosaurus rex*: preliminary description and implications. *Journal of Vertebrate Paleontology* 16, 175-178.
- Faith, T.J., 2007. Sources of variation in carnivore tooth-mark frequencies in a modern spotted hyena (*Crocuta crocuta*) den assemblage, Amboseli Park, Kenya. *Journal of Archaeological Science*, 34, 1601-1609.
- Faith, T.J., Marean, C.W., Behrensmeyer, A.K., 2007. Carnivore competition bone destruction, and bone density. *Journal of Archaeological Science*, 34, 2025-2034.

- Fiorillo, A.R., 1991. Prey bone utilization by predatory dinosaurs. *Paleogeography, Paleoclimatology, Paleoecology*, 88, 157-166.
- Foley, R., 2001. The evolutionary consequences of increase carnivory in hominids. In Stanford, C.B., Bunn, H.T. (Eds.), *Meat-Eating and Human Evolution*. Oxford University Press, New York, pp. 305-331.
- Friess, M. (2010). Calvarial shape variation among Middle Pleistocene hominins: an application of surface scanning in palaeoanthropology. *Comptes Rendus Palevol*, 9(6), 435-443.
- Garvin, H. M., & Ruff, C. B. (2012). Sexual dimorphism in skeletal browridge and chin morphologies determined using a new quantitative method. *American journal of physical anthropology*, 147(4), 661-670.
- Gidna, A., Yravedra, J., & Domínguez-Rodrigo, M. (2013). A cautionary note on the use of captive carnivores to model wild predator behavior: a comparison of bone modification patterns on long bones by captive and wild lions. *Journal of Archaeological Science*, 40(4), 1903-1910.
- Gifford, D.P., 1981. Taphonomy and paleoecology: a critical review of archaeology's sister disciplines. *Advances in Archaeological Method and Theory*, 4, 365-438.
- Gifford-Gonzalez, D., 1991. Bones are not enough: analogues, knowledge and interpretive strategies in zooarchaeology. *Journal of Anthropological Archaeology*, 1, 355-381.
- Gilbert, W. H., & Richards, G. D. (2000). Digital imaging of bone and tooth modification. *The Anatomical Record*, 261(6), 237-246.
- Gould, S.J., 1965. Is uniformitarianism necessary? *American Journal of Science*, 263, 223-228.
- Grosman, L., Smikt, O., & Smilansky, U. (2008). On the application of 3-D scanning technology for the documentation and typology of lithic artifacts. *Journal of Archaeological Science*, 35(12), 3101-3110.
- Gumrukcu, M., Muttart, M.V., Pante, M.C., 2017. Assessing the effects of fluvial abrasion on bone surface modifications using high-resolution 3D scanning. Abstracts of the Paleoanthropology Society 2017 Meeting. *PaleoAnthropology* A1-A34.
- Guy, F., Gouvard, F., Boistel, R., Euriat, A., & Lazzari, V. (2013). Prospective in (Primate) dental analysis through tooth 3D topographical quantification. *PloS one*, 8(6), e66142.
- Harris, J.W.K., Capaldo, S.D., 1993. The earliest stone tools. In Berthelet, A., Chavaillon, J. (Eds.), *The Use of Tools by Human and Non-Human Primates*. Oxford: Clarendon Press, Oxford, pp. 196-200.
- Harstone-Rose, A. (2008). *Evaluating the hominin scavenging niche through analysis of the carcass-processing abilities of the carnivore guild*. Doctoral dissertation. Duke University.
- Haynes, G., 1980. Evidence of carnivore gnawing on Pleistocene and recent mammal bones. *Paleobiology*, 5, 341-351.
- Haynes, G., 1982. Utilization and skeletal disturbances of North American prey carcasses. *Artic* 35, 266-281.

- Hayes, G., 1983. A guide for differentiating mammalian carnivore taxa responsible for gnaw damage to herbivore limb bones. *Paleobiology*, 9, 164-172.
- Höner, O.P., Wachter, B., East, M.L. and Hofer, H., 2002. The response of spotted hyaenas to long-term changes in prey populations: functional response and interspecific kleptoparasitism. *Journal of Animal Ecology*, 71(2), pp.236-246.
- Hunt, K.D., 1994. The evolution of human bipedality: ecology and functional morphology. *Journal of Human Evolution*, 26(3), pp.183-202.
- Kaiser, T. M., & Katterwe, H. (2001). The application of 3D-microprofilometry as a tool in the surface diagnosis of fossil and sub-fossil vertebrate hard tissue. An example from the Pliocene Upper Laetolil Beds, Tanzania. *International Journal of Osteoarchaeology*, 11(5), 350-356.
- Karasik, A., & Smilansky, U. (2008). 3D scanning technology as a standard archaeological tool for pottery analysis: practice and theory. *Journal of Archaeological Science*, 35(5), 1148-1168.
- Klein, R.G., 1982. Age (mortality) profiles as a means of distinguishing hunted species from scavenged ones in Stone Age archaeological sites. *Paleobiology*, 8, 151-158.
- Koch PL, Barnosky AD. 2006. Late Quaternary extinctions: State of the debate. *Annual Review of Ecology, Evolution, and Systematics* 37: 215–250.
- Kruuk, H., 1972. *The Spotted Hyaena: A Study of Predation and Social Behavior*. University of Chicago Press, Chicago.
- Kupczik K., Stynder D.D. 2012 Tooth root morphology as an indicator for dietary specialization in carnivores (Mammalia: Carnivora) *Biological Journal of the Linnean Society* 105:456-471
- Kuzminsky, S. C., & Gardiner, M. S. (2012). Three-dimensional laser scanning: potential uses for museum conservation and scientific research. *Journal of Archaeological Science*, 39(8), 2744-2751.
- Lam, Y.M., 1992. Variability in the behaviour of spotted hyaenas as taphonomic agents. *Journal of Archaeological Science*, 19(4), pp.389-406.
- Lam, Y.M., Chen, X., Pearson, O. M., 1999. Intertaxonomic variability in patterns of bone density and the differential representation of bovid, cervid and equid elements in the archaeological record. *American Antiquity* 64(2), 343-362.
- Lansing, S.W., Cooper, S.M., Boydston, E.E., Holekamp, K.E., 2009. Taphonomic and zooarchaeological implications of spotted hyena (*Crocuta crocuta*) bone accumulations in Kenya: a modern behavioural ecological approach. *Paleobiology*, 35, 289-309.
- Larsen CS. 2003. Animal source foods and human health during evolution. *Journal of Nutrition* 133: 3893-3897.
- Leigh, S.R., 2012. Brain size growth and life history in human evolution. *Evolutionary Biology*, 39(4), pp.587-599.
- Liebenberg, L., 2006. Persistence hunting by modern hunter-gatherers. *Current Anthropology*, 47(6), pp.1017-1026.

- Lemorini, C., Plummer, T. W., Braun, D. R., Crittenden, A. N., Ditchfield, P. W., Bishop, L. C., Potts, R. (2014). Old stones' song: use-wear experiments and analysis of the Oldowan quartz and quartzite assemblage from Kanjera South (Kenya). *Journal of human evolution*, 72, 10-25.
- Leonard, W. R., Snodgrass, J. J., & Robertson, M. L. (2007). Effects of brain evolution on human nutrition and metabolism. *Annu. Rev. Nutr.*, 27, 311-327.
- Lewis, M.E., 1996. Carnivoran paleoguilds of Africa: implications for hominid food procurement strategies. *Journal of Human Evolution*, 32, 257-288.
- Lin, S. C., Douglass, M. J., Holdaway, S. J., & Floyd, B. (2010). The application of 3D laser scanning technology to the assessment of ordinal and mechanical cortex quantification in lithic analysis. *Journal of Archaeological Science*, 37(4), 694-702.
- Lupo KD. 1995. Hadza bone assemblages and hyena attrition: An ethnographic example of the influence of cooking and mode of discard on the intensity of scavenger ravaging. *Journal of Anthropological Archaeology* 14: 288–314.
- Lupo, K.D., O'Connell, J.F., 2002. Cut and tooth mark distributions on large animal bones: ethnoarchaeological data from the Hadza and their implications for current ideas about early human carnivory. *Journal of Archaeological Science*, 29, 85-109.
- Lyman, R.L., 1987. On the analysis of vertebrate mortality profiles: sample size, mortality type, and hunting pressure. *American Antiquity*, 52, 125-142.
- Lyman, R.L., 1994. *Vertebrate Taphonomy*. Cambridge University Press, Cambridge.
- Lyman, R. L. (2005). Analyzing cut marks: lessons from artiodactyl remains in the northwestern United States. *Journal of Archaeological Science*, 32(12), 1722-1732.
- Marean, C.W., Spencer, L.M., 1991. Impact of carnivore ravaging on zooarchaeological measures of element abundance. *American Antiquity* 56, 645-658.
- Marean, C.W., Spencer, L.M., Blumenschine, R.J., Capaldo, S.D., 1992. Captive hyaena bone choice and destruction, the schlepp effect, and Olduvai archaeofaunas. *Journal of Archaeological Science*, 19, 101-121.
- Marean, C.W., 1995. Of taphonomy and zooarchaeology. *Evolutionary Anthropology*, 4, 64-72.
- Marean, C.W., Ehrhardt, C.L., 1995. Paleoanthropological implications of a sabertooth's den. *Journal of Human Evolution*, 29, 515-547.
- Marean, C.W., 1998. A critique of the evidence for scavenging by Neanderthals and early modern humans: new data from Kobeh Cave (Zagros Mountain, Iran) and Die Kelders Cave 1 Layer 10 (South Africa). *Journal of Human Evolution*, 35, 111-136.
- Marean, C.W., Kim, S.Y., 1998. Mousterian large-mammal remains from Kobeh Cave – Behavioral implications for Neanderthals and early modern humans. *Current Anthropology*, 39, S70-S113.

- Maté-González, M. Á., Yravedra, J., González-Aguilera, D., Palomeque-González, J. F., & Domínguez-Rodrigo, M. (2015). Micro-photogrammetric characterization of cut marks on bones. *Journal of Archaeological Science*, 62, 128-142.
- Maté-González, M. Á., Palomeque-González, J. F., Yravedra, J., González-Aguilera, D., & Domínguez-Rodrigo, M. (2016). Micro-photogrammetric and morphometric differentiation of cut marks on bones using metal knives, quartzite, and flint flakes. *Archaeological and Anthropological Sciences*, 1-12.
- Meachen-Samuels J., Van Valkenburgh B. 2009. Craniodental indicators of prey size preference in the Felida. *Biological Journal of the Linnean Society* 96:784-799
- Merritt, S. R. (2015). Cut mark cluster geometry and equifinality in replicated Early Stone Age butchery. *Int. J. Osteoarchaeol.*(doi: 10.1002/oa. 2448).
- McPherron, S.P., Alemseged, Z., Marean, C., Wynn, J.G., Reed, D., Geraads, D.,Bobe, R., Béarat, H., 2011. Tool-marked bones from before the Oldowan change the paradigm. *Proc. Natl. Acad. Sci.* 108. E116-E116.
- Moleón, M., Sánchez-Zapata, J.A., Selva, N., Donázar, J.A. and Owen-Smith, N., 2014. Inter-specific interactions linking predation and scavenging in terrestrial vertebrate assemblages. *Biological Reviews*, 89(4), pp.1042-1054.
- Molina, A., & Martin-de-las-Heras, S. (2015). Accuracy of 3d scanners in tooth mark analysis. *Journal of forensic sciences*, 60(s1).
- Monahan, C.M., 1999. Quantifying bone modification by African wild dogs and spotted hyaenas: implications of models estimating the timing of hominid and carnivore access to animal carcasses. *Journal of Human Evolution*, 36, A14.
- Montani, I., Sapin, E., Sylvestre, R., & Marquis, R. (2012). Analysis of Roman pottery graffiti by high resolution capture and 3D laser profilometry. *Journal of Archaeological Science*, 39(11), 3349-3353.
- Morales, J. I., Lorenzo, C., & Vergès, J. M. (2015). Measuring retouch intensity in lithic tools: a new proposal using 3D scan data. *Journal of Archaeological Method and Theory*, 22(2), 543-558.
- Moretti, E., Arrighi, S., Boschin, F., Crezzini, J., Aureli, D., & Ronchitelli, A. (2015). Using 3D microscopy to analyze experimental cut marks on animal bones produced with different stone tools. *Ethnobiology Letters*, 6(2), 267-275.
- Nascou, A., Morin, E. (2014) Arctic Wolf and Spotted Hyena Gnawing Damage on an Experimental Faunal Assemblage. *Journal of Taphonomy*, 12(1), 1-36.
- Njau J.K., Blumenschine R.J. 2006 A diagnosis of crocodile feeding traces on larger mammal bone, with fossil examples from the Plio-Pleistocene Olduvai Basin, Tanzania *Journal of Human Evolution* 50:142-162
- Oliver, J.S., 1994. Estimates of hominid and carnivore involvement in the FLK *Zinjanthropus* fossil assemblage: some socioecological implications. *J. Hum. Evol.* 27, 267-294.
- Palmqvist, P.B., Martínez-Navarro, B., Arribas, A., 1996. Prey selection by terrestrial carnivores in a Lower Pleistocene community. *Paleobiology*, 22(4), 514-534.

Palmqvist, P.B., Arribas, A., 2001. Taphonomic decoding of the paleobiological information locked in a lower Pleistocene assemblage of large mammals. *Paleobiology* 27(3), 512-530.

Palmqvist P., Martinez-Navarro B., Perez-Claros J.A., Torregros V., Figuerido B., Espigares M.P., De Renzi M. 2011. The giant hyena *Pachycrocuta brevirostris*: Modelling the bone cracking behavior of an extinct carnivore *Quaternary International* 243:61-79

Pante, M. C., & Blumenschine, R. J. (2010). Fluvial transport of bovid long bones fragmented by the feeding activities of hominins and carnivores. *Journal of Archaeological Science*, 37(4), 846-854.

Pante, M.C., Blumenschine, R.J., Capaldo, S.D., Scott, R.S., 2012. Validation of bone surface modification models for inferring fossil hominin and carnivore feeding interactions, with reapplication to FLK 22, Olduvai Gorge, Tanzania. *J. Hum. Evol.* 63, 395-407.

Pante, M.C., 2013. The larger mammal fossil assemblage from JK2, Bed III, Olduvai Gorge, Tanzania: implications for the feeding behavior of *Homo erectus*. *Journal of human evolution*, 64(1), pp.68-82.

Pante, M.C., Scott, R.S., Blumenschine, R.J. and Capaldo, S.D., 2015. Revalidation of bone surface modification models for inferring fossil hominin and carnivore feeding interactions. *Quaternary International*, 355, pp.164-168.

Pante, M. C., Muttart, M. V., Keevil, T. L., Blumenschine, R. J., Njau, J. K., & Merritt, S. R. (2017). A new high-resolution 3-D quantitative method for identifying bone surface modifications with implications for the Early Stone Age archaeological record. *Journal of Human Evolution*, 102, 1-11.

Park, H. K., Chung, J. W., & Kho, H. S. (2006). Use of hand-held laser scanning in the assessment of craniometry. *Forensic science international*, 160(2), 200-206.

Parkinson, J. A., Plummer, T., Hartstone-Rose, A. (2015). Characterizing felid tooth marking and gross bone damage patterns using GIS image analysis: An experimental feeding study with large felids. *J. Hum. Evol.* 80:114-134.

Pickering, T.R., Wallis, J., 1997. Bone modifications resulting from captive chimpanzee mastication: implications for the interpretation of Pliocene archaeological faunas. *Journal of Archaeological Science*, 24, 1115-1127.

Pickering, T.R., 2001. Carnivore voiding: a taphonomic process with the potential for the deposition of forensic evidence. *Journal of Forensic Sciences* 46, 406-411.

Pickering, T., Dominguez-Rodrigo, M., Egeland, C.P., Brain, C.K., 2004. Beyond leopards: tooth marks and the contribution of multiple carnivore taxa to the accumulation of the Swartkrans Member 3 fossil assemblage. *Journal of Human Evolution*, 46, 595-604.

Pickering, T.R., Egeland, C.P. 2006. Experimental patterns of hammerstone percussion damage on bones: implications for inferences of carcass processing by humans. *Journal of Archaeological Science*, 33, 459-469.

Plummer, T.W., Bishop, L.C., Ditchfield, P., Hicks, J., 1999. Research on Late Pliocene Oldowan sites at Kanjera South, Kenya. *Journal of Human Evolution*, 36, 151-170.

- Plummer, T.W., Stanford, C.B., 2000. Analysis of a bone assemblage made by chimpanzees at Gombe National Park, Tanzania. *Journal of Human Evolution*, 39, 345-365.
- Pobiner, B.L., Blumenschine, R.J., 2003. A taphonomic perspective on the Oldowan hominid encroachment on the carnivoran paleoguild. *Journal of Taphonomy* 1(2), 115-141.
- Pobiner B.L. 2007. Hominin-carnivore interactions: evidence from modern carnivore bone modification and Early Pleistocene archaeofauna (Koobi Fora, Kenya; Olduvai Gorge, Tanzania) *Doctoral Dissertation, Rutgers, The State University of New Jersey*
- Pobiner, B. L. (2015). New actualistic data on the ecology and energetics of hominin scavenging opportunities. *Journal of human evolution*, 80, 1-16.
- Polychronis, G., Christou, P., Mavragani, M., & Halazonetis, D. J. (2013). Geometric morphometric 3D shape analysis and covariation of human mandibular and maxillary first molars. *American journal of physical anthropology*, 152(2), 186-196.
- Potts, R., & Shipman, P. (1981). Cutmarks made by stone tools on bones from Olduvai Gorge, Tanzania. *Nature*, 291(5816), 577-580.
- Potts, R., 1983. Foraging for faunal resources by early hominids at Olduvai Gorge, Tanzania. In Clutton-Brock, J., Grigson, C., (Eds.), *Animals and Archaeology 1: Hunters and Their Prey*. British Archaeological Reports International Series 163, Oxford, pp. 51-62.
- Potts, R., 1998. Environmental hypotheses of hominid evolution. *Yearbook of Physical Anthropology*, 41, 93-136.
- Pradhan, G.R., Tennie, C. and van Schaik, C.P., 2012. Social organization and the evolution of cumulative technology in apes and hominins. *Journal of Human Evolution*, 63(1), pp.180-190.
- Ragir S. 2000. Diet and food preparation: Rethinking early hominid behavior. *Evolutionary Anthropology* 9: 153–155.
- Roche, H., Delagnes, A., Brugal, J.P., Feibel, C., Kibunjia, M., Mourre, V., Texier, P.J., 1999 Early hominid stone tool production and technical skill 2.34 Myr ago in West Turkana, Kenya. *Nature*, 399, 57-60.
- Rogers, M.J., Harris, J.W.K., Feibel, C.S., 1994. Changing patterns of land use by Plio-Pleistocene hominids in the Lake Turkana Basin. *Journal of Human Evolution*, 27, 139-158.
- Rudwick, M.J.S., 1976. *The Meaning of Fossils*. Neale Watson Academic Publications, New York.
- Ruck, L. (2014). Manual praxis in stone tool manufacture: Implications for language evolution. *Brain and language*, 139, 68-83.
- Sacco T., Van Valkenburgh B. 2004. Ecomorphological indicators of feeding behavior in the bears (Carnivore: Ursidae) *Journal of Zoology London* 263:41-54
- Schroettner, H., Schmied, M., & Scherer, S. (2006). Comparison of 3D surface reconstruction data from certified depth standards obtained by SEM and an infinite focus measurement machine (IFM). *Microchimica Acta*, 155(1), 279-284.

Selvaggio, M.M., 1994. Evidence from carnivore tooth marks and stone-tool-butchery marks for scavenging by hominids at FLK *Zinjanthropus*, Olduvai Gorge, Tanzania. Ph.D. dissertation, Rutgers University.

Selvaggio, M.M., 1998. Evidence for a three-stage sequence of hominid and carnivore involvement with long bones at FLK *Zinjanthropus*, Olduvai Gorge, Tanzania. *J. Archaeol. Sci.* 25, 191-202.

Selvaggio, M.M., Wilder, J., 2001. Identifying the involvement of multiple carnivore taxa with archaeological bone assemblages. *Journal of Archaeological Science* 28(5), 465-470.

Shipman, P., Rose, J., 1983. Early hominid hunting, butchering and carcass-processing behaviors: approaches to the fossil record. *Journal of Anthropological Archaeology*, 2, 57-98.

Shipman, P., Walker, A., 1989. The costs of becoming a predator. *Journal of Human Evolution*, 18, 373-392.

Sholts, S. B., Wärmländer, S. K., Flores, L. M., Miller, K. W., & Walker, P. L. (2010). Variation in the measurement of cranial volume and surface area using 3D laser scanning technology. *Journal of forensic sciences*, 55(4), 871-876.

Sholts, S. B., Walker, P. L., Kuzminsky, S. C., Miller, K. W., & Wärmländer, S. K. (2011). Identification of group affinity from cross-sectional contours of the human midfacial skeleton using digital morphometrics and 3D laser scanning technology. *Journal of forensic sciences*, 56(2), 333-338.

Slater, G. J., and B. Van Valkenburgh. Allometry and performance: the evolution of skull form and function in felids. *Journal of evolutionary biology* 22.11 (2009): 2278-2287.

Songsasen, N., & Rodden, M. D. (2010). The role of the species survival plan in maned wolf *Chrysocyon brachyurus* conservation. *International Zoo Yearbook*, 44(1), 136-148.

Stanford CB, Bunn HT, eds. 2001. Meat-Eating and Human Evolution. Oxford University Press.

Steele, T.E., 2003. Using mortality profiles to infer behavior in the fossil record. *Journal of Mammalogy*, 84(2), pp.418-430.

Stemp, J.W., Childs, B. E., & Vionnet, S. (2010). Laser profilometry and length-scale analysis of stone tools: second series experiment results. *Scanning*, 32(4), 233-243.

Stinner, M.C., 1990. The use of mortality patterns in archaeological studies of hominid predatory adaptations. *Journal of Anthropological Archaeology*, 9, 305-351.

Stinner, M.C., 1991. Food procurement and transport by human and non-human predators. *Journal of Archaeological Science*, 18, 455-482.

Tanner J.B., Dumont E.R., Sakai S.T., Lundrigan B.L. Holekamp K.E. 2008. Of arcs and vaults: the biomechanics of bone-cracking in spotted hyenas *Biological Journal of the Linnean Society* 95:256-255.

Tappen, M., Wrangham, R., 2000. Recognizing hominoid-modified bones: the taphonomy of colobus bones partially digested by free-ranging chimpanzees in the Kibale Forest, Uganda. *American Journal of Physical Anthropology*, 113, 217-234.

- Thali, M. J., Taubenreuther, U., Karolczak, M., Braun, M., Brueschweiler, W., Kalender, W. A., & Dirnhofer, R. (2003). Forensic microradiology: micro-computed tomography (Micro-CT) and analysis of patterned injuries inside of bone. *Journal of forensic sciences*, 48(6), 1336-1342.
- Therrien F. 2005. Feeding behavior and bite force of sabretoothed predators. *Zoological Journal of the Linnean Society* 145:393-426.
- Thompson, J. C., McPherron, S. P., Bobe, R., Reed, D., Barr, W. A., Wynn, J. G., ... & Alemseged, Z. (2015). Taphonomy of fossils from the hominin-bearing deposits at Dikika, Ethiopia. *Journal of human evolution*, 86, 112-135.
- Treves, A., & Naughton-Treves, L. (1999). Risk and opportunity for humans coexisting with large carnivores. *Journal of Human Evolution*, 36(3), 275-282.
- Tseng Z.J., Binder W.J. 2010. Mandibular biomechanics of *Crucuta crocuta*, *canis lupus*, and the late Miocene *Dinocrocuta gigantea*. *Zoological Journal of the Linnean Society* 158:683-696
- Tseng Z.J. 2013. Testing adaptive hypotheses of convergence with functional landscapes: A case study of bone-cracking hypercarnivores *PLoS One* 8(5)1-16
- Tseng Z.J., Flynn J.J. 2015. Are cranial biomechanical simulation data linked to known diets in extant taxa? A method for applying diet-biomechanics linkage models to infer feeding capability of extinct species *Plos One* 10(4):1-25
- Turillazzi, E., Karch, S. B., Neri, M., Pomara, C., Riezzo, I., & Fineschi, V. (2008). Confocal laser scanning microscopy. Using new technology to answer old questions in forensic investigations. *International journal of legal medicine*, 122(2), 173-177.
- Turner, A., 1988. Relative scavenging opportunities of East and South African Plio-Pleistocene hominids. *Journal of Archaeological Science*, 15, 327-341.
- Turner, A., 1992. Large carnivores and earliest European hominids: Changing determinants of resource availability during the Lower and Middle Pleistocene. *Journal of Human Evolution*, 22, 349-368.
- Ungar, P. (2004). Dental topography and diets of *Australopithecus afarensis* and early *Homo*. *Journal of Human Evolution*, 46(5), 605-622.
- Ungar PS, Grine FE, Teaford MF. 2006. Diet in early *Homo*: A review of the evidence and a new model of adaptive versatility. *Annual Review of Anthropology* 35: 209–228.
- Van Valkenburgh, B., 1985. Locomotor diversity within past and present guilds of large predatory mammals. *Paleobiology*, 11, 406-428.
- Van Valkenburgh, B., Teaford, M.F., Walker, A., 1990. Molar microwear and diet in large carnivores: inferences concerning diet in the sabretooth cat, *Smilodon fatalis*. *Journal of Zoology London* 222, 319-340.
- Van Valkenburgh, B., 1996. Feeding behavior in free-ranging, large African carnivores. *Journal of Mammalogy*, 77, 240-254.

- Van Valkenburgh, B., 1999. Major patterns in the history of carnivorous mammals. *Annual Review of Earth and Planetary Sciences*, 27, 462-493.
- Van Valkenburgh B., Molnar R. E., 2002. Dinosaurian and Mammalian Predators Compared *Paleobiology* 28(4):527-543
- Van Valkenburgh B., Wang X., Damuth J. 2004. Cope's Rule Hypercarnivory, and Extinction in North American Canids *Science* 306:101-104
- Van Valkenburgh B. 2007. Déjà vu: The Evolution of Feeding Morphologies in the Carnivora *Integrative and Comparative Biology* 47(1):147-163
- Van Valkenburgh B. 2009. Costs of carnivory: tooth fracture in Pleistocene and recent carnivorans *Biological Journal of the Linnean Society* 96:68-81
- Vrba, E.S., 1975. Some evidence of chronology and paleoecology of Sterkfontein, Swartkrans and Kromdraai from the fossil Bovidae. *Nature*, 254, 301-304.
- Vrba, E.S., 1980. The significance of bovid remains as indicators of environment and predation patterns. In Behrensmeyer, A.K., Hill, A. (Eds.), *Fossils in the Making*. University of Chicago Press, Chicago, pp. 247-271.
- Wayne, R.K. 1986. Limb morphology of domestic and wild canids: The influence of development in morphologic change. *Journal of Morphology*. 197:301-319.
- Werdelin L., Lewis M.E. 2005. Plio-Pleistocene Carnivora of eastern Africa: Species richness and turnover patterns *Zoological Journal of the Linnean Society* 144:121-144
- Wood, B.A., Collard, M. 1999. The human genus. *Science*, 284, 65-71.
- Wroe S., McHenry C., Thomason J. 2005. Bite club: comparative bite force in big biting mammals and the prediction of predatory behavior in fossil taxa *Proceeding of the Royal British Society* 272:619-625
- Wroe S. 2008. Cranial mechanics compared in extinct marsupial and extant African lions using a finite-element approach *Journal of Zoology* 274:332-339
- Yirga G., De Iongh HH., Leirs H., Gebrihiwot K., Deckers J., Bauer H. 2012. Adaptability of large carnivores to changing anthropogenic food sources: Diet change of spotted hyena (*Crocuta crocuta*) during Christian fasting period in northern Ethiopia. *Journal of Animal Ecology*. 81:1052-1055.
- Yravedra, J., Dominguez-Rodrigo, M., 2009. The shaft-based methodological approach to the quantification of long limb bones and its relevance to understanding hominin subsistence in the Pleistocene: application to four Paleolithic sites. *Journal of Quaternary Science*, 23, 85-96.
- Yravedra, J., Lagos, L., Biarcena, F., 2011. A taphonomic study of wild wolf (*Canis lupus*) modification of horse bones in northwestern Spain. *Journal of Taphonomy*, 9, 37-65.
- Yravedra, J., Rubio-Jara, S., Panera, J., Uribebarrea, D., & Pérez-González, A. (2012). Elephants and subsistence. Evidence of the human exploitation of extremely large mammal bones from the Middle Palaeolithic site of PRERESA (Madrid, Spain). *Journal of Archaeological Science*, 39(4), 1063-1071.

Yravedra, J., Andres, M., Dominguez-Rodrigo, M., 2014. A taphonomic study of the African wild dog (*Lycaon pictus*). *Archaeology ANthropol. Scie.*, 6, 113-124.

Yravedra, J., Maté-González, M. Á., Palomeque-González, J. F., Aramendi, J., Estaca-Gómez, V., San Juan Blazquez, M., ... & Cobo-Sánchez, L. (2017). A new approach to raw material use in the exploitation of animal carcasses at BK (Upper Bed II, Olduvai Gorge, Tanzania): a micro-photogrammetric and geometric morphometric analysis of fossil cut marks. *Boreas*. 10.1111/bor.12224

APPENDIX A – ALL MEASURED DATA FROM CAPTIVE AND WILD CARNIVORES

CARNIVORE TAXA	MARK ID	THREE DIMENSIONAL MEASUREMENTS						PROFILE MEASUREMENTS					
		SURFACE	VOLUME	MAXIMUM DEPTH	MEAN DEPTH	MAXIMUM LENGTH	MAXIMUM WIDTH	MAXIMUM DEPTH	AREA	WIDTH	ROUGHNESS	OPENING ANGLE	FLOOR RADIUS
African Wild Dog	DZD1-1	1.83E+06	1.60E+08	152.77	87.34	2548.56	1120.68	111.27	6.35E+04	1170.00	3.32	152.85	1506.81
African Wild Dog	DZD1-2	1.41E+06	1.03E+08	170.10	73.62	2231.62	796.32	164.43	6.16E+04	685.00	10.62	132.50	440.44
African Wild Dog	DZD1-4A	2.83E+06	2.96E+08	216.56	104.67	2488.69	1617.95	192.00	1.49E+05	1480.00	6.64	155.19	2209.57
African Wild Dog	DZD1-4B	2.97E+06	3.27E+08	222.44	110.26	2529.04	1522.95	264.59	2.38E+05	1635.00	20.83	150.67	1681.39
African Wild Dog	DZD1-5	5.13E+06	4.00E+08	160.04	78.00	5959.28	1130.40	142.25	8.20E+04	1370.00	2.56	167.43	4567.77
African Wild Dog	DZD2-1	1.79E+06	8.56E+07	114.52	47.71	2324.54	1094.37	103.23	4.65E+04	1030.00	4.39	166.14	8862.49
African Wild Dog	DZD4-2	4.48E+05	2.35E+07	116.14	52.54	949.43	555.98	74.66	1.47E+04	490.00	2.37	149.70	675.27
African Wild Dog	DZD4-3A	7.64E+05	5.27E+07	153.01	68.97	1727.03	626.35	151.74	5.18E+04	895.00	7.45	144.81	912.59
African Wild Dog	DZD4-3B	5.92E+05	4.12E+07	127.31	60.75	1249.72	584.48	93.48	2.91E+04	640.00	3.80	142.59	706.44
African Wild Dog	DZD4-4	2.89E+05	2.54E+07	158.55	87.85	883.85	383.25	103.53	2.10E+04	460.00	2.28	116.45	261.55
African Wild Dog	DZD4-5	6.77E+05	2.00E+07	77.34	29.56	1201.15	704.14	70.82	2.40E+04	915.00	3.55	163.90	2475.28
African Wild Dog	DZD4-6	1.01E+06	3.11E+07	74.19	30.86	1371.11	1096.13	66.85	3.45E+04	950.00	2.58	170.41	2560.81
African Wild Dog	DZD4-7	3.14E+05	6.98E+06	60.97	22.26	829.14	486.13	59.40	1.18E+04	430.00	1.95	162.95	700.08
African Wild Dog	DZD4-8	1.17E+06	5.14E+07	118.13	44.02	1895.51	896.04	107.78	4.92E+04	850.00	3.77	153.95	1187.57
African Wild Dog	DZD4-9	2.25E+06	1.54E+08	136.96	68.23	2407.39	1052.44	131.15	9.52E+04	1290.00	3.43	157.75	1757.20
African Wild Dog	DZD4-10	1.24E+06	7.07E+07	105.36	44.83	1710.68	811.54	99.44	5.21E+04	850.00	3.05	158.21	1214.95
African Wild Dog	DZD4-11	9.87E+05	4.28E+07	112.45	43.29	2740.38	653.08	117.28	3.70E+04	665.00	5.66	151.74	796.71
African Wild Dog	DZD4-12	2.14E+06	1.83E+08	222.28	85.69	2389.20	1244.71	206.03	1.32E+05	1345.00	3.05	144.37	1334.24
African Wild Dog	DZD4-14	3.74E+05	5.48E+06	54.50	14.65	1481.22	325.52	52.48	6.79E+03	340.00	2.61	156.93	536.03
African Wild Dog	DZD4-15A	3.58E+05	5.11E+06	47.86	14.24	1467.33	307.30	49.77	8.47E+03	360.00	1.99	162.63	608.61
African Wild Dog	DZD4-15B	3.89E+05	5.86E+06	61.15	15.05	1495.12	343.75	55.19	5.11E+03	320.00	3.22	151.23	463.46
African Wild Dog	DZD6-1	1.24E+06	6.03E+07	117.85	48.43	2870.47	590.17	127.54	4.77E+04	735.00	4.38	139.31	569.75
African Wild Dog	DZD7-1	7.01E+05	2.62E+07	92.08	37.45	1164.13	809.66	92.33	3.92E+04	830.00	2.11	153.91	1307.27

African Wild Dog	DZD7-2	2.06E+05	5.40E+06	76.29	26.15	612.26	363.18	61.48	8.56E+03	315.00	2.90	144.95	271.17
African Wild Dog	DZD7-3	5.16E+05	1.42E+07	73.54	26.83	1157.82	573.18	68.59	2.01E+04	550.00	2.57	155.02	925.25
African Wild Dog	DZD7-4	6.42E+05	1.09E+07	52.26	16.89	1697.08	546.69	51.95	1.26E+04	525.00	2.68	166.20	1197.31
African Wild Dog	DZD8-1A	5.50E+05	2.47E+07	83.25	44.86	1106.38	643.35	98.37	4.90E+04	870.00	3.22	157.39	1114.74
African Wild Dog	DZD8-1B	2.47E+05	9.97E+06	77.66	40.28	615.02	496.32	53.10	1.27E+04	460.00	2.68	157.58	635.73
African Wild Dog	DZD8-1C	2.84E+05	1.30E+07	98.42	45.96	723.07	454.13	77.10	1.44E+04	380.00	1.91	153.30	470.14
African Wild Dog	DZB8-2A	2.79E+05	4.93E+06	47.95	17.67	810.57	567.17	43.22	9.54E+03	580.00	3.04	152.04	3683.77
African Wild Dog	DZB8-2B	3.38E+04	7.66E+05	43.82	22.64	223.56	191.42	35.12	3.95E+03	180.00	1.96	145.23	166.97
Grey Wolf	WSN1-1	2.29E+06	1.08E+08	137.79	47.37	2387.33	1423.28	147.28	1.14E+05	1780.00	7.22	164.73	3786.26
Grey Wolf	WSN2-1	8.93E+05	7.42E+07	224.92	83.04	1141.91	1049.63	216.63	1.35E+05	1240.00	8.88	141.16	1018.87
Grey Wolf	WSN2-2	4.85E+05	2.48E+07	127.99	51.17	1099.15	549.96	139.35	7.15E+04	975.00	3.64	146.42	894.66
Grey Wolf	WSN2-3	2.06E+06	9.36E+07	123.09	45.42	2018.95	1454.91	115.94	9.51E+04	1515.00	3.85	159.42	3366.62
Grey Wolf	WSH1-2	2.92E+06	2.07E+08	147.21	70.84	1839.34	2112.37	162.62	2.21E+05	2055.00	6.74	164.65	4340.53
Grey Wolf	WSH1-3	4.30E+06	5.78E+08	381.85	134.57	3136.30	1725.36	401.54	3.92E+05	2070.00	12.81	134.10	1417.46
Grey Wolf	WSH1-4	4.15E+06	4.78E+08	324.23	115.22	3393.46	1844.67	331.90	2.77E+05	1675.00	9.69	132.61	1150.83
Grey Wolf	WSH1-5	2.79E+06	1.73E+08	150.47	61.99	2625.05	1163.29	158.42	1.06E+05	1610.00	7.07	156.65	4149.35
Grey Wolf	WSH1-7	8.72E+05	5.96E+07	156.06	68.35	1620.73	974.32	163.27	9.08E+04	1190.00	5.51	150.50	1202.62
Grey Wolf	WSH1-8	1.54E+06	7.77E+07	140.64	50.57	3277.93	789.47	144.03	5.02E+04	955.00	4.30	147.00	972.05
Grey Wolf	WSH1-9	1.98E+06	1.16E+08	141.38	58.48	2514.72	988.30	133.29	6.99E+04	1195.00	2.57	158.49	1764.41
Grey Wolf	WSH1-10	3.86E+06	2.61E+08	188.01	67.72	3216.49	1558.85	211.50	1.88E+05	1720.00	8.24	153.13	1951.53
Grey Wolf	WSH1-13	9.58E+05	5.20E+07	155.48	54.24	1108.25	1104.31	121.18	5.45E+04	900.00	6.61	146.92	859.89
Grey Wolf	WSH3-1	1.11E+06	3.89E+07	109.27	35.16	4626.59	479.27	119.99	2.51E+04	545.00	7.47	141.61	475.08
Grey Wolf	WST1-1	1.39E+06	4.11E+07	69.61	29.49	1913.90	761.12	70.05	2.69E+04	900.00	1.78	148.18	3112.31
Grey Wolf	WST1-2A	3.50E+05	1.26E+07	85.36	36.15	800.61	583.42	87.66	2.96E+04	620.00	2.64	149.95	645.39
Grey Wolf	WST1-2B	2.90E+05	9.77E+06	89.02	33.71	742.06	468.93	92.72	2.46E+04	670.00	2.26	153.56	713.52
Grey Wolf	WST1-7	1.10E+06	1.59E+07	49.68	14.51	3213.06	477.40	62.40	2.06E+04	710.00	2.05	163.76	1529.92
Grey Wolf	WST1-8	2.95E+05	4.33E+06	46.93	14.69	640.65	707.26	41.67	9.56E+03	585.00	2.69	166.15	1479.03
Grey Wolf	WST1-9	3.38E+05	8.26E+06	69.31	24.43	724.81	687.32	82.88	2.27E+04	530.00	3.09	146.49	483.04
Grey Wolf	WST1-11	2.55E+06	9.31E+07	110.07	36.52	3872.67	967.99	98.57	4.80E+04	1390.00	2.92	158.05	9218.50
Grey Wolf	WST1-12	1.02E+06	7.67E+07	169.82	75.18	1065.68	1110.57	119.47	6.22E+04	1045.00	4.85	154.12	1262.51

Grey Wolf	WST1-15	1.73E+06	1.67E+08	168.77	96.31	1418.31	2082.20	189.87	1.61E+05	1415.00	6.35	166.81	3423.53
Grey Wolf	WST1-17	6.67E+05	2.13E+07	92.72	31.86	1075.18	766.70	93.02	3.35E+04	715.00	4.08	151.11	748.51
Grey Wolf	WST1-18A	6.01E+05	2.40E+07	84.12	39.94	1060.34	875.30	81.33	4.06E+04	995.00	2.37	160.87	1501.21
Grey Wolf	WST1-18B	5.14E+05	1.76E+07	73.12	34.17	984.59	763.81	73.12	3.25E+04	785.00	3.01	160.50	1182.38
Grey Wolf	WST1-21	3.05E+06	3.18E+08	247.47	104.50	2755.85	1639.66	258.59	2.25E+05	1650.00	9.68	143.64	1403.27
Grey Wolf	WST1-23	1.91E+06	1.42E+08	180.57	74.25	1730.39	1325.04	182.73	1.50E+05	2115.00	7.33	160.20	3201.08
Grey Wolf	WST1-3	3.86E+05	2.08E+07	104.29	53.94	991.98	632.37	110.37	3.42E+04	520.00	5.32	140.34	444.28
Spotted Hyena*	NGO25-3-1	6.19E+05	3.10E+08	169.00	50.12	4267.00	2332.55	174.78	2.09E+05	2395.00	8.71	163.58	4767.01
Spotted Hyena*	NGO25-3-3	2.66E+06	1.72E+08	159.98	64.76	4316.62	816.00	146.94	6.18E+04	850.00	5.01	146.73	832.28
Spotted Hyena*	NGO25-3-7	1.96E+06	7.59E+07	96.11	38.63	1949.33	1582.92	114.40	6.33E+04	1005.00	2.97	159.35	1478.61
Spotted Hyena*	NGO25-6-2	5.22E+06	5.64E+08	267.93	107.93	2589.39	2826.95	241.88	4.10E+05	2815.00	5.21	161.76	4582.58
Spotted Hyena*	NGO25-7-1	5.08E+06	3.52E+08	225.35	69.25	5013.29	1366.49	214.74	1.41E+05	1455.00	3.36	150.98	1651.11
Spotted Hyena*	NGO25-18-1	3.31E+06	2.11E+08	215.62	63.90	3163.37	2199.23	208.59	2.08E+05	2150.00	9.29	155.91	3544.51
Spotted Hyena*	NGO25-18-2	1.04E+07	7.06E+08	184.13	67.74	5968.97	2342.90	196.45	2.82E+05	2520.00	6.25	162.23	4463.52
Spotted Hyena*	NGO25-21-1	2.73E+06	1.36E+08	114.40	49.67	2448.59	1440.71	109.22	7.70E+04	1275.00	2.03	163.36	2458.72
Spotted Hyena*	NGO25-22-1	4.47E+05	3.24E+07	163.83	72.46	842.63	764.00	139.72	5.94E+04	775.00	6.15	138.18	557.44
Spotted Hyena*	NGO25-14-1	2.72E+06	3.86E+08	317.90	142.05	3555.33	1255.44	302.53	2.38E+05	1465.00	4.39	136.55	1055.39
Spotted Hyena*	NGO25-14-2	7.57E+05	5.32E+07	172.26	70.25	1215.48	945.44	177.67	8.78E+04	1015.00	3.71	135.44	745.97
Spotted Hyena*	NGO25-14-3	5.25E+06	1.14E+09	592.78	217.58	3349.72	1887.57	575.99	5.14E+05	2065.00	20.71	117.50	1142.10
Spotted Hyena*	NGO25-14-5	3.16E+06	4.89E+08	367.72	154.65	2476.15	1328.26	369.16	2.87E+05	1500.00	6.08	126.30	914.23
Spotted Hyena*	NGO25-10-2	4.29E+06	3.55E+08	222.67	82.72	5359.92	1217.27	252.90	1.84E+05	1455.00	5.09	141.38	1218.83
Spotted Hyena*	NGO25-10-3	6.52E+06	8.17E+08	296.03	125.38	5209.10	2758.19	299.32	4.23E+05	2750.00	2.93	151.36	4425.51
Spotted Hyena*	NGO25-1-1	4.02E+06	2.43E+08	180.99	60.29	3971.66	1583.73	164.65	9.60E+04	1205.00	7.88	143.23	951.29
Spotted Hyena*	NGO25-1-2	2.00E+06	6.58E+07	104.98	32.92	4026.02	823.81	103.91	2.06E+04	690.00	9.17	149.04	957.81
Spotted Hyena*	NGO25-1-4	5.96E+06	2.74E+08	101.12	45.96	4777.30	2808.64	92.54	9.55E+04	2845.00	4.45	170.57	18191.97
Spotted Hyena*	NGO25-1-5	1.26E+06	4.34E+07	82.13	34.45	1680.25	1370.79	86.17	3.44E+04	755.00	2.81	159.45	929.77
Spotted Hyena*	NGO25-2 - 1	3.02E+06	1.90E+08	209.49	62.96	4320.04	1377.22	170.16	4.66E+04	455.00	4.54	82.14	244.91
Spotted Hyena*	NGO25-2 - 2A	3.49E+06	5.00E+08	364.23	143.36	3644.29	1463.64	346.69	1.77E+05	980.00	9.60	106.07	490.44
Spotted Hyena*	NGO25-2 - 2B	9.98E+05	5.47E+07	189.92	54.74	1777.57	941.88	195.75	9.08E+04	910.00	8.79	135.62	589.11
Spotted Hyena*	NGO25-2 - 3A	3.31E+06	1.01E+08	106.21	30.56	3852.18	2042.71	90.67	2.83E+04	850.00	4.84	157.14	1315.58

Spotted Hyena*	NGO25-2 - 3B	1.09E+06	4.76E+07	128.57	43.75	2307.12	759.98	130.11	4.17E+04	660.00	6.70	132.51	465.78
Spotted Hyena*	NGO25-2 - 3C	7.44E+05	3.02E+07	98.44	40.51	1565.14	694.23	90.44	2.50E+04	565.00	3.66	145.22	508.01
Spotted Hyena*	NGO25-2 - 4A	3.94E+05	1.67E+07	126.34	42.45	706.52	857.35	119.70	4.70E+04	840.00	4.45	146.99	827.30
Spotted Hyena*	NGO25-2 - 4B	1.24E+05	3.59E+06	63.40	28.87	592.38	282.20	63.23	9.75E+03	295.00	2.24	139.50	226.13
Spotted Hyena*	NGO25-2 - 5	1.77E+06	9.86E+07	148.60	55.57	3522.16	1263.57	135.27	7.78E+04	1300.00	5.56	160.69	2288.07
Spotted Hyena*	NGO25-1 - 6	2.66E+06	2.98E+08	261.58	111.68	1980.23	1881.95	246.41	2.40E+05	1995.00	13.88	144.27	2741.71
Spotted Hyena	DZHP1-1	8.22E+06	1.29E+09	272.72	157.14	4214.52	2139.35	150.26	1.67E+05	2340.00	5.99	168.84	6167.43
Spotted Hyena	DZHP1-2	8.71E+05	4.43E+07	124.84	50.91	1125.83	968.01	129.10	7.22E+04	1000.00	6.12	150.90	1138.32
Spotted Hyena	DZHP1-3	1.03E+06	8.86E+07	200.15	85.68	1319.70	931.22	184.89	7.64E+04	1030.00	6.38	140.35	878.22
Spotted Hyena	DZHP2-1	7.40E+06	1.35E+09	482.45	182.81	3288.04	3037.92	472.81	9.53E+05	3220.00	11.38	122.33	7569.14
Spotted Hyena	DZHP2-2	5.00E+06	5.07E+08	286.26	101.29	3148.47	2208.34	292.77	2.98E+05	2270.00	12.18	154.88	2764.70
Spotted Hyena	DZHP3-1A	3.39E+06	2.10E+08	226.45	62.10	1644.73	1730.05	202.59	1.15E+05	1365.00	5.01	144.50	1630.70
Spotted Hyena	DZHP3-1B	2.70E+06	1.68E+08	191.53	62.23	2833.53	981.61	179.42	1.17E+05	1545.00	4.82	149.70	1655.59
Spotted Hyena	DZHP3-2	4.93E+06	4.64E+08	249.24	94.24	4255.88	1624.56	269.66	3.25E+05	2055.00	6.56	122.31	2418.80
Spotted Hyena	DZHP4-1	4.96E+06	4.85E+08	267.75	97.76	3702.18	1916.45	281.21	3.11E+05	2160.00	9.37	138.60	2591.75
Spotted Hyena	DZHP4-3	3.66E+06	2.92E+08	182.66	79.79	2845.76	1760.91	206.49	1.91E+05	1660.00	8.67	153.20	1867.69
Spotted Hyena	DZHP5-1	1.21E+07	8.31E+08	197.69	68.63	11203.91	1431.17	181.47	1.33E+05	1515.00	4.13	150.27	1795.53
Spotted Hyena	DZHP5-2	7.64E+06	4.96E+08	150.02	59.48	7680.75	1164.36	144.41	1.05E+05	1470.00	3.28	158.20	2790.63
Spotted Hyena	DZHP5-3	3.17E+06	1.60E+08	102.34	50.33	4157.58	897.56	107.35	7.74E+04	1425.00	2.44	166.13	3785.73
Spotted Hyena	DZHP5-5	3.25E+06	2.12E+08	164.81	65.23	3119.15	1294.85	175.95	1.20E+05	1460.00	2.90	153.24	1638.69
Spotted Hyena	DZHP5-7	9.07E+06	8.47E+08	219.49	93.43	5529.54	2386.25	191.83	2.29E+05	2620.00	5.73	161.96	4922.99
Spotted Hyena	DZHP5-11	1.33E+07	1.12E+08	202.67	83.55	1627.91	721.68	205.35	1.12E+05	1040.00	7.68	148.21	1013.92
Spotted Hyena	DZHP5-12A	8.30E+05	1.88E+07	59.60	22.66	2355.85	613.77	61.39	1.59E+04	580.00	3.27	163.10	958.97
Spotted Hyena	DZHP5-13	2.53E+06	1.09E+08	121.41	43.01	3674.14	775.04	132.48	6.49E+04	1180.00	3.41	153.71	1962.43
Spotted Hyena	DZHP5-15	6.89E+05	3.82E+07	117.76	55.42	801.29	1054.56	115.68	6.18E+04	1060.00	4.52	153.20	1201.19
Spotted Hyena	DZHP5-16	3.16E+06	3.29E+08	268.33	104.18	2161.22	1901.36	239.04	2.04E+05	1985.00	15.13	150.93	2140.47
Spotted Hyena	DZHP5-17	1.04E+07	2.10E+09	493.03	203.31	4735.33	2980.85	479.02	7.85E+05	3255.00	6.88	146.72	3125.76
Spotted Hyena	DZHP5-18	1.47E+06	8.39E+11	149.71	60.43	1128.09	1096.05	136.08	7.94E+04	1155.00	136.74	136.74	1907.98
Spotted Hyena	DZHP6-1A	6.14E+05	1.98E+07	80.35	32.22	959.92	916.31	72.65	3.42E+04	860.00	3.08	162.61	1519.75
Spotted Hyena	DZHP6-1B	2.44E+06	7.98E+07	86.76	32.76	3568.05	1081.82	85.36	6.65E+04	1785.00	8.48	173.14	9290.13

Spotted Hyena	DZHP6-4	2.14E+07	4.77E+09	595.21	223.22	8309.44	3810.50	506.87	9.55E+05	3685.00	14.18	148.80	3617.70
Spotted Hyena	DZHP6-5	8.70E+06	1.41E+09	448.40	162.33	3814.52	2343.27	452.69	6.86E+05	3090.00	10.43	149.52	3545.18
Spotted Hyena	DZHP6-6	9.73E+06	2.42E+09	655.89	248.27	4455.00	2440.24	580.70	6.19E+05	3250.00	20.21	142.73	7327.62
Spotted Hyena	DZHP6-7	1.22E+07	2.04E+09	412.97	167.01	4199.33	3375.58	358.64	4.75E+05	2680.00	14.02	149.89	3346.94
Spotted Hyena	DZHP6-8	1.91E+06	2.42E+08	242.75	126.94	1837.84	1234.45	239.18	3.09E+05	1940.00	8.01	154.44	2419.89
Spotted Hyena	DZHP9-1	1.84E+06	2.17E+08	220.32	117.67	1999.34	1281.72	207.36	1.63E+05	1390.00	2.95	130.21	1362.20
Striped Hyena	DZHT1-2	1.30E+07	1.17E+09	252.74	89.67	9324.77	2020.67	245.93	2.17E+05	1895.00	6.45	155.75	2359.01
Striped Hyena	DZHT1-3	1.23E+07	8.35E+08	173.50	67.97	9557.73	1734.40	173.75	1.42E+05	1705.00	5.77	155.12	2944.49
Striped Hyena	DZHT1-4	7.69E+06	1.57E+08	85.87	20.38	8070.27	1145.65	91.71	3.94E+04	1270.00	3.14	165.58	3497.30
Striped Hyena	DZHT1-5	5.60E+07	2.77E+08	141.52	49.41	7957.42	1297.51	132.55	5.94E+04	1100.00	5.48	161.40	1859.26
Striped Hyena	DZHT1-6	4.79E+06	1.35E+08	123.56	28.25	11501.28	1095.80	125.84	6.14E+04	1065.00	5.19	162.98	1928.80
Striped Hyena	DZHT1-7	5.48E+06	2.46E+08	178.82	44.97	5824.42	1453.63	172.18	8.86E+04	1340.00	4.79	151.65	1512.89
Striped Hyena	DZHT1-8	7.18E+06	4.13E+08	171.99	51.51	8154.06	1024.43	191.25	7.37E+04	1130.00	7.93	148.74	1794.22
Striped Hyena	DZHT1-9	3.04E+06	2.41E+08	218.03	79.27	1985.36	1863.96	212.79	1.65E+05	1815.00	10.85	159.86	2560.65
Striped Hyena	DZHT1-10	4.14E+07	7.56E+09	507.30	182.51	16038.27	4263.77	601.46	1.35E+06	4600.00	16.48	151.47	5264.94
Striped Hyena	DZHT1-11	5.36E+06	3.58E+08	193.39	66.82	3178.40	2165.33	214.69	2.05E+05	2505.00	8.51	168.47	6815.64
Striped Hyena	DZHT2-1	2.93E+07	3.56E+09	293.81	121.45	14237.68	2172.54	268.60	2.64E+05	2130.00	16.35	165.85	4979.85
Striped Hyena	DZHT2-2A	1.43E+06	5.49E+07	105.00	38.48	2283.61	1033.69	99.59	5.13E+04	1020.00	3.48	163.67	2136.92
Striped Hyena	DZHT2-2B	9.37E+05	3.69E+07	94.32	39.41	1457.21	582.31	80.73	2.43E+04	565.00	2.31	146.79	563.07
Striped Hyena	DZHT2-3	7.49E+05	4.69E+07	158.80	62.64	1191.55	911.85	158.90	6.69E+04	990.00	6.48	154.38	963.50
Striped Hyena	DZHT2-4	2.11E+06	8.94E+07	94.43	42.46	2948.54	1046.01	117.43	6.55E+04	1150.00	4.39	160.61	2060.22
Striped Hyena	DZHT2-5	3.52E+06	6.30E+07	81.48	17.90	5313.80	972.58	86.39	3.00E+04	910.00	6.02	167.12	2448.24
Striped Hyena	DZHT2-6	3.98E+06	1.06E+08	90.26	26.64	4500.20	1054.75	99.29	7.08E+04	1675.00	6.05	168.46	4649.48
Striped Hyena	DZHT2-7	1.76E+06	1.25E+08	175.67	71.20	1863.17	1101.92	186.25	1.18E+05	1135.00	3.67	155.58	1371.60
Striped Hyena	DZHT2-8	3.12E+06	1.71E+08	151.54	54.82	3334.27	1256.20	125.36	5.64E+04	1020.00	3.77	156.65	1386.74
Striped Hyena	DZHT2-9	5.24E+06	4.68E+08	241.37	89.31	3726.74	1837.28	211.74	1.40E+05	1470.00	10.39	159.24	3319.66
Striped Hyena	DZHT2-10	2.37E+07	2.70E+09	247.59	113.96	12870.53	2549.76	248.31	2.10E+05	1905.00	15.48	156.36	2735.89
Striped Hyena	DZHT3-1A	1.59E+06	7.57E+07	121.62	47.47	2447.77	753.70	130.45	5.64E+04	925.00	6.63	152.90	977.39
Striped Hyena	DZHT3-1B	9.88E+05	3.59E+07	93.13	36.32	1765.26	722.64	99.56	4.32E+04	925.00	3.10	163.85	3286.82
Striped Hyena	DZHT3-2	1.06E+07	1.32E+09	382.43	124.51	5786.80	2716.25	321.21	2.87E+05	2370.00	8.13	127.42	5952.96

Striped Hyena	DZHT3-3	7.16E+06	6.06E+08	224.82	84.68	3901.92	3028.46	192.54	2.68E+05	3130.00	8.85	165.48	8736.59
Striped Hyena	DZHT3-4A	2.55E+06	1.70E+08	209.98	66.51	2229.30	1412.46	203.18	1.47E+05	1830.00	15.77	157.05	2811.31
Striped Hyena	DZHT3-4B	2.89E+06	1.90E+08	141.18	65.68	3135.52	1249.03	151.51	1.15E+05	1605.00	5.38	160.39	2347.30
Striped Hyena	DZHT3-5	6.10E+06	1.07E+09	359.30	175.83	3189.35	2273.81	367.06	4.71E+05	2820.00	8.39	147.86	2906.18
Striped Hyena	DZHT3-7A	2.97E+06	4.26E+08	316.66	143.50	2242.34	1411.86	339.80	2.86E+05	1810.00	10.47	144.17	1637.59
Striped Hyena	DZHT3-7B	1.38E+06	5.61E+07	93.05	40.50	1507.17	1520.08	86.55	4.17E+04	1015.00	4.58	164.61	2089.81
African Lion*	A1	2.15E+06	5.89E+07	73.97	27.36	2451.92	766.84	65.85	2.00E+04	835.00	3.05	165.05	1767.36
African Lion*	A2	5.53E+06	3.45E+08	128.78	62.40	5537.56	1395.55	75.02	5.16E+04	1480.00	3.46	171.73	5806.12
African Lion*	A3	4.57E+06	2.29E+08	132.61	50.01	5479.61	1095.60	82.64	3.18E+04	800.00	3.83	165.72	2102.62
African Lion*	B1	2.11E+06	4.50E+07	66.08	21.33	9083.30	407.91	56.47	1.31E+04	490.00	2.39	156.77	2015.21
African Lion*	B2	2.49E+06	5.26E+07	57.63	21.08	6235.34	578.13	51.74	1.36E+04	500.00	2.40	161.33	830.40
African Lion*	C1	1.55E+06	3.99E+07	85.74	25.77	3030.01	625.59	96.91	3.67E+04	725.00	3.67	150.74	866.78
African Lion*	C2	3.32E+05	1.65E+07	100.26	49.62	801.10	475.14	104.41	2.98E+04	520.00	5.00	138.32	388.19
African Lion*	E1	1.47E+06	2.68E+07	56.77	18.27	3500.72	567.67	52.85	1.65E+04	580.00	2.97	160.27	893.37
African Lion*	E2	1.90E+06	4.08E+07	78.60	21.46	4685.78	515.80	70.17	1.63E+04	455.00	1.92	147.15	426.64
African Lion*	E3	3.11E+06	6.51E+07	64.77	20.90	7513.43	953.56	73.59	3.79E+04	855.00	3.02	165.26	1775.78
African Lion*	I1	1.65E+06	3.38E+07	66.68	20.45	3066.75	853.44	77.29	2.30E+04	580.00	3.52	143.26	840.31
African Lion*	J1	8.10E+06	3.77E+08	175.58	46.52	9062.31	1123.90	200.60	1.03E+05	1160.00	5.90	142.54	1030.48
African Lion*	J2	6.73E+06	5.36E+08	201.39	79.67	7024.37	1387.35	205.29	1.56E+05	1250.00	4.36	147.53	1170.37
African Lion*	K1	1.21E+06	8.62E+07	160.06	71.36	1851.20	1017.51	163.52	1.06E+05	1050.00	6.08	150.19	1142.23
African Lion*	K2	1.34E+06	2.57E+07	67.96	19.25	3278.61	662.68	70.61	2.27E+04	545.00	4.13	160.71	835.02
African Lion*	L1	6.44E+06	4.52E+08	219.71	70.19	7395.96	1288.27	226.70	1.26E+05	1295.00	5.32	138.16	993.66
African Lion*	N1	2.69E+06	8.56E+07	89.05	31.81	6043.11	815.13	85.30	3.49E+04	695.00	1.51	154.21	807.87
African Lion*	N2	3.94E+06	9.79E+07	91.52	24.85	7946.21	762.06	84.90	3.43E+04	745.00	2.78	150.24	770.89
African Lion*	N3	4.98E+06	1.85E+08	105.37	37.08	6877.84	916.79	115.47	5.12E+04	1200.00	2.33	154.49	2032.16
African Lion*	O1	2.11E+06	7.60E+07	84.27	35.99	4338.88	561.90	50.57	1.56E+04	550.00	2.09	162.91	1046.11
African Lion*	O2	4.26E+06	1.20E+08	74.41	28.27	6161.08	864.36	56.93	2.67E+04	905.00	3.43	168.55	4416.67
African Lion*	O3	3.02E+06	1.38E+08	147.45	45.70	5533.27	964.82	162.35	7.24E+04	1135.00	5.28	158.27	1667.40
African Lion*	O4	9.06E+06	7.24E+08	206.98	79.10	7922.34	1944.66	231.14	1.34E+05	1270.00	6.41	143.93	1071.72
African Lion*	O5	1.03E+06	9.03E+07	234.70	87.71	1218.44	1147.91	256.81	1.73E+05	1325.00	5.28	141.58	1159.03

African Lion*	P1	3.00E+06	2.88E+08	225.69	96.03	4861.98	1185.50	237.56	1.67E+05	1345.00	3.67	146.29	1121.40
African Lion*	P2	3.92E+06	4.37E+08	246.61	11.46	5278.23	1009.86	206.73	1.10E+05	975.00	6.05	149.17	938.15
African Lion*	Q1	1.09E+07	2.41E+09	460.43	220.18	6948.70	2481.36	410.37	4.52E+05	2185.00	19.43	139.72	1851.40
African Lion*	S1	2.67E+06	1.87E+08	167.48	69.88	3090.43	1194.00	168.61	1.13E+05	1205.00	3.27	149.78	1255.65
African Lion*	S2	1.15E+06	8.14E+07	165.55	10.66	1105.91	1310.29	165.28	1.27E+05	1335.00	5.24	149.55	1776.02
African Lion	DZL1-1	1.04E+06	1.04E+08	237.25	100.27	1331.03	1077.22	219.77	8.99E+04	810.00	12.43	110.03	436.01
African Lion	DZL1-4	2.11E+06	6.00E+07	77.68	28.49	3602.80	873.19	77.92	2.07E+04	625.00	3.38	163.96	1087.42
African Lion	DZL1-6	4.28E+06	2.64E+08	170.91	61.70	6679.88	1275.09	143.19	6.20E+04	1070.00	4.68	148.05	1411.68
African Lion	DZL1-7A	2.84E+05	6.23E+06	54.30	21.95	630.40	536.82	53.17	1.36E+04	480.00	1.86	153.69	775.18
African Lion	DZL1-7B	3.30E+05	8.56E+06	73.38	25.93	847.57	480.53	78.08	2.20E+04	480.00	1.37	147.77	501.45
African Lion	DZL1-7C	2.99E+06	9.74E+07	101.19	32.56	5391.34	640.49	99.26	3.47E+04	775.00	4.18	156.95	1017.64
African Lion	DZL1-7D	8.06E+05	2.40E+07	76.72	29.74	1857.38	698.64	73.16	2.57E+04	775.00	2.16	160.06	1282.34
African Lion	DZL1-7E	6.63E+05	1.81E+07	67.38	27.31	1211.38	591.84	70.38	2.73E+04	715.00	1.85	158.21	1240.77
African Lion	DZL1-10	2.04E+06	3.24E+07	58.21	15.93	3840.83	600.17	65.14	1.88E+04	780.00	3.76	161.67	1591.91
African Lion	DZL2-3	2.22E+06	6.04E+07	74.50	29.57	3852.22	912.57	81.24	2.08E+04	655.00	3.85	183.15	1182.34
African Lion	DZL3-2	1.89E+05	4.65E+06	76.11	24.57	503.24	403.86	78.43	1.47E+04	430.00	1.47	141.96	368.14
African Lion	DZL3-3	1.86E+05	5.05E+06	67.60	27.15	544.06	500.00	65.35	1.53E+04	395.00	1.25	141.31	330.08
African Lion	DZL3-4	9.18E+05	1.51E+07	54.55	16.42	1972.41	585.02	25.74	1.37E+03	440.00	1.43	163.97	17847.49
African Lion	DZL3-5B	6.22E+05	1.17E+07	48.84	18.80	2596.23	359.96	44.00	6.50E+03	330.00	1.22	145.63	310.23
African Lion	DZL3-5C	5.98E+05	1.69E+07	70.84	28.70	2785.11	300.34	63.05	1.00E+04	285.00	1.56	119.52	169.11
African Lion	DZL3-5D	4.95E+05	8.04E+06	43.61	16.25	1930.96	313.69	36.40	5.29E+03	265.00	1.09	144.75	280.92
African Lion	DZL3-5E	5.85E+05	7.39E+06	41.63	12.64	4514.74	214.93	40.36	1.68E+03	175.00	0.45	156.06	230.73
African Lion	DZL3-5F	5.02E+05	6.98E+06	64.03	13.90	2963.64	234.53	58.13	5.54E+03	285.00	2.84	136.36	290.99
African Lion	DZL3-6	1.20E+06	1.10E+08	209.69	91.82	2215.47	777.01	202.53	1.02E+05	900.00	4.46	126.77	547.87
African Lion	DZL3-7	5.72E+05	2.60E+07	95.87	45.49	1969.23	363.16	86.82	2.38E+04	575.00	3.08	127.13	516.76
African Lion	DZL3-8	4.96E+05	1.36E+07	65.25	27.30	1886.76	294.29	64.27	8.38E+03	400.00	1.81	143.94	365.51
African Lion	DZL3-9	6.97E+05	4.39E+07	164.05	62.98	1109.63	781.50	156.33	6.30E+04	945.00	6.43	143.55	785.09
African Lion	DZL3-12A	2.45E+05	6.73E+06	61.37	27.41	1008.24	254.11	67.80	1.05E+04	320.00	2.01	132.03	216.33
African Lion	DZL3-12B	2.54E+05	5.38E+06	54.79	21.17	994.92	389.60	54.15	7.72E+03	315.00	2.04	147.70	313.89
African Lion	DZL3-12C	2.47E+05	8.40E+06	76.19	33.96	587.37	466.93	79.84	2.52E+04	575.00	3.94	146.31	526.25

African Lion	DZL3-12D	1.45E+05	4.17E+06	60.92	28.82	570.98	277.01	45.42	7.39E+03	345.00	2.45	154.44	462.77
African Lion	DZL3-13A	6.57E+05	2.03E+07	75.54	30.97	1829.81	545.91	41.65	9.94E+03	565.00	1.35	165.64	1229.83
African Lion	DZL3-13B	1.24E+06	5.54E+07	98.89	44.80	3724.34	585.01	75.39	2.72E+04	625.00	2.87	149.51	769.69
African Lion	DZL3-13C	2.88E+05	1.46E+07	134.86	50.63	597.79	609.96	122.39	4.17E+04	700.00	3.58	143.51	613.59
Nile Crocodile	SCP4.1 1A	9.36E+06	9.61E+08	327.32	102.70	10117.18	1620.12	314.14	2.28E+05	1700.00	21.54	139.52	1347.34
Nile Crocodile	SCP4.1 1B	7.29E+06	8.36E+08	325.05	114.73	7273.36	1703.94	313.43	2.84E+05	1620.00	12.63	132.60	1135.76
Nile Crocodile	FEM 1A	1.59E+07	1.17E+09	222.71	73.50	11347.61	1645.79	228.69	2.50E+05	2180.00	11.76	158.45	3174.76
Nile Crocodile	FEM 1B	9.21E+06	1.01E+09	202.00	109.13	5818.99	2142.63	211.35	1.92E+05	1600.00	4.79	153.92	2026.88
Nile Crocodile	FEM 1C	6.53E+06	5.45E+08	160.34	83.45	5181.27	1398.86	156.37	1.46E+05	1750.00	10.17	158.73	2469.87
Nile Crocodile	HUM4.2 3	5.85E+05	1.71E+07	76.57	29.25	3243.23	321.12	77.17	9.52E+03	255.00	2.15	121.46	142.81
Nile Crocodile	HUM4.2 4	6.28E+06	7.92E+08	293.93	126.10	5138.83	1694.62	297.61	2.91E+05	1905.00	10.31	147.37	1869.30
Nile Crocodile	HUM4.2 6A	1.50E+06	5.37E+07	77.07	35.79	1665.02	1197.99	85.14	5.87E+04	1315.00	3.68	167.19	3059.76
Nile Crocodile	HUM4.2 6B	1.35E+06	6.26E+07	152.96	46.20	2180.24	1279.99	146.34	5.45E+04	775.00	6.73	150.74	749.10
Nile Crocodile	HUM4.2 7	8.15E+06	8.74E+08	310.60	107.27	3947.20	3104.19	310.11	4.85E+05	4495.00	9.61	156.90	19148.23
Nile Crocodile	HUM4.2 8	1.97E+07	7.54E+09	1097.59	383.08	11409.17	3410.24	111.06	2.16E+06	3750.00	16.71	115.38	1918.86
Nile Crocodile	HUM4.2 9	4.10E+06	1.10E+08	91.56	26.91	9151.51	670.86	95.00	3.43E+04	825.00	2.63	150.88	899.11
Nile Crocodile	HUM4.2 10	2.15E+06	1.23E+08	154.73	57.12	3027.15	984.03	156.52	7.34E+04	1080.00	3.13	143.22	1499.10
Nile Crocodile	KRM4 1	1.20E+07	2.22E+09	402.60	185.18	10819.70	1761.01	373.05	3.13E+05	1670.00	18.60	132.80	1170.12
Nile Crocodile	RAD4.3 1	9.99E+06	9.58E+08	315.16	95.85	12251.63	1909.03	300.69	2.79E+05	2075.00	11.44	135.34	2340.72
Nile Crocodile	RAD4.3 3A	7.77E+06	1.87E+09	562.67	240.77	3978.42	2952.22	552.10	8.80E+05	2740.00	12.10	146.31	3696.23
Nile Crocodile	RAD4.3 3B	2.26E+06	2.35E+08	331.67	104.25	1740.52	1922.32	331.44	2.44E+05	1800.00	17.34	137.74	1538.88
Nile Crocodile	RAD4.3 4	6.28E+06	1.65E+09	642.68	262.47	3421.55	2696.09	626.77	9.19E+05	2850.00	13.03	131.31	1984.42
Nile Crocodile	RAD4.3 5	7.22E+06	1.07E+09	486.59	148.41	3012.22	3399.95	492.90	7.56E+05	3800.00	15.86	153.91	5565.28
Nile Crocodile	RAD4.3 6	4.97E+06	2.42E+08	128.74	48.71	2662.83	3720.65	133.49	1.68E+05	2300.00	5.34	168.26	6463.34
Nile Crocodile	RAD4.3 7	1.44E+07	3.59E+09	562.21	249.00	7054.92	3047.10	553.27	9.35E+05	2950.00	12.53	136.24	2117.63
Nile Crocodile	RAD4.3 9	7.28E+06	1.48E+08	73.75	20.31	10630.12	1169.57	72.65	3.89E+04	1350.00	2.56	170.86	5871.13
Nile Crocodile	RAD4.3 10	6.51E+06	1.65E+09	674.55	252.49	4093.53	2940.70	668.93	1.10E+06	2900.00	23.68	131.71	1970.03
Nile Crocodile	RAD4.3 11	4.03E+06	1.31E+08	111.84	32.54	2945.09	2421.60	118.09	1.47E+05	2300.00	4.98	170.35	7827.87
Nile Crocodile	RAD4.3 12	2.34E+06	2.00E+08	217.29	85.24	3802.23	1130.26	224.14	1.21E+05	1190.00	6.01	135.71	1059.42
Nile Crocodile	RAD4.3 13	5.58E+05	2.06E+07	85.53	36.88	1284.62	688.44	84.43	2.78E+04	765.00	4.75	147.23	987.19

Nile Crocodile	RAD4.3 14	1.15E+07	8.97E+08	214.29	78.12	6211.48	4067.54	215.94	1.75E+05	2600.00	15.00	161.92	5397.40
Nile Crocodile	RAD4.3 15	1.33E+07	3.05E+09	588.23	229.45	5660.53	3398.20	609.85	9.51E+05	3795.00	13.01	142.21	3350.86
Nile Crocodile	RAD4.3 16A	3.96E+06	5.00E+08	343.69	125.99	2995.21	2200.98	359.92	3.25E+05	1730.00	23.72	133.50	1336.68
Nile Crocodile	RAD4.3 16B	2.69E+06	3.03E+08	338.61	112.51	2543.55	1834.22	340.17	3.04E+05	1920.00	18.15	139.28	1658.46
Nile Crocodile	RAD4.3 17	8.24E+06	6.12E+08	219.30	74.25	11079.79	1381.59	212.47	1.94E+05	1550.00	4.19	147.04	1511.39
Nile Crocodile	RAD4.3 18	9.14E+05	7.77E+07	241.69	84.95	1221.40	980.02	217.67	9.67E+04	1185.00	9.95	123.16	1138.42
Nile Crocodile	RAD4.3 21	1.45E+06	3.49E+07	83.64	24.04	2784.00	1058.39	96.43	4.41E+04	1230.00	4.08	162.80	2603.44
Nile Crocodile	RAD4.3 23A	1.64E+06	8.05E+07	180.34	49.17	2432.09	988.73	176.66	8.22E+04	1015.00	4.75	146.92	1057.57
Nile Crocodile	RAD4.3 23B	4.51E+05	9.89E+06	60.55	21.96	2428.82	433.42	55.68	1.25E+04	425.00	1.72	149.19	421.73
Nile Crocodile	RAD4.3 24	1.06E+06	2.79E+07	69.04	26.21	3609.61	940.90	60.10	3.10E+04	960.00	1.39	163.88	2833.52
Nile Crocodile	RAD4.3 27	1.46E+07	4.67E+09	913.19	318.97	8782.66	3230.50	875.18	1.47E+06	3475.00	26.39	116.53	1890.12
Nile Crocodile	RAD4.3 28	5.95E+06	1.56E+09	651.41	261.49	2849.27	3651.07	623.34	9.33E+05	3540.00	20.31	147.64	3611.68
Nile Crocodile	RAD4.3 29A	9.75E+05	5.39E+07	162.60	55.28	2758.97	572.22	172.54	4.06E+04	600.00	11.47	123.07	355.07
Nile Crocodile	RAD4.3 31A	1.25E+06	6.49E+07	122.59	51.78	2848.37	828.22	122.53	3.90E+04	625.00	3.68	121.99	684.22
Nile Crocodile	RAD4.3 31B	1.17E+06	3.09E+07	85.15	26.30	1965.23	907.26	89.04	2.25E+04	940.00	5.65	160.07	2518.31
Nile Crocodile	RAD4.3 32	1.39E+06	1.52E+08	253.06	109.66	2818.63	744.93	252.42	1.08E+05	1005.00	6.27	123.16	579.82
Nile Crocodile	RAD4.3 35	3.06E+06	1.85E+08	146.54	60.25	5012.31	863.23	143.12	5.82E+04	745.00	2.96	133.94	514.07
Brown Bear	DZB1-1	1.34E+07	1.30E+09	270.16	96.77	8638.12	3028.90	227.53	1.85E+05	2630.00	9.40	31.74	12807.60
Brown Bear	DZB1-2	3.52E+07	3.49E+09	342.18	99.28	12000.99	3166.24	368.19	5.69E+05	3440.00	21.90	167.30	8120.90
Brown Bear	DZB1-3	1.31E+07	1.46E+09	257.18	111.41	6996.70	2216.41	276.93	3.40E+05	2090.00	10.73	160.16	3417.42
Brown Bear	DZB2-1A	6.23E+06	2.51E+08	144.61	40.30	8365.34	1465.39	149.32	7.67E+04	1295.00	4.74	164.36	2442.75
Brown Bear	DZB2-1B	5.02E+06	1.46E+08	110.59	29.08	7324.13	1127.52	115.01	4.78E+04	1050.00	4.24	147.17	2506.08
Brown Bear	DZB2-2	3.59E+07	3.43E+09	276.04	95.55	12469.57	3574.25	247.30	2.95E+05	3065.00	8.60	171.11	8379.33
Brown Bear	DZB2-4	3.23E+07	1.80E+09	188.98	55.68	1057.67	4112.18	173.21	1.14E+05	2040.00	9.29	12.70	44263.55
Brown Bear	DZB2-4	9.86E+06	5.00E+08	164.40	50.71	5744.07	2368.08	146.21	1.31E+05	2490.00	7.38	168.18	6917.05
Brown Bear	DZB2-6	1.93E+07	1.69E+09	230.01	77.32	8824.11	2737.11	225.16	2.70E+05	2455.00	9.89	131.44	10785.37
Brown Bear	DZB2-7	2.25E+07	2.88E+09	315.97	117.12	9053.92	3575.03	322.77	6.68E+05	4320.00	12.71	160.20	8213.63
Brown Bear	DZB2-8	1.60E+07	1.79E+09	270.03	111.90	4632.33	4895.18	299.20	7.72E+05	5325.00	9.15	172.71	19759.86
Brown Bear	DZB2-9	4.84E+06	4.92E+08	252.95	101.55	3448.99	1943.18	248.01	4.05E+05	3535.00	6.97	171.37	15156.56
Brown Bear	DZB2-10	3.48E+06	1.78E+08	198.96	51.14	3923.05	1169.25	198.07	1.06E+05	1345.00	8.49	159.84	2564.78

Brown Bear	DZB3-1	3.40E+06	3.43E+08	229.08	100.74	1460.95	3391.07	228.75	3.57E+05	3530.00	14.42	172.50	1883.61
Brown Bear	DZB3-2B	1.93E+06	1.38E+08	176.75	71.46	2903.78	985.08	181.99	8.38E+04	750.00	3.62	132.55	506.99
Brown Bear	DZB3-2A	3.37E+06	3.78E+08	247.04	112.21	1654.42	3182.06	250.18	4.89E+05	3515.00	6.05	164.62	7060.38
Brown Bear	DZB3-3	1.15E+07	1.00E+09	243.52	86.91	9415.53	1745.21	253.03	1.92E+05	2025.00	20.57	152.65	2834.55
Brown Bear	DZB3-4	3.67E+07	6.86E+09	472.63	187.06	10251.75	4158.61	367.98	7.29E+05	4615.00	14.17	168.24	15659.26
Brown Bear	DZB3-5	2.41E+07	2.47E+09	299.68	105.35	9498.84	2691.33	322.56	4.55E+05	2765.00	16.32	163.73	8179.22
Brown Bear	DZB4-1	4.09E+07	7.72E+09	343.40	188.59	14367.91	3641.99	233.43	4.42E+05	3605.00	6.72	169.45	10768.42
Brown Bear	DZB4-2	2.96E+07	4.22E+09	297.21	140.07	10278.45	3856.21	267.13	4.12E+05	3055.00	8.25	178.35	8597.51
Brown Bear	DZB4-3	2.44E+07	2.01E+09	254.65	82.41	8486.03	3965.80	242.82	3.75E+05	2865.00	7.08	166.15	6464.56
Brown Bear	DZB4-5	4.50E+07	5.80E+09	372.47	128.92	12151.94	4726.30	337.13	4.09E+05	4235.00	21.50	172.71	16796.53
Brown Bear	DZB5-3	3.34E+07	2.52E+09	220.83	75.58	12380.39	4193.71	197.34	2.93E+05	3510.00	6.84	169.60	11576.59
Brown Bear	DZB5-4	9.15E+06	4.55E+08	123.79	49.76	6957.23	1933.50	130.93	1.28E+05	1950.00	7.68	165.89	4429.13
Brown Bear	DZB6-1	5.27E+07	5.12E+09	284.68	97.14	17318.87	4355.49	294.49	6.58E+05	4690.00	7.96	172.72	27220.58
Brown Bear	DZB6-3	1.88E+07	5.17E+09	693.03	274.68	6350.42	3827.17	732.56	7.92E+05	2625.00	32.19	121.18	1559.85
Brown Bear	DZB6-4	1.04E+07	1.95E+09	370.37	186.74	4283.06	3389.13	423.74	6.66E+05	3060.00	15.89	154.39	3810.03

APPENDIX B – ALL MEASURED DATA FOR MARKS INFERRED ON FOSSILS

MARK ID	THREE DIMENSIONAL MEASUREMENTS						PROFILE MEASUREMENTS					
	SURFACE	VOLUME	MAXIMUM DEPTH	MEAN DEPTH	MAXIMUM LENGTH	MAXIMUM WIDTH	MAXIMUM DEPTH	AREA	WIDTH	ROUGHNESS	OPENING ANGLE	FLOOR RADIUS
HWKEE 1652	1969100	1.03E+08	144.348	52.326	3014.31	952.34	129.174	57317.88	940	3.948	150.088	1053.434
HWKEE 2908A	6399000	4.01E+09	1145.7	626.982	9585.20	2015.26	1262.103	1824795	2335	32.142	82.182	1090.356
HWKEE 2908B	4679175	1.59E+09	772.938	340.494	2658.15	1729.93	901.158	1268403	2585	22.746	109.79	1335.181
HWKEE 4107	5957125	5.74E+08	216.989	96.3	3923.00	1793.61	231.674	267013.2	2060	8.835	160.863	3260.48
HWKEE 4242	1489100	7.94E+07	122.652	53.315	3561.14	655.48	91.656	25468.22	535	4.98	153.061	641.767
HWKEE 4268	6208800	5.08E+08	198.52	81.817	8317.57	1479.15	138.199	95719.21	1595	3.581	157.455	3695.462
HWKEE 60025	690774.7	1.75E+09	496.88	253.736	4450.79	1913.58	504.117	513632	1890	13.77	119.924	1274.025
HWKEE 2743(L7)	4647850	3.33E+08	171.417	71.74	4992.97	1161.67	176.062	89551.79	1020	3.113	148.465	1012.618
HWKEE 356(L1)	1666125	2.78E+08	395.844	166.695	1471.15	1445.91	351.917	273716.6	1425	6.851	128.08	899.964
HWKEE 3833A(L1)	7860525	2.01E+09	595.894	255.334	4673.85	2045.55	501.908	561489	1995	17.415	124.511	1169.007
HWKEE 3833B(L1)	1378600	1.48E+08	198.516	107.117	1503.12	1252.47	184.984	176247.2	1440	3.117	145.244	1478.021
HWKEE 4168(L1)	3386625	1.66E+08	126.805	48.855	6558.03	752.61	156.068	56531.4	730	3.554	133.578	521.457
HWKEE 4176A(L1)	1.01E+07	1.33E+09	398.457	131.088	9600.57	1644.47	382.988	255718.2	1730	20.87	127.633	1399.829
HWKEE 4176B1(L1)	2628475	1.65E+08	134.35	62.9	4141.24	843.39	95.984	31011.08	685	6.502	143.758	585.084
HWKEE 4176B2(L1)	1097250	4.17E+07	86.358	38.011	3376.85	421.34	46.446	7532.924	260	1.364	145.642	232.905
HWKEE 4176B3(L1)	292125	1.39E+07	98.022	47.45	657.89	466.30	102.238	30523.79	605	4.475	145.034	553.162
HWKEE 1975-2(L2)	1.19E+07	3.80E+09	812.25	319.994	3623.63	3628.37	755.724	1380591	4605	11.868	143.08	4060.098
HWKEE 677A(L6)	3121750	2.82E+08	194.489	90.308	1925.23	1781.62	152.927	160162.3	1895	6.018	153.098	3672.922
HWKEE 677B(L6)	5774775	4.77E+08	173.861	82.511	3986.84	1613.16	154.523	157412	2295	7.353	162.655	4898.702
HWKEE 1045A(L6)	1503175	1.44E+08	257.98	95.731	2198.55	1379.46	255.059	76962.05	880	7.843	118.258	569.681
HWKEE 1045B(L6)	835225	5.74E+07	147.725	68.672	1696.17	677.46	154.952	50328.47	575	5.947	102.563	387.331
HWKEE 1045C(L6)	1.47E+07	1.85E+09	291.505	125.646	11652.27	1782.88	257.109	247717.6	2215	15.443	153.586	2708.534
HWKEE 3969	1.16E+07	7.27E+08	167.637	62.528	8427.33	1776.35	129.128	95491.18	1845	9.022	161.59	4135.396

HWKEE 1886A	2822225	1.26E+08	108.846	44.704	5057.28	1150.06	87.218	27480.23	730	7.626	159.089	1153.368
HWKEE 1886B	915375	3.17E+07	93.332	34.628	1473.78	995.46	92.473	24719.17	595	3.412	148.263	609.395
HWKEE 60021A	312175	1.26E+07	85.391	40.412	1056.72	363.47	100.601	27780.73	545	3.678	135.718	739.021
HWKEE 60021B	1038700	6.24E+07	133.426	60.079	1214.77	967.30	132.364	82543.66	1045	3.978	152.679	1291.862
HWKEE 60275	2614750	3.08E+08	267.067	117.587	3297.81	919.56	204.448	112248.4	1165	4.261	139.423	913.114
HWKEE 60050	3210775	3.16E+08	276.183	98.476	3694.54	1251.74	259.176	109852	960	7.009	134.701	640.715

APPENDIX C – ALL MEASURED FROM TESTING THE ACCURACY OF REPLICAS

ORIGINAL / REPLICA	MARK ID	THREE DIMENSIONAL MEASUREMENTS						PROFILE MEASUREMENTS					
		SURFACE	VOLUME	MAXIMUM DEPTH	MEAN DEPTH	MAXIMUM LENGTH	MAXIMUM WIDTH	MAXIMUM DEPTH	AREA	WIDTH	ROUGHNESS	OPENING ANGLE	FLOOR RADIUS
ORIGINAL	NGO25-1-1	4.02E+06	2.43E+08	1.81E+02	6.03E+01	3.97E+03	1.58E+03	1.65E+02	9.60E+04	1.21E+03	7.88E+00	1.43E+02	9.51E+02
ORIGINAL	NGO25-1-2	2.00E+06	6.58E+07	1.05E+02	3.29E+01	4.03E+03	8.24E+02	1.04E+02	2.06E+04	6.90E+02	9.17E+00	1.49E+02	9.58E+02
ORIGINAL	NGO25-1-4	5.96E+06	2.74E+08	1.01E+02	4.60E+01	4.78E+03	2.81E+03	9.25E+01	9.55E+04	2.85E+03	4.45E+00	1.71E+02	1.82E+04
ORIGINAL	NGO25-1-5	1.26E+06	4.34E+07	8.21E+01	3.45E+01	1.68E+03	1.37E+03	8.62E+01	3.44E+04	7.55E+02	2.81E+00	1.59E+02	9.30E+02
ORIGINAL	NGO25-1-6	2.66E+06	2.98E+08	2.62E+02	1.12E+02	1.98E+03	1.88E+03	2.46E+02	2.40E+05	2.00E+03	1.39E+01	1.44E+02	2.74E+03
ORIGINAL	NGO25-2-1	3.02E+06	1.90E+08	2.09E+02	6.30E+01	4.32E+03	1.38E+03	1.70E+02	4.66E+04	4.55E+02	4.54E+00	8.21E+01	2.45E+02
ORIGINAL	NGO25-2-2A	3.49E+06	5.00E+08	3.64E+02	1.43E+02	3.64E+03	1.46E+03	3.47E+02	1.77E+05	9.80E+02	9.60E+00	1.06E+02	4.90E+02
ORIGINAL	NGO25-2-2B	9.98E+05	5.47E+07	1.90E+02	5.47E+01	1.78E+03	9.42E+02	1.96E+02	9.08E+04	9.10E+02	8.79E+00	1.36E+02	5.89E+02
ORIGINAL	NGO25-2-4A	3.94E+05	1.67E+07	1.26E+02	4.25E+01	7.07E+02	8.57E+02	1.20E+02	4.70E+04	8.40E+02	4.45E+00	1.47E+02	8.27E+02
ORIGINAL	NGO25-3-1	6.19E+05	3.10E+08	1.69E+02	5.01E+01	4.27E+03	2.33E+03	1.75E+02	2.09E+05	2.40E+03	8.71E+00	1.64E+02	4.77E+03
ORIGINAL	NGO25-3-3	2.66E+06	1.72E+08	1.60E+02	6.48E+01	4.32E+03	8.16E+02	1.47E+02	6.18E+04	8.50E+02	5.01E+00	1.47E+02	8.32E+02
ORIGINAL	NGO25-3-7	1.96E+06	7.59E+07	9.61E+01	3.86E+01	1.95E+03	1.58E+03	1.14E+02	6.33E+04	1.01E+03	2.97E+00	1.59E+02	1.48E+03
ORIGINAL	NGO25-6-2	5.22E+06	5.64E+08	2.68E+02	1.08E+02	2.59E+03	2.83E+03	2.42E+02	4.10E+05	2.82E+03	5.21E+00	1.62E+02	4.58E+03
ORIGINAL	NGO25-7-1	5.08E+06	3.52E+08	2.25E+02	6.93E+01	5.01E+03	1.37E+03	2.15E+02	1.41E+05	1.46E+03	3.36E+00	1.51E+02	1.65E+03
ORIGINAL	NGO25-10-2	4.29E+06	3.55E+08	2.23E+02	8.27E+01	5.36E+03	1.22E+03	2.53E+02	1.84E+05	1.46E+03	5.09E+00	1.41E+02	1.22E+03
ORIGINAL	NGO25-10-3	6.52E+06	8.17E+08	2.96E+02	1.25E+02	5.21E+03	2.76E+03	2.99E+02	4.23E+05	2.75E+03	2.93E+00	1.51E+02	4.43E+03
ORIGINAL	NGO25-14-1	2.72E+06	3.86E+08	3.18E+02	1.42E+02	3.56E+03	1.26E+03	3.03E+02	2.38E+05	1.47E+03	4.39E+00	1.37E+02	1.06E+03
ORIGINAL	NGO25-14-2	7.57E+05	5.32E+07	1.72E+02	7.03E+01	1.22E+03	9.45E+02	1.78E+02	8.78E+04	1.02E+03	3.71E+00	1.35E+02	7.46E+02
ORIGINAL	NGO25-18-1	3.31E+06	2.11E+08	2.16E+02	6.39E+01	3.16E+03	2.20E+03	2.09E+02	2.08E+05	2.15E+03	9.29E+00	1.56E+02	3.54E+03
ORIGINAL	NGO25-21-1	2.73E+06	1.36E+08	1.14E+02	4.97E+01	2.45E+03	1.44E+03	1.09E+02	7.70E+04	1.28E+03	2.03E+00	1.63E+02	2.46E+03
ORIGINAL	NGO25-22-1	4.47E+05	3.24E+07	1.64E+02	7.25E+01	8.43E+02	7.64E+02	1.40E+02	5.94E+04	7.75E+02	6.15E+00	1.38E+02	5.57E+02
REPLICA	NGO25-1-1	2.06E+06	1.51E+08	1.82E+02	7.35E+01	2.99E+03	1.10E+03	1.87E+02	1.17E+05	1.15E+03	3.62E+00	1.41E+02	9.49E+02
REPLICA	NGO25-1-2	1.99E+06	9.40E+07	1.44E+02	4.73E+01	4.00E+03	8.90E+02	1.43E+02	6.73E+04	9.05E+02	5.55E+00	1.50E+02	9.20E+02

REPLICA	NGO25-1-4	5.11E+06	2.35E+08	1.09E+02	4.61E+01	4.55E+03	2.21E+03	1.25E+02	1.52E+05	2.64E+03	5.91E+00	1.72E+02	9.39E+03
REPLICA	NGO25-1-5	1.08E+06	3.97E+07	9.24E+01	3.68E+01	1.72E+03	1.08E+03	7.88E+01	2.60E+04	7.80E+02	4.00E+00	1.52E+02	1.49E+03
REPLICA	NGO25-1-6	2.82E+06	3.09E+08	2.67E+02	1.10E+02	2.06E+03	1.95E+03	2.53E+02	2.50E+05	1.94E+03	9.44E+00	1.43E+02	2.52E+03
REPLICA	NGO25-2-1	3.03E+06	1.60E+08	1.76E+02	5.28E+01	4.44E+03	1.19E+03	1.71E+02	9.17E+04	1.00E+03	6.36E+00	1.37E+02	9.30E+02
REPLICA	NGO25-2-2A	3.66E+06	6.04E+08	4.22E+02	1.65E+02	3.11E+03	1.76E+03	4.03E+02	2.23E+05	1.07E+03	1.20E+01	9.99E+01	4.90E+02
REPLICA	NGO25-2-2B	1.40E+06	9.17E+07	2.41E+02	6.55E+01	1.83E+03	1.17E+03	2.31E+02	1.27E+05	1.07E+03	1.34E+01	1.16E+02	7.37E+02
REPLICA	NGO25-2-4A	3.91E+05	1.54E+07	1.45E+02	3.93E+01	7.41E+02	7.83E+02	1.35E+02	3.39E+04	6.70E+02	3.94E+00	1.48E+02	6.95E+02
REPLICA	NGO25-3-1	6.59E+05	3.70E+08	1.87E+02	5.61E+01	4.12E+03	2.44E+03	1.83E+02	2.23E+05	2.44E+03	9.03E+00	1.62E+02	5.01E+03
REPLICA	NGO25-3-3	2.78E+06	1.62E+08	1.53E+02	5.82E+01	4.27E+03	8.47E+02	1.56E+02	6.58E+04	8.65E+02	8.11E+00	1.44E+02	7.73E+02
REPLICA	NGO25-3-7	1.83E+06	9.47E+07	1.24E+02	5.18E+01	2.16E+03	1.23E+03	1.33E+02	7.02E+04	8.80E+02	6.38E+00	1.43E+02	9.63E+02
REPLICA	NGO25-6-2	5.17E+06	6.45E+08	3.09E+02	1.25E+02	2.17E+03	3.09E+03	3.15E+02	4.98E+05	2.92E+03	9.81E+00	1.62E+02	4.78E+03
REPLICA	NGO25-7-1	5.68E+06	3.57E+08	2.14E+02	6.28E+01	5.06E+03	1.37E+03	1.76E+02	1.49E+05	1.42E+03	3.94E+00	1.57E+02	1.87E+03
REPLICA	NGO25-10-2	4.48E+06	3.57E+08	2.24E+02	7.97E+01	5.87E+03	1.39E+03	2.60E+02	1.74E+05	1.12E+03	5.47E+00	1.34E+02	7.52E+02
REPLICA	NGO25-10-3	6.78E+06	8.43E+08	3.13E+02	1.24E+02	5.35E+03	2.74E+03	3.24E+02	4.31E+05	2.47E+03	9.74E+00	1.47E+02	3.35E+03
REPLICA	NGO25-14-1	2.99E+06	3.82E+08	3.21E+02	1.28E+02	3.49E+03	1.40E+03	3.39E+02	2.63E+05	1.40E+03	5.38E+00	1.27E+02	8.55E+02
REPLICA	NGO25-14-2	7.49E+05	5.48E+07	1.90E+02	7.32E+01	1.19E+03	1.01E+03	1.97E+02	9.64E+04	9.05E+02	5.79E+00	1.33E+02	6.65E+02
REPLICA	NGO25-18-1	4.27E+06	2.40E+08	2.20E+02	5.63E+01	3.11E+03	2.77E+03	1.92E+02	1.86E+05	2.23E+03	1.07E+01	1.58E+02	4.76E+03
REPLICA	NGO25-21-1	3.15E+06	1.12E+08	1.09E+02	3.55E+01	2.59E+03	1.57E+03	1.14E+02	8.95E+04	1.22E+03	2.13E+00	1.64E+02	2.80E+03
REPLICA	NGO25-22-1	5.22E+05	3.70E+07	1.75E+02	7.08E+01	8.98E+02	8.62E+02	1.88E+02	9.74E+04	9.60E+02	8.08E+00	1.33E+02	1.01E+03